University of Louisville
ThinkIR: The University of Louisville's Institutional Repository

Electronic Theses and Dissertations

5-2019

# Novel mechanisms and biomarkers in alcohol-induced organ injury.

Christine E. Dolin
*University of Louisville*

Follow this and additional works at: https://ir.library.louisville.edu/etd

 Part of the Diagnosis Commons, Digestive System Diseases Commons, Hepatology Commons, Medical Molecular Biology Commons, Medical Toxicology Commons, and the Nephrology Commons

Recommended Citation
Dolin, Christine E., "Novel mechanisms and biomarkers in alcohol-induced organ injury." (2019). *Electronic Theses and Dissertations.* Paper 3195.
Retrieved from https://ir.library.louisville.edu/etd/3195

This Doctoral Dissertation is brought to you for free and open access by ThinkIR: The University of Louisville's Institutional Repository. It has been accepted for inclusion in Electronic Theses and Dissertations by an authorized administrator of ThinkIR: The University of Louisville's Institutional Repository. This title appears here courtesy of the author, who has retained all other copyrights. For more information, please contact thinkir@louisville.edu.

# NOVEL MECHANISMS AND BIOMARKERS IN ALCOHOL-INDUCED ORGAN INJURY

By

Christine E. Dolin

B.S. University of Louisville, 2015

M.S., University of Louisville, 2017

A Dissertation

Submitted to the Faculty of the

School of Medicine of the University of Louisville

In Partial Fulfillment of the Requirements

for the Degree of

Doctor of Philosophy in Pharmacology and Toxicology

Department of Pharmacology and Toxicology

University of Louisville

Louisville, KY

May 2019

NOVEL MECHANISMS AND BIOMARKERS IN ALCOHOL-INDUCED ORGAN INJURY

By Christine E. Dolin

B.S., University of Louisville, 2015

M.S. University of Louisville, 2017

Dissertation Approved on

04/12/2019

By the following Committee:

_____
Michael L. Merchant, Ph.D. (Mentor)

_____
Gavin E. Arteel, Ph.D. (Co-Mentor)

_____
Michelle T. Barati, Ph.D.

_____
Juliane I. Beier, Ph.D.

_____
Jonathan H. Freedman, Ph.D.

_____
Gary W. Hoyle, Ph.D.

# DEDICATION

This dissertation is lovingly dedicated

to my parents

Owen and Ann Dolin

And to my husband

Neal Taylor

for their constant love, encouragement and support

In all my endeavors.

ACKNOWLEDGEMENTS

First, I would like to thank my mentors, Dr. Gavin Arteel and Dr. Michael Merchant, for their steadfast guidance and support in my research and learning. Their encouragement, patience and confidence in my abilities during my first scientific investigations and throughout my graduate career has been instrumental in the success of my research. I would also like to thank my dissertation committee members, Dr. Michelle Barati, Dr. Juliane Beier, Dr. Jonathan Freedman, and Dr. Gary Hoyle, for their guidance and support throughout my graduate career.

I would like to thank Dr. Craig McClain and Dr. Vatsalya Vatsalya for their help in providing the alcoholic hepatitis samples and clinical data. I would also like to thank Dr. Shesh Rai and Dr. Sudhir Srivastava for their statistical support. I would also like to thank Dr. Wolfgang Zacharias, Sabine Waigel, and Vennila Arumugam for their help with RNA-seq, and Dr. Eric Rouchka and Dr. Julia Chariker for bioinformatics support.

Many thanks to my lab mates who have been an instrumental part of my graduate experience: Daniel Wilkey, for his proteomics expertise, Susan Isaacs, for her expertise in immunoblot, Ming Li, Kim Head, and Deanna Siow for their guidance and lab management, Dr. Veronica Massey, Dr. Lauren Poole, Dr. Shanice Hudson, Dr. Anna Lang, Dr. Liya Chen, Regina Schnegelberger, Brenna

Kaelin, and Calvin Nguyen-Ho for their peer mentorship and their help with various experiments.

Thank you to everyone in the University of Louisville Department of Pharmacology and Toxicology, Alcohol Research Center, and Division of Nephrology for your support. Thanks also to my cohort mates for making coursework more enjoyable.

Finally, I would also like to thank my friends and family for their support through my years in graduate school. Special thanks to Kelsey Durrenberg and Adrienne Bushau-Sprinkle for their steadfast friendship. I would like to thank my husband, Neal Taylor, for his endless love, patience and encouragement. Many thanks to my family- Owen, Ann, Matt, and Brad Dolin– for all of their loving support throughout my life that made me who I am. I thank God for each of these individuals, and for the opportunity and ability to do the work that is summarized herein.

ABSTRACT

NOVEL MECHANISMS AND BIOMARKERS IN ALCOHOL-INDUCED ORGAN INJURY

Christine E. Dolin

April 12, 2019

**Background.** Ethanol (EtOH) consumption is known to affect multiple organs; this is unsurprising, as the concentration of EtOH in the blood at relevant doses reaches the millimolar range. The overarching goal of this dissertation was to elucidate mechanisms of alcohol-induced organ injury, specifically the effects of alcohol on the hepatic extracellular matrix (ECM) proteome, the alcoholic hepatitis (AH) plasma peptidome, and the effects of alcohol on the renal cortex proteome and transcriptome. **Methods.** Mice were pair-fed ethanol-containing liquid diet chronically, and then some mice were administered lipopolysaccharide (LPS). Liver sections from these mice were processed in a series of increasingly rigorous extraction buffers to separate proteins by 'age' and crosslinking. Extracted proteins were identified using liquid chromatography-tandem mass spectrometry (LC-MS/MS). For the AH study, a workflow was developed for the peptidomic analysis of plasma from healthy participants or AH patients. AH severity was stratified by MELD score as mild (<12; n=45), moderate (12-19;

n=23) or severe (>19; n=37). The peptidome in AH and control plasma was analyzed with LC-MS/MS. For the kidney study, renal cortex proteins were extracted in lysis buffer, and RNA was also isolated. Extracted proteins were identified using LC-MS/MS, and RNA sequencing (i.e. transcriptomics) identified transcripts. **Results.** Chapter III introduced a new proteomic approach for characterizing the hepatic matrisome, which demonstrated that the hepatic matrisome responds dynamically to both acute (LPS) and chronic (ethanol) stresses, long before more dramatic fibrotic changes to the liver. Chapter IV demonstrated that AH causes detectable changes in the plasma ECM degradome/peptidome of patients, and that the LC-MS/MS analysis of the plasma peptidome is a novel, minimally-invasive method for prognosis stratification in patients with AH. Finally, Chapter V revealed that chronic, moderate ethanol consumption affects renal cortical oxidant response pathways at the protein and transcript level. **Conclusions.** The work presented in this dissertation has, in conclusion, revealed that the hepatic ECM responds dynamically to stress, plasma peptides, including ECM peptides, change with AH severity, and chronic ethanol consumption affects renal cortical oxidant response pathways.

TABLE OF CONTENTS

DEDICATION……iii
ACKNOWLEDGEMENTS……iv
ABSTRACT……vi
LIST OF TABLES……xv
LIST OF FIGURES…… xvi

CHAPTER

I. INTRODUCTION

A. Background and rationale for this study...……1

1. Alcohol consumption and human health……..…… 1

2. The extracellular matrix: more than a scaffold …..……..……2

3. The role of the ECM in inflammation and disease..……... 4

4. ECM remodeling and the “degradome”……... 7

5. Natural history of liver disease.…… 8

6. Alcoholic liver disease..…...……9

7. Alcoholic hepatitis ……...11

8. Alcohol and the kidney..……...……....12

9. Statement of goals.…….....  13

B. Aims and proposals……13

1. Characterization of alcohol-induced matrisome changes in liver ….  13

2. Novel biomarkers in alcoholic hepatitis: analysis of the plasma peptidome/degradome ……..……14

3. Pathways affected by alcohol in the kidney.....16

II. EXPERIMENTAL PROCEDURES…… 18

A. Animals and exposures…….. 18

1. Animal sacrifice, tissue collection and storage..…….. 18

2. Carbon tetrachloride model of hepatic fibrosis……... 18

3. Chronic model of alcohol exposure……...19

4. Chronic+binge model of alcohol exposure……20

B. Proteomics…… 21

1. 3-step ECM extraction……21

2. Total protein extraction…….23

3. Sample cleanup and preparation for liquid chromatography and mass spectrometry…… 24

4. TMT labeling…….25

5. Liquid chromatography and tandem mass spectrometry……..… 26

6. Informatics……..28

C. Immunoblots…… 29

1. Dot blot……...29

2. Western blot…….....30

D. Transcriptomics…… 30

1. RNA isolation…… 30

2. RNA sequencing…….....30

3. RNASeq data analysis…… 31

E. Histology and Immunohistochemistry..…….. 31

1. Histology…….……31

2. Immunohistochemistry..……...31

F. Clinical chemistry…… 32

1. Blood urea nitrogen analysis……...…32

G. Clinical study……32

1. Study participants……..……32

2. Inclusion criteria…… 33

3. Study paradigm…….33

4. Collection of clinical data…….34

5. Plasma collection..……..…….... 34

H. Peptidomics……..……..35

1. Peptidomic workflow optimization……..35

2. Plasma peptide purification…….36

3. Peptide sample cleanup and preparation for liquid chromatography and mass spectrometry……..…….36

4. Liquid chromatography and tandem mass spectrometry……...…37

I. Informatics……..…….. 38

1. Liver ECM proteomic data analysis……..38

2. Renal cortex proteomic data analysis..…….38

3. Multivariate analysis of renal cortex proteomic and transcriptomic data sets…….39

4. AH plasma peptidome data analysis…….39

J. Statistics……..…….. 40

1. Statistical analysis of liver ECM proteomic data……..…….40

2. Statistical analysis of alcoholic hepatitis plasma peptidomic data…….41

3. Statistical analysis of renal cortex proteomic and transcriptomic data..42

III. THE HEPATIC “MATRISOME” RESPONDS DYNAMICALLY TO INJURY: CHARACTERIZATION OF TRANSITIONAL CHANGES TO THE EXTRACELLULAR MATRIX IN MICE……..44

A. Introduction……44

B. Experimental procedures……46

1. Animals and exposures……... 46

2. Three-step ECM extraction……..……..49

3. Sample cleanup and preparation for LC-MS/MS……... 49

4. Liquid chromatography and mass spectrometry ……..…….…. 49

5. Data analysis ……49

6. Statistical analysis…….49

C. Results……..……50

1. Analysis of changes to the ECM proteome caused by carbon tetrachloride-induced hepatic fibrosis……50

2. Ethanol and LPS exposure cause global changes to the hepatic matrisome……..……53

3. Three-step serial extraction creates distinct protein profiles……....53

4. Qualitative changes to the ECM proteome in response to stress…... 74

5. Quantitative changes to the ECM proteome in response to stress….. 80

D. Discussion……...…..95

IV. NOVEL BIOMARKERS IN ALCOHOLIC HEPATITIS: ANALYSIS OF THE PLASMA PEPTIDOME/DEGRADOME……..……103

A. Introduction……..…103

B. Experimental procedures……...104

1. Study participants and inclusion criteria…….……104

2. Study paradigm……104

3. Plasma collection....……..……..……..……105

4. Plasma peptide purification....……..……105

5. Liquid chromatography and tandem mass spectrometry……..105

6. Data analysis……105

7. Statistical analysis……..…105

C. Results……..108

1. Patient demographics...……..……..108

2. Plasma peptides change between MELD groups……..……108

3. ECM peptides change between MELD groups…… 114

D. Discussion……..…… 122

V. CHRONIC MODERATE ALCOHOL CONSUMPTION INFLUENCES RENAL CORTICAL OXIDANT RESPONSE PATHWAYS……..126

A. Introduction……...126

B. Experimental procedures……...128

1. Animals and exposures……..128

2. Histology and immunohistochemistry..……128

3. Blood urea nitrogen analysis…….……128

4. Proteomic sample handling……128
5. Liquid chromatography and tandem mass spectrometry ……129
6. RNA seq analysis……129
7. Multivariate analysis of proteomic and transcriptomic data……129
8. Immunoblot analysis……129
9. Statistical analyses……130
C. Results……130
1. Ethanol, LPS, and the combination increase blood urea nitrogen……130
2. Ethanol alone contributes little-to-no morphological changes to mouse renal cortex……130
3. Ethanol attenuates LPS-induced cortical recruitment of MPO-positive cells……135
4. Ethanol and LPS each cause unique protein abundance patterns……135
5. RNA seq data support proteomic data for LPS effect……140
6. Ethanol alone downregulates Nrf2-mediated oxidative stress response pathway at the protein level and transcript level……143
7. Effects of ethanol and LPS on catalase abundance……148
8. Data sharing……148
D. Discussion……151
VI. DISCUSSION AND CONCLUSIONS…… 158
A. Restatement of goals and questions……158
B. Major findings of this dissertation…… 158
1. The hepatic “matrisome” responds dynamically to stress…… 158

2. The plasma ECM degradome profile of alcoholic hepatitis patients changes between MELD groups ……..… 160

3. Alcohol consumption alters renal cortical oxidant response pathways…….. 162

C. Significance of new findings…… 163

D. Strengths and weaknesses of this dissertation…… 165

1. Strengths…… 165

2. Weaknesses…… 168

E. Future directions…… 170

1. Does targeting the regulated “matrisome” proteins identified in Chapter III prevent, halt, or reverse alcohol-induced organ injury?..... 170

2. Do the regulated peptides and features identified in Chapter IV predict alcoholic hepatitis patient outcome and/or response to treatment in longitudinal studies?..... 171

3. Do the regulated peptide features identified in Chapter V predict alcoholic hepatitis patient outcome and/or response to treatment in longitudinal studies?..... 171

F. Summary and Conclusions……172

REFERENCES……174
PUBLISHER’S NOTICE OF APPROVAL……..…… 192
ABBREVIATIONS……..…… 192
CURRICULUM VITAE…… 198

LIST OF TABLES

TABLES

Table 3.1: Qualitative presence of ECM proteins in sample extracts..... 57

Table 3.2: Clustering of proteins in response to ethanol and/or LPS..... 91

Table 4.1: Patient demographics..... 109

Table 4.2: Pairwise comparison of peptidomes..... 115

Table 4.3: ECM matrisome annotation for pairwise regulated peptides……..119

Table 5.1: Effects of EtOH and LPS on differentially regulated cortical RNA transcripts, differentially regulated genes, and one-hit/two-hit associated Top-5 Gene Ontology (GO) terms..... 146

LIST OF FIGURES

FIGURES

Figure 3.1: Scheme of transitional ECM changes and extraction methodology.. 47

Figure 3.2: Validation of extraction technique with CCl4 model of fibrosis ..... 51

Figure 3.3: Liver extracts have unique protein profiles based on fraction type and experimental group..... 54

Figure 3.4: Ethanol and LPS cause dynamic changes in the matrisome……..75

Figure 3.5: Shared and unique changes to the hepatic matrisome……78

Figure 3.6: Quantitative changes to the matrisome……..81

Figure 3.7: Clustered profiles of protein abundances for proteins identified in the NaCl fraction……..……..…….83

Figure 3.8: Clustered profiles of protein abundances for proteins identified in the SDS fraction……..……..85

Figure 3.9: Clustered profiles of protein abundances for proteins identified in the GnHCl fraction…….……..87

Figure 3.10: Clustered profiles of protein abundances for proteins identified in the pellet ……..……..……..89

Figure 4.1: Scheme of peptidomic workflow ..... 106

Figure 4.2: Multivariate analysis of the plasma peptidome using principal component analysis biplots and heat maps with hierarchical clustering..... 112

Figure 4.3: Pairwise comparison of the peptidomes of patients with different AH severity by volcano plots ..... 116
Figure 4.4: Regulated peptides common to HC to AH pairwise comparisons include ECM peptides..... 120
Figure 5.1: Effects of chronic moderate EtOH feeding and low dose (10mg/kg intra-peritoneal (i.p.) lipopolysaccharide (LPS) on blood urea nitrogen (BUN) . 131
Figure 5.2: Mild effects of EtOH and/or LPS on renal architecture ..... 133
Figure 5.3: LPS induced infiltration of myeloperoxidase (MPO) positive cells into the renal parenchyma..... 136
Figure 5.4: Workflow and characterization of the global effect of EtOH and LPS on the cortical proteome ..... 138
Figure 5.5: Quantitative cluster analysis reveals EtOH-regulated protein clusters ..... 141
Figure 5.6: Workflow and characterization of the EtOH and 4h LPS regulated transcriptomes..... 144
Figure 5.7: Effects of EtOH feeding on Cat abundance in the renal cortex ..... 149

# CHAPTER I

# INTRODUCTION

## A. Background and rationale for this study

### 1. Alcohol consumption and human health

Alcoholic beverages were valued in ancient cultures as an antimicrobial agent, a source of hydration and nourishment, as well as a “social lubricant” (1). Today, alcohol consumption is nearly ubiquitous worldwide. In the United States alone, 86.4% of adults report consuming alcohol at some point in their lives (2). Just as alcohol use is common worldwide, so is alcohol abuse. Chronic, compulsive alcohol abuse characterizes clinically recognized alcohol use disorder (AUD), which is defined with specific criteria in the Diagnostic and Statistical Manual of Mental Disorders (DSM). AUDs affect approximately 15 million adults in the United States (2). Worldwide, an estimated 64 million people are dependent on alcohol (3).

While AUD is, in itself, a brain disorder, the serious health consequences of alcohol abuse are much more extensive. In addition to the brain (4), chronic alcohol consumption/abuse directly damages several organs, including the liver (5), lung (6), skeletal muscle and heart (7), and pancreas (8). Alcohol

consumption is a risk factor for over 200 health conditions (9). Alcohol consumption accounts for ~6% of all disability-adjusted life years lost in the United States, and alcohol-related disease and disability costs the United States approximately 250 billion dollars annually (2). There is a great need for mechanism-based therapies to treat and/or protect against alcohol-induced organ damage, especially given the high rate of relapse of AUDs (10). Unfortunately, current therapies for alcohol-induced organ damage are palliative, at best, and do not prevent or reverse the progression of organ injuries. The overarching goal of this project is to develop such means of detection and treatment of alcohol-induced end organ damage.

## 2. The extracellular matrix: more than a scaffold

The extracellular matrix (ECM) is a non-cellular three-dimensional scaffold within all tissues and organs (11) that is critical for structure and cell signaling. Genetic mutations in matrix components can cause a myriad of connective tissue pathologies (12-14), if not embryonic lethality (15, 16). Therefore, the ECM is essential to normal tissue homeostasis.

The most obvious function of the ECM is to physically support cells and thereby provide structure to tissue. The composition of the ECM allows for its structural role. A network of collagens, which provides tensile strength, is a major component of the ECM of the basement membranes and interstitial matrices in all physiological domains (17). In all solid organs, fibroblasts secrete

fibrous glycoproteins and proteoglycans that adhere to this collagen scaffold in a highly cross-linked meshwork (17).

In addition to its structural role, the ECM can also play a role in cell signaling. The heparin and heparan sulfate components of many proteoglycans readily bind soluble growth factors, cytokines, and chemokines and can even regulate their activation and presentation to cells (18). Additionally, these signaling molecules can become spatially distributed and form gradients by binding to the ECM (18). These gradients are important for tissue development and inflammatory cell migration (18).

In addition to binding signaling molecules, ECM proteins can directly engage in signaling. Indeed, ECM proteins are ligands of cell surface receptors, including integrins, which bind specific ECM protein domains (e.g., the RGD motif) (19). Through interaction with cell-surface receptors, the ECM can activate intracellular signaling (19)

The ECM is far from static; it is full of activities required to maintain homeostasis or (mal)adapt to insult. Proteases and protease inhibitors are key players in maintaining and regulating other ECM components (20). Proteases may deposit (e.g., proteases involved in the complement and coagulation cascades) or degrade (e.g. matrix metalloproteinases, MMPs) matrix components to facilitate rapid changes in ECM organization. Alterations in the extracellular landscape, including changes in ECM topography, crosslinking, and biochemistry, can affect cell migration, adhesion, and activation (21). Indeed, protease-mediated modification of the ECM can have physical and/or

biochemical significance. For example, ECM proteolytic degradation can create physical space through which cells can migrate (22). Alternatively, ECM proteolysis can expose or remove binding sites; for example, protease cleavage of laminin-5 exposes integrin-binding sites that are necessary for cell adhesion (23). Proteases can also contribute to ECM dynamics by modulating the activity of other enzymes (e.g., proteinase precursors (24) and soluble mediators (e.g., IL-8, (21)). Degradation of ECM components, such as the glycosaminoglycan components of proteoglycans, can release growth factors (18). The broad, consequential activity of proteases necessitates intricate, and often redundant, mechanisms of regulation. Indeed, proteases are not only regulated at the levels of transcription and secretion, but also at the level of activity (25). Proteases are often activated through cleavage by another protease, and can be targeted by inhibitors, such as tissue inhibitors of matrix metalloproteinases (TIMPs) (22). Therefore, regulation of the ECM is important for the function of tissues and organs.

## 3. The role of the ECM in inflammation and disease

As previously discussed, tight regulation of the ECM is critical for normal tissue homeostasis. Such regulation also facilitates rapid changes that allow the ECM to play a dynamic and responsive role during inflammation and tissue repair. Perturbations in the ECM during either of these physiological states can contribute to disease initiation and progression. Indeed, ECM dysregulation is often a hallmark of tissue pathology (16).

During hepatic inflammation of any cause, hepatocytes express many different chemokines and inflammatory mediators (26). During hepatocyte injury or death, they also release damage-associated molecular patterns (DAMPs), which activate resident macrophages (Kupffer cells, KCs). Additionally, pathogen-associated molecular patterns (PAMPs, e.g. LPS) activate pattern recognition receptors (PRRs) (27). DAMPs and PAMPs cause the release of cytokines and acute phase proteins (APPs), such as TNFα, IL-1, IL-6. Hepatic stellate cells become activated, and deposit new ECM and alter matrix degradation. Although this response is important for normal immune/inflammatory function, dysregulation of this response can cause inappropriate inflammation, tissue damage, and hepatic fibrosis. During inflammation and injury, the functions of the ECM include providing structure, facilitating adhesion, presenting cytokines to receptors, sequestering and storing cytokines, and mechanical signal transduction.

The ECM plays an important structural role during inflammation and disease. Under normal conditions, the ECM defines tissue boundaries (28). When the tissue is injured, the super- and ultra- structure of the ECM is altered. As a result, tissue boundaries are perturbed. Additionally, injury alters structural components of the ECM (e.g. collagens I, IV, V, fibronectin, elastin) and thereby affects the normal elasticity provided by the ECM (29).

Another role of the ECM during inflammation is regulation of the signaling of cytokines and other APPs. The ECM acts as a chemokine reservoir. Additionally, ECM binding of cytokines, including IL-2, TNFα, TGFβ, and

RANTES ((30-32), has been shown to regulate cell activation, adhesion, and migration. For example, CCL2 is concentrated in the ECM at the site of injury. Furthermore, glycosaminoglycan binding of chemokines can protect them from proteolytic cleavage.

The ECM also acts as an adhesive substrate during inflammation. The ECM directs inflammatory cells. For example, the ECM is critical in the process of leukocyte adhesion and transmigration (33). Initial leukocyte capture and rolling is mediated by selectins, arrest is medicated by integrins, and transmigration involves adhesion molecules. The aforementioned chemokine gradients mediated by the ECM also play an important role in directing immune cells.

During inflammation, the ECM also plays an important role in mechanical signaling. During an acute inflammatory response, the ECM plays a pivotal role by serving as a structural barrier. The ECM defines mechanical properties permissive and/or instructive to inflammation. Indeed, studies have shown that neutrophil transmigration is greater through vascular areas with lower ECM concentration (34). The interaction between the ECM and cell infiltration is bidirectional; as leukocytes integrate structural and biochemical signals from the ECM, they in turn release matrix-degrading proteases (35) which alter the extracellular composition and allow for easier cell migration.

ECM dysregulation during chronic inflammation can cause pathological tissue remodeling. Over time, this remodeling can culminate in disease states such as hepatic fibrosis (36, 37), pulmonary fibrosis (38-40), atherosclerosis (41, 42), and cancer (43, 44). Dysregulated ECM synthesis and/or degradation can lead to

altered matrix accumulation, which is the etiologic basis of these pathologies. For example, robustly increased collagen Iα1 secretion by hepatic stellate cells (HSCs) (45), increased crosslinking, and a decrease in enzymatic degradation (46) all characterize hepatic fibrosis. These dynamic ECM changes can initiate and perpetuate disease through multiple mechanisms, including altered tissue biomechanics (i.e. tissue stiffness) (47, 48), increased integrin-mediated cell adhesion (49) and activation of immune cells (50).

## 4. ECM remodeling and the "degradome"

As discussed previously, the ECM always has some level of dynamicity, even under normal conditions, but can undergo more dramatic, rapid changes (i.e. remodeling) during inflammation and disease. Changes in ECM components can occur at all different levels, from protein synthesis to crosslinking or activation. One important means of regulation of ECM components is through proteases (e.g. MMPs). At different stages of liver injury, hepatic stellate cells express and secrete different profiles of proteases and inhibitors (51), as do hepatocytes (52), neutrophils (53), and macrophages (54). These proteases can release cytokines from the matrix (55), but can also release a myriad of other peptides that may or may not be bioactive. The roles of protease degradation products (i.e. the 'degradome') in various diseases are becoming increasingly understood. For example, ECM degradation rate, the production rate of matrix degrading enzymes (MDE), and the conversion of ECM into soluble ECM have been demonstrated to strongly influence tumor growth and morphology (56).

Understanding the role of the ECM degradome in disease is facilitated by modern mass spectrometry methods that allow widespread characterization of the degradome (i.e. peptidomics or ‘degradomics’) (57). Even if degradation products do not play a critical role in disease mechanisms, they may be useful surrogate biomarkers. These peptides are particularly attractive biomarker candidates because they are often secreted into bodily fluids (58, 59). This means that they could be detected using minimally invasive procedures (e.g. blood draw).

## 5. Natural history of liver disease

No matter their etiology, liver diseases share a common natural history that has been thoroughly documented. This natural history is comprised of a spectrum of disease states including earlier stages of fatty accumulation and inflammation, such as steatosis and steatohepatitis, and later stages of disease such as fibrosis and cirrhosis (60, 61). Simple steatosis is the earliest stage of liver disease and is characterized by micro- and macro-vesicular fat accumulation. Steatosis may be reversible with lifestyle modifications or progress to steatohepatitis. Steatohepatitis is characterized by persistent fat accumulation, chronic inflammation, and necrosis (27). Fibrosis and cirrhosis, the later stages of liver disease, are characterized by accumulation of fibrillar collagens and regenerative nodules, respectively (61, 62).

Although there is a great need for and large amount of money spent on liver disease treatment, therapeutic options are palliative at best. Currently there is no

FDA-approved therapy to halt or reverse liver disease progression. A better understanding of mechanisms of disease progression is needed, and new therapeutic targets must be identified if a rational, targeted therapy is to be developed.

## 6. Alcoholic liver disease

The liver is the primary site of alcohol metabolism and therefore the primary target organ of alcohol toxicity. Indeed, after absorption from the small intestine, milli-molar concentrations of ethanol flow through the portal circulation and to the liver for degradation. Ethanol is at least 2-3 times more concentrated in portal blood than in systemic circulation (63). Oxidative metabolism of ethanol in hepatocytes by alcohol dehydrogenase (Adh) and cytochrome P450 2E1 (Cyp2e1) produces toxic intermediate metabolites (e.g., acetaldehyde). Ethanol metabolism also causes a robust increase in the NADH/NAD+ ratio, which creates a more reduced cellular environment. This reduced microenvironment blocks the beta-oxidation of fatty acids and increases fatty acid esterification. The accumulation of excess fatty acids, which are stored in lipid droplets, characterizes steatosis, the earliest stage of alcoholic liver disease (ALD).

Most individuals who consume moderate amounts of alcohol develop steatosis. Steatosis most often has no health consequences, and may even be considered a protective mechanism, as it prevents plasma lipid levels from rising. However, chronic alcohol consumption can cause progression to later stages of ALD, including alcoholic steatohepatitis (ASH), fibrosis, and cirrhosis. Only a

minority of even the heaviest drinkers will develop the most serious stages of ALD. This suggests a 2-hit hypothesis in which progression to later stages of liver disease requires multiple insults, or 'hits' (64, 65). The first 'hit,' such as hepatic steatosis, sensitizes the liver to a second hit such as oxidative stress (65) or inflammatory cytokine signaling (66), both of which are increased by ethanol consumption.

Therefore, alcohol is one of the most commonly recognized causes of liver disease. ALD affects more than 10 million Americans each year with medical costs of more than $166 billion annually (67). There are no targeted therapies for ALD, and current therapy focuses on achieving and maintaining abstinence. Individuals with severe ALD are at risk of such acute alcoholic hepatitis (AH) or cirrhosis (68). These sequelae of ALD have a poor prognosis and limited therapeutic options. Without a successful liver transplant, patients typically die from the effects of decompensation (e.g., hepatorenal syndrome) (69). Additionally, cirrhosis increases the overall risk for hepatocellular carcinoma (HCC) by roughly 20-fold, even in the case of compensated cirrhosis (70). Once the HCC is symptomatic, it is usually unresectable (71). This cancer has a dismal prognosis, with a median survival of less than 6 months and a five year survival of almost nil (71). While the stages of ALD have been well-characterized, targeted therapies to prevent or reverse this process in humans are still needed. Therefore, additional research is needed to improve understanding of risk factors and mechanisms of disease progression and to develop rational therapies to prevent or reverse ALD.

### Alcoholic hepatitis

AH is characterized by severe, acute hepatic inflammation, liver failure, and jaundice (72). It is a sequelae of ALD that typically occurs after many years of heavy alcohol consumption, and it has a high mortality rate (30-50% at 3 months, (73)). Cause of death in AH patients is usually due to multiple organ failure secondary to liver injury (74). AH patients are also at risk of systemic inflammatory response syndrome (SIRS), which is associated with increased mortality (75).

Therapeutic options for AH are limited. Liver transplantation for AH is controversial and is currently not recommended, largely due to organ shortages (76). Current pharmacologic treatment options for AH are limited to corticosteroids or pentoxifylline, although the outcomes from the therapies are poor. The benefits of anti-inflammatory pharmaceuticals only outweigh the risks (e.g. infection) in patients with more severe AH (72). For this reason, assessing AH severity and predicting patient outcome is important.

Predicting outcomes of AH patients is challenging. AH patients typically have an AST/ALT greater than 2, but this measure is neither specific nor sensitive (77). Alternatively, several clinical scoring systems have been developed. The Maddrey discriminant function (DF) is based on serum bilirubin and PT/INR (78) which are independent predictors of short-term mortality in AH (79). The Model for End-Stage Liver Disease (MELD) score similarly utilizes serum bilirubin and INR, but also considers creatinine. MELD has been shown to more accurately

predict short-term mortality in AH compared to DF (80). Other validated scores include ABIC, Glasgow Alcoholic Hepatitis Score, the Child-Turcotte-Pugh score; these have similar prognostic efficiency as MELD (81-83). These models are highly limited in patients with coexisting kidney disease or chronic hemolysis not related to the underlying liver disease (78). Furthermore, scores such as MELD are more limited in predicting outcome of patients with more moderate AH (84).

## 7. Alcohol and the kidney

It is well established that ethanol is both directly toxic to the liver and can sensitize the liver to a second-hit insult. Although the liver is the primary target organ of ethanol toxicity, it is becoming increasingly understood that ethanol has some level of toxicity in other organs, such as the brain, gut, lungs, and pancreas. Chronic, heavy ethanol consumption causes kidney damage secondary to hepatic cirrhosis, a phenomenon known as hepato-renal syndrome. Moderate alcohol consumption, however, is currently not considered a risk factor for chronic kidney disease. Furthermore, population based studies have shown moderate alcohol consumption to be inversely associated with kidney injury (85). However, the direct renal effects of chronic moderate EtOH consumption and sensitization to secondary hits are unclear. Rodent studies have identified several mechanisms of alcohol-induced kidney injury that parallel those observed in the liver (86-88). These investigations have been driven by the hypothesis that alcohol affects the kidneys similarly to the liver. It certainly is not surprising that these parallel mechanisms have been confirmed, considering similarities

between these two organs, such as the expression of *CYP2E1* (86). However, it is certainly possible that ethanol affects the kidneys by mechanisms that do not parallel those in the liver. Therefore, further investigation into the effects of ethanol on the kidneys is needed. Additionally, it is not known whether ethanol exposure alters renal response to a second inflammatory 'hit', as has been observed in the liver.

### 8. Statement of goals

It is well established that ethanol is toxic to the liver, and the natural history of ALD is well characterized. However, there are no targeted therapies to halt or reverse liver disease. Development of such therapies requires a better understanding of mechanisms of disease progression as well as identification of novel drug targets. Therefore, one goal of this dissertation is to shed new insight into mechanisms of progression of ALD. In contrast to the liver, the effects of ethanol on the kidneys are largely unknown. Therefore, another goal of this dissertation is to elucidate mechanisms by which ethanol affects the kidneys. Taken together, the goal of this dissertation is to examine new potential mechanisms by which ethanol affects the liver and kidneys.

## B. Aims and proposals

### 1. Characterization of alcohol-induced matrisome changes in liver

As discussed in earlier sections, the role of the ECM in later stages of liver disease (i.e., fibrosis) is well established. Previous studies from our group and others have also demonstrated changes in the ECM in early liver disease, prior to fibrogenesis (89-91). These studies suggest that these transitional ECM changes may play an important role in the sensitization of the liver to insult. While several matrix proteins have been implicated as players in liver injury and inflammation (i.e., fibrin, fibronectin), this is only a small portion of the >1000 known ECM related proteins (92). Indeed, other ECM proteins likely also contribute to hepatic injury. Identification of new ECM proteins that ethanol exposure alters would help elucidate mechanisms of ALD progression. There are likely changes in the hepatic ECM that have not yet been identified, due to the insolubility of matrix proteins that makes them difficult to extract and analyze. A limitation of previous studies focused on the role of the ECM in ALD is that they generally studied changes in one ECM protein at a time and did not consider structural changes that may accompany altered ECM protein turnover. Additionally, the study of alterations to the hepatic ECM has primarily been hypothesis-driven, which limits the discovery of novel potential players. This study couples a serial extraction method that allows solubilization and enrichment of tightly cross-linked proteins with LC-MS/MS analysis. This approach allows analysis of global changes in the hepatic ECM.

## 2. Novel biomarkers in alcoholic hepatitis: analysis of the plasma peptidome/degradome

AH is characterized by acute liver inflammation and liver failure. It was hypothesized that this inflammation would involve transitional remodeling of the hepatic ECM, and that this remodeling would cause the accumulation of ECM degradation products (peptides) in the blood. Therefore, the plasma peptidome in AH patients was analyzed. This builds upon the work in Aim 1 of this dissertation, which will demonstrated that the hepatic ECM undergoes significant remodeling during inflammatory liver injury (93). This remodeling involves protease cleavage of ECM proteins, which yields ECM peptide fragments (94). During remodeling, peptide fragments of the degraded ECM have been shown to increase in biologic fluids (e.g. plasma) (58, 59). Peptidomic analysis of the degraded ECM (i.e., 'degradome) has been identified as a useful diagnostic/prognostic tool in other diseases of ECM remodeling, such as chronic obstructive pulmonary disease (COPD) (58) and metastatic cancers (59). Current methods of predicting AH outcome (i.e. clinical scores, e.g. MELD) are limited in their abilities to predict at-risk patients with moderate disease (84). Therefore, the purpose of this study was to test the hypothesis that the severe inflammatory liver injury caused by AH would yield a unique degradome profile in patient plasma. This was done using a peptidomic workflow analysis of plasma from healthy participants or AH patients. This is expected to reveal unique patterns of ECM peptides or 'features' across different severity groups of AH patients This analysis lays the groundwork for further studies investigating the plasma ECM degradome as potential surrogate or mechanistic biomarkers for

AH patient outcome. The characterization of the AH plasma degradome also supports future mechanistic studies on the role of ECM remodeling in AH.

### 3. Pathways affected by alcohol in the kidney

The effects of ethanol consumption on the kidneys are poorly understood in contrast to the liver. Some human studies have reported benefits of chronic moderate EtOH consumption for preservation of renal function (85, 95). However, the small number of rodent studies on the effects of ethanol on the kidneys have reported that chronic ethanol consumption upregulates Cyp2e1 (88), causes neutrophil infiltration (88), and increases acetylation of mitochondrial proteins (86) in the kidney. However, these previous studies have been limited by the hypothesis that ethanol affects the kidneys by mechanisms parallel to those in the liver. It was hypothesized that there are additional mechanisms by which ethanol affects the kidneys that do not necessarily parallel mechanisms in the liver. Aim 3 of this dissertation tests this hypothesis using a discovery-based proteomic and transcriptomic approach to discover novel players and pathways affected by ethanol and LPS in the renal cortex.

## Overall aim of this dissertation.

The overall aim of this dissertation is to provide new insight into mechanisms of alcohol-induced organ injury. To this end, a novel method of analyzing the hepatic matrisome will be used to determine the effects of chronic, moderate ethanol consumption and acute inflammation on the hepatic matrisome in mice

(Aim 1). Next, ECM degradome (peptidome) in AH patient plasma will be analyzed (Aim 2), allowing for future investigation into the use of plasma ECM peptides as surrogate or mechanistic biomarkers. Finally, a discovery based ‘omics approach will be used to elucidate the effects of ethanol consumption on the kidneys (Aim 3). Taken together, this work will shed new mechanistic insight into alcohol-induced organ injury.

# CHAPTER II

# EXPERIMENTAL PROCEDURES

## A. Animals and exposures

Animal experiments were carried out by the Arteel laboratory. Mice were housed in a pathogen-free barrier facility accredited by the Association for Assessment and Accreditation of Laboratory Animal Care, and procedures were approved by the University of Louisville's Institutional Animal Care and Use Committee.

### 1. Animal sacrifice, tissue collection and storage

At time of sacrifice, animals were anesthetized with ketamine/xylazine (100/15 mg/kg, intraperitoneally (i.p.)). Blood was collected from the vena cava just before sacrifice. Citrated plasma was stored at -80 ºC for further analysis. Portions of liver and renal cortex tissue were snap-frozen in liquid nitrogen, fixed in 10% neutral buffered formalin for subsequent sectioning and mounting on microscope slides, or frozen-fixed in Tissue Tek OCT-Compound (Sakura Finetek, Torrance, CA).

### 2. Carbon tetrachloride model of hepatic fibrosis

Male (4-6 weeks old) C57BL6/J mice were purchased from Jackson Laboratory (Bar Harbor, ME). Mice were injected with $CCl_4$ (1 mL/kg i.p.; diluted 1:4 in olive oil; Sigma-Aldrich, St. Louis, MO) or vehicle twice a week for 4 weeks (96).

**3. Chronic model of alcohol exposure**

Male (8 weeks old) C57BL6/J mice were purchased from the Jackson Laboratory (Bar Harbor, ME). Mice were given ethanol-containing Lieber-DeCarli diet (Dyets, Inc.) *ad libitum* or pair-fed isocaloric/isovolumetric maltose-dextrin control diet (97). During the exposure period, animals were housed in pairs in shoebox cages in a room held at 75 °F. Diet was provided in vacuum tubes and replaced between 4 and 5 pm daily. Both ethanol-fed animals and their pair-fed counterparts received control diet for the first two days of liquid diet feeding to allow acclimation to the liquid diet feeders. After 2 days of acclimation, ethanol concentrations increased incrementally over the course of three weeks before reaching the highest ethanol concentration, 6% (vol/vol) for the final three weeks of exposure. Ethanol concentrations in the ethanol-containing diets were as follows: 0% for two days of acclimation, 1% for two days, 2% for two days, 4% for one week, 5% for one week, and 6% for three weeks. Ethanol-containing diet was provided *ad libitum* for the entire course of the study. Because of the relatively high caloric content of ethanol, pair-fed control animals received an iso-caloric control diet; the calories in the iso-caloric diet were matched by adding a calorie-equivalent of maltose-dextrin. To account for the reduced food

consumption of ethanol-fed mice, pair-fed mice were given the volume of diet consumed by their ethanol-fed counterparts the night before. At the conclusion of the feeding period, the two diet groups were further separated into additional groups that received either LPS (*Escherichia coli*; 10 mg/kg i.p. Sigma, St. Louis, MO) or vehicle (saline). Animals were euthanized 4 or 24 h after LPS (or vehicle) injection (97). 6 control mice, 5 ethanol mice, 6 24-h LPS mice, and 4 ethanol+24h LPS mice were used for the hepatic matrisome analysis. 3 control mice, 3 ethanol mice, 3 4h LPS mice, and 3 ethanol+4h LPS mice were used for the renal cortex proteomic and transcriptomic analyses. The same mice were used for the renal cortex proteomics and transcriptomics, except for 1 4h LPS mouse and 1 ethanol+4h LPS mouse that were different.

**4. Chronic+binge model of alcohol exposure**

Male (10 weeks old) C57BL6/J mice were purchased from the Jackson Laboratory (Bar Harbor, ME). Mice were exposed to ethanol as described by Bertola et al. (98). During the exposure period, animals were housed in pairs in shoebox cages in a room held at 75 °F. Diet was provided in vacuum tubes and replaced between 4:00 and 5:00 PM daily. Animals were acclimatized to control (0% EtOH) Lieber-DeCarli liquid diet (Dyets, Inc., Bethlehem, PA) for 5 days. Mice were then split into two groups fed ethanol-containing (5% v/v) or iso-caloric control liquid diet for 10 days. To account for the reduced food consumption of ethanol-fed mice, pair-fed mice were given the volume of diet consumed by their ethanol-fed counterparts the night before. On day 11, mice received ethanol (5

g/kg) or iso-caloric maltose dextran binge via oral gavage. Mice were sacrificed 9 hours post-gavage. Tissues were collected as described in section A1.

## B. Proteomics

### 1. 3-step ECM extraction

Sequential extraction of the hepatic ECM was performed as described by de Castro Bras et al. for heart tissue (99), with minor modifications for liver. Sample preparation and wash. Snap frozen liver tissue (75-100 mg) was immediately added to ice-cold phosphate-buffered saline (pH 7.4) wash buffer containing commercially available protease and phosphatase inhibitors (Sigma Aldrich) and 25 mM EDTA to inhibit proteinase and metalloproteinase activity, respectively. While immersed in wash buffer, liver tissue was diced into small fragments using a scalpel. The diced sample was washed 5 times to remove contaminants. Between washes, samples were pelleted by centrifugation (12,000×g, 5 min), and wash buffer was decanted.

NaCl extraction. Diced samples were incubated in 10 volumes of 0.5 M NaCl buffer, containing 10 mM Tris HCl (pH 7.5), proteinase/phosphatase inhibitors, and 25 mM EDTA. The samples were mildly mixed on a plate shaker (800 rpm) overnight at room temperature. The following day, the remaining tissue pieces were pelleted by centrifugation (10,000×g for 10 min). The pellet was used for the SDS extraction (see below). The supernatant was collected and desalted using ZebaSpin columns (Pierce) according to manufacturer's instructions. To precipitate proteins, desalted supernatant was incubated with 5x

supernatant volume of 100% acetone overnight at -20 °C, centrifuged (16,000×g, 45 min), and dried in a rotary evaporator. Proteins were resuspended in deglycosylation buffer. SDS extraction. The pellet from the NaCl extraction was subsequently incubated in 10 volumes (based on original weight) of 1% SDS solution, containing proteinase/phosphatase inhibitors and 25 mM EDTA. The samples were mildly mixed on a plate shaker (800 rpm) overnight at room temperature. The following day, the remaining tissue pieces were pelleted by centrifugation at 10,000×g for 10 min. The pellet was used for the GnHCl extraction (see below). The supernatant was collected and desalted using ZebaSpin columns (Pierce) according to manufacturer's instructions. To precipitate proteins, desalted supernatant was incubated with 5× supernatant volume of 100% acetone overnight at -20 °C, centrifuged (16,000×g, 45 min), and dried in a rotary evaporator. Proteins were resuspended in deglycosylation buffer. Guanidine HCl extraction. The pellet from the SDS extraction was incubated with 5 volumes (based on original weight) of a denaturing guanidine buffer containing 4 M guanidine HCl (pH 5.8), 50 mM sodium acetate, 25 mM EDTA, and proteinase/phosphatase inhibitors. The samples were vigorously mixed on a plate shaker at 1200 rpm for 48 hours at room temperature; vigorous shaking is necessary at this step to aid in the mechanical disruption of ECM components. The remaining insoluble components were pelleted by centrifugation at 10,000×g for 10 minutes. This insoluble pellet was retained and solubilized as described below. To precipitate proteins, the supernatant was mixed with 6× supernatant volume of 100% ice cold ethanol overnight at 20 °C,

centrifuged (16,000×g, 45 min), and washed with 90% ethanol. Pellets were dried in a rotary evaporator and resuspended in deglycosylation buffer.

Deglycosylation and solubilization. The supernatants from each extraction were dried in a rotary evaporator and resuspended in deglycosylation buffer containing 150 mM NaCl, 50 mM sodium acetate, 10 mM EDTA, and proteinase/phosphatase inhibitors. Resuspended samples were desalted using ZebaSpin columns (Pierce) according to manufacturer's instructions. The desalted extracts were then mixed with 5 volumes of 100% acetone and stored at -20°C overnight to precipitate proteins. The precipitated proteins were pelleted by centrifugation at 16,000×g for 45 minutes. Acetone was evaporated by vacuum drying in a rotary evaporator for 1 hour. Dried protein pellets were resuspended in 500 µL deglycosylation buffer containing 150 mM NaCl, 50 mM sodium acetate, pH 6.8, 10 mM EDTA, and proteinase/phosphatase inhibitors that contained chondroitinase ABC (*P. vulgaris*; 0.025 U/sample), endo-beta-galactosidase (*B. fragilis*; 0.01 U/sample) and heparitinase II (*F. heparinum*; 0.025 U/sample). Samples were incubated overnight at 37°C. 20 uL DMSO was added to the insoluble fraction (pellet from guanidine HCl extraction) to aide in solubilization. Protein concentrations were estimated by absorbance at 280 nm using bovine serum albumin (BSA) in deglycosylation buffer for reference standards.

### 2. Total protein extraction

This extraction was carried out in the Merchant laboratory. Proteins were extracted from snap frozen renal cortex tissue using lysis buffer (1:1 w/v) containing 10% glycerol, 50 mM HEPES, 100 mM KCl, 2 mM EDTA, 0.1% Nonidet p-40 (NP-40), 2 mM DTT, 10 mM NaF, 0.25 mM $NaVO_3$, and 1x Halt Protease and Phosphatase Inhibitor Cocktail (ThermoFisher). Samples were placed in a sonication bath for 5 minutes, incubated on ice for 1 hour, and centrifuged at 12,000×g for 30 minutes. Extract was removed from insoluble matter. Protein concentrations were assayed using standard Bradford assay with BSA for reference standards.

### 3. Sample cleanup and preparation for liquid chromatography and mass spectrometry

Liver ECM extracts in deglycosylation buffer were pooled by experimental group and subsequently analyzed by the University of Louisville Proteomics Biomarkers Discovery Core (PBDC). At the PBDC, samples in deglycosylation buffer were thawed to room temperature and clarified by centrifugation at 5,000xg for 5 min at 4°C. 50 µL (25 µg) of each sample were reduced by adding 5.55 µL of 1 M DTT and incubating at 60°C for 30 min. 144.45 µL of 8 M urea in 0.1 M Tris-HCl, pH 8.5, was added to each sample. Each reduced and diluted sample was digested with a modified Filter-Aided Sample Preparation (FASP) method developed by Jacek R. Wisniewski, et al. (100). Recovered material was dried in a rotary evaporator and redissolved in 200 µL of 2% (v/v) acetonitrile (ACN)/0.4% formic acid (FA). The samples were then trap-cleaned with a C18

PROTO™ 300Å Ultra MicroSpin Column (The Nest Group, Southborough, MA). The sample eluates were stored at -80°C for 30 min, dried in a rotary evaporator, and stored at -80°C. Before liquid chromatography, dried samples were warmed to room temperature and dissolved in 2% (v/v) ACN/0.1% FA to a final concentration of 0.25 µg/µL. 16 µL (4 µg) of sample was injected into the Orbitrap Elite.

Renal cortical proteins (100µg) were digested using a FASP protocol (100) to remove NP-40 detergent used for sample preparation. Proteomic analysis of tissue lysates was conducted as previously described (101) with the following modifications. Proteins were digested with Lys-c (Promega #V167A) and trypsin (Promega #V5111), each at a 1:100 w/w enzyme:protein ratio. Peptides were desalted using HLB extraction (Waters Oasis HLB 1cc, WAT094225) (102). 50 µg peptide were dried and resuspended in 100µL 100mM triethylammonium bicarbonate (TEABC). Peptide concentrations were measured using an A205 nm assay with an external peptide standard curve.

**4. TMT labeling**

Tandem mass tag (TMT) 10-plex labeling (Thermo 90111) of renal cortical digests was carried out according to manufacturer's instructions. 50 µg peptide in 100 µL 100 mM TEABC were added to each label tube. Labeled samples were admixed, dried, and resuspended in 800 µL 0.1% v/v FA. Peptide concentrations were measured using an A205 nm assay with an external peptide standard curve. 200 µg peptide were fractionated by strong cation exchange

using 30-300 µg capacity SCX MacroSpin Columns (SMM HIL-SCX.25, Nest Group, Inc. Southborough, MA, USA) according to manufacturer's instructions. Sample cleanup was performed using C18 PROTO, 300 Å Ultra Microspin Columns (Nest Group, Inc., Southborough, MA, USA).

**5. Liquid chromatography and tandem mass spectrometry**

At the PBDC, liver digest samples were separated on a Dionex Acclaim PepMap 100 75 µm x 2 cm nanoViper (C18, 3 µm, 100 Å) trap and Dionex Acclaim PepMap RSLC 50 µM x 15 cm nanoViper (C18, 2 µm, 100 Å) separating columns. An EASY n-LC (Thermo, Waltham, MA) UHPLC system was used with buffer A = 2% (v/v) ACN/ 0.1% (v/v) FA and buffer B = 80% (v/v) ACN / 0.1% (v/v) FA as mobile phases. Following injection of the sample onto the trap, separation was accomplished with a 140 min linear gradient from 0% B to 50% B, followed by a 30 min linear gradient from 50% B to 95% B, and lastly a 10 min wash with 95% B. A 40 mm stainless steel emitter (Thermo, Waltham, MA; P/N ES542) was coupled to the outlet of the separating column. A Nanospray Flex source (Thermo, Waltham, MA) was used to position the end of the emitter near the ion transfer capillary of the mass spectrometer. The ion transfer capillary temperature of the mass spectrometer was set at 225°C, and the spray voltage was set at 1.6 kV.

An Orbitrap Elite – ETD mass spectrometer (Thermo) was used to collect data from the LC eluate. An Nth Order Double Play with ETD Decision Tree method was created in Xcalibur v2.2. Scan event one of the method obtained an

FTMS MS1 scan for the range 300-2000 m/z. Scan event two obtained ITMS MS2 scans on up to ten peaks that had a minimum signal threshold of 10,000 counts from scan event one. A decision tree was used to determine whether collision induced dissociation (CID) or electron transfer dissociation (ETD) activation was used. An ETD scan was triggered if any of the following held: an ion had charge state 3 and m/z less than 650, an ion had charge state 4 and m/z less than 900, an ion had charge state 5 and m/z less than 950, or an ion had charge state greater than 5; a CID scan was triggered in all other cases. The lock mass option was enabled (0% lock mass abundance) using the 371.101236 m/z polysiloxane peak as an internal calibrant.

TMT-labeled renal cortex tryptic digest SCX fractions underwent 1D-LC-MS/MS analysis using a Proxeon EASY-nLC 1000 UHPLC and nanoelectrospray ionization into an Orbitrap Elite mass spectrometer (Thermo) using a transfer capillary temperature set of 225°C and the spray voltage of 1.6kV. An Nth Order Double Play method was used with scan event one. An FTMS MS1 scan (normal mass range; 60,000 resolution; full scan type) for the 400-2000 m/z range was used, with charge state screening and monoisotopic precursor selection enabled. Charge state rejection was enabled for unassigned charge states and +1 charge states. The lock mass option was enabled (0% lock mass abundance) using the 445.120028 m/z polysiloxane peak as an internal calibrant. Scan event two obtained HCD FTMS MS2 scans (normal mass range; 60,000 resolution; centroid data type) on up to twelve peaks that had a minimum signal threshold of 5,000 counts from scan event one. Dynamic exclusion was enabled

with a repeat count of one, a repeat duration of 60 seconds, an exclusion list size of 500, an exclusion duration of 60 seconds, and an exclusion mass width of ±0.001% relative to reference mass (93).

**6. Informatics**

The hepatic ECM mass spectrometry data were analyzed at the University of Louisville PBDC using Proteome Discoverer v1.4.0.288. The database used in Mascot v2.4 and SequestHT searches was the 6/2/2015 version of the UniprotKB *Mus musculus* reference proteome canonical and isoform sequences. +57 on C (Carbamidomethylation) was selected as a fixed modification, and +1 on N (Asn->Asp) and +16 on MP (Oxidation) were selected as variable modifications. A maximum of two missed cleavages were allowed. A Target Decoy PSM Validator node was included in the Proteome Discoverer workflow in order to estimate the false discovery rate (FDR).

The Proteome Discoverer analysis workflow allows for extraction of MS2 scan data from the Xcalibur RAW file, separate searches of CID and ETD MS2 scans in Mascot and Sequest, and collection of the results into a single file (.msf extension). The resulting .msf files from Proteome Discoverer were loaded into Scaffold Q+S v4.3.2. Scaffold was used to calculate the FDR using the Peptide and Protein Prophet algorithms. Protein identification probability of the sequences was set to >95% on the software. The results were annotated with mouse GO information from the Gene Ontology Annotations Database.

Renal cortex mass spectrometry data were analyzed at the University of Louisville PBDC using Proteome Discoverer v1.4.0.288 and Scaffold Q+S v4.3.2 with the 6/2/2014 version of the UniprotKB *Mus musculus* reference proteome canonical and isoform sequences. A Target Decoy PSM Validator node was used to control the FDR and a Reporter Ions Quantifier node was included for quantification of the TMT reporter ions considering TMT purity correction factors obtained from the manufacturer. Intensity based normalization of reporter ions was achieved using the mean calculation type, modeled on unique peptides, and using an average protein reference. Scaffold was used to calculate the FDR using the Peptide and Protein Prophet algorithms.

## C. Immunoblots

### 1. Dot blot

Liver samples from the chronic EtOH model were homogenized in radioimmunoprecipitation assay (RIPA) buffer containing protease and phosphatase inhibitor cocktails (Sigma; St. Louis, MO). 10 µg protein in 100 µl RIPA buffer were loaded onto nitrocellulose membranes (GE Healthcare) using a vacuum-assisted microfiltration system (Bio-Dot; Bio-Rad, Hercules, CA). The membrane was blocked for one hour with 5% non-fat milk in TBST. Primary antibodies against collagen type I α1 (Meridian T40777R) and GAPDH (Santa Cruz SC-25778) were used. Densitometric analysis was performed using UN-SCAN-IT gel (Silk Scientific Inc., Orem, Utah) software.

### 2. Western blot

Renal cortex immunoblot was carried out as described previously (103) using a primary antibody against Cat (Cell Signaling D5N7V). Densitometry of exposed film was analyzed using the ImageJ software (ImageJ, NIH, http://rsb.info.nih.gov/ij/).

## D. Transcriptomics

### 1. RNA isolation

Snap frozen renal cortex sections were stored at -80° C and then incubated in RNAlater-ICE (Life Technologies, Carlsbad, CA) at -20° C for 72 hours prior to RNA extraction. RNA was isolated using the mirVana kit (Life Technologies, Carlsbad, CA) according to manufacturer's instructions for total RNA isolation. RNA quality was evaluated by Nanodrop ND-1000 (Thermo Fisher Scientific, Grand Island, NY) and Agilent 2100 Bioanalyzer (Agilent, Santa Clara, CA) analysis. Ribosomal depletion was carried out at the University of Louisville Center for Genetics and Molecular Medicine (CGeMM) prior to RNA seq analysis.

### 2. RNA sequencing

RNA libraries were prepared using the TruSe Stranded Total RNA LT sample preparation Kit- Set A with Ribo-Zero Gold. Sequencing was performed on the University of Louisville CGeMM's Illumina NextSeq 500/550 75 cycle High Output Kit v2.

### 3. RNASeq data analysis

RNA Seq data were analyzed at the University of Louisville CGeMM using the Tuxedo suite data analysis pipeline. Differentially expressed transcripts were identified by filtering by analysis of variance (ANOVA) p-value cutoff ($p<0.05$), a more stringent Benjamini-Hochberg (BH) q-value cutoff ($q<0.01$) and FC cutoffs of 1.2 (to explore pathways analysis) and 2 (to address larger changes in RNA expression).

## E. Histology and Immunohistochemistry

### 1. Histology

In the Arteel laboratory, paraffin-embedded, formalin fixed liver sections from the $CCl_4$ study were stained with Sirius Red/Fast Green to visualize fibrosis (96).

Paraffin-embedded, formalin fixed renal cortex sections from the chronic EtOH study were periodic acid-Schiff (PAS) stained (103) in collaboration with Dr. Michelle Barati. Blinded histology was reviewed by a fellowship-trained, board certified pathologist. It was determined that there were no differences between groups, and so staining was not quantified.

### 2. Immunohistochemistry

In collaboration with Dr. Michelle Barati, immunohistochemistry (IHC) was carried out on renal cortex sections using a primary antibody against myeloperoxidase (Mpo, Abcam ab9535) and catalase (Cat, Cell Signaling

D5N7V) (103). Mpo staining was quantified as average number of Mpo positive cells per visual field (40x) with an average number of 33 ± 4 visual fields per kidney section. An n of 3 samples in each experimental group were analyzed. Differences between groups were determined by 2-way ANOVA and post-hoc t-tests.

## F. Clinical chemistry

### 1. Blood urea nitrogen analysis

Blood urea nitrogen (BUN) in mouse plasma from the chronic and chronic+binge EtOH studies was measured using the Urea Assay Kit (Abnova KA1652) according to manufacturer's instructions.

## G. Clinical study

### 1. Study participants

Plasma samples and clinical data from the following study were provided through collaboration with Dr. Craig McClain and Dr. Vatsalya Vatsalya. This study was approved by the Institutional Review Boards at all the participating centers. This study was a part of a large national multisite clinical trial indexed at clinicaltrials.gov: NCT01922895 and NCT01809132. All moderate and severe AH patients were enrolled at the University of Louisville, the University of Massachusetts Medical School, the University of Texas-Southwestern and the Cleveland Clinic. All AUD ("mild") patients were enrolled at NIAAA, NIH. All healthy volunteers were recruited at the Louisville site. All AH patients were

diagnosed using clinical and laboratory criteria described by the NIAAA consortium on AH (104). Individuals with or without liver injury met the criteria for AUD based on DSM 4 XR or DSM 5 manual. All healthy participants were free of any clinically diagnosed disease (liver or organ systems) that might contribute to altered laboratory values in comparison analyses. All patient specimens and data were analyzed at the University of Louisville.

**2. Inclusion criteria**

Eligible participants were 21 years old or older. The following individuals were ineligible for participation 1) those unwilling or unable to provide informed consent; and/or 2) those who had significant comorbid conditions (heart, kidney, lung, neurological or psychiatric illnesses, sepsis) and/or active drug abuse; and/or 3) pregnant/lactating women; and/or 4) prisoners or other vulnerable persons.

**3. Study paradigm**

112 adult male and female individuals participated in this NIH-funded study. This investigation was a single time point assessment of patients between the study cohorts. The cohorts included healthy participants (n=7), patients with AUDs (“mild” , MELD<12; n=45), patients with “moderate” AH (MELD=12-19; n=23), patients with “severe” AH (>19; n=37). The mild/AUD group was both analyzed as whole and also as sub-groups without liver injury (“mild-A”, serum alanine aminotransferase (ALT)<40, n=14) and with liver injury (“mild-B”,

ALT≥40, n=31). Informed consent was obtained from all study participants before collection of data and bodily samples. Clinical data, relevant medical history, measures of severity of ALD, and drinking history [using the Alcohol Use Disorders Identification Test (AUDIT) (105) (only in moderate and severe AH patients) and lifetime drinking history (LTDH) in all AH and AUD patients (106) were collected. The study was designed to analyze plasma peptides for comparison between healthy volunteers, AUD patients (with or without liver injury), patients with moderate AH, and patients with severe AH for potential associations between parameters. All data collected from the enrolled study participants were de-identified, coded, and analyzed.

**4. Collection of clinical data**

Clinical data include participant demographics [age, sex, body mass index (BMI)], drinking history (AUDIT and LTDH), medical assessments at admission (after obtaining consent, specific for the study to exclude any condition that might affect liver tests), and medical history. Confirmatory tests for AH (laboratory and imaging), and markers of liver disease severity [Child-Turcotte-Pugh (CTP), MELD, Maddrey DF] were also obtained. Laboratory tests included a comprehensive metabolic profile with indices of liver injury [including serum ALT), aspartate aminotransferase (AST), total bilirubin (Tbili)] and coagulation.

**5. Plasma collection**

Blood samples were collected from each study participant following consent. Blood was collected in lavender- top Vacutainer tubes containing K3 EDTA. Blood was separated by centrifugation, and plasma was apportioned into 1 mL aliquots and stored at -80 °C until use. Freeze-thaw cycles were avoided to maintain the integrity of the plasma.

## H. Peptidomics

### 1. Peptidomic workflow optimization

During workflow optimization, peptides were purified by ACN precipitation. 100 µL plasma were acidified with 100 µL 10% v/v acetic acid. To precipitate proteins and impurities, 600 µL 99.9% v/v ACN / 0.1% v/v trifluoroacetic acid was added to each sample, on ice. Samples were vortexed for 30 seconds, and precipitate was pelleted by centrifugation at 15,000 × g for 15 minutes at 4 °C. Pellets were discarded. Supernatants were collected and centrifuged again as before. Again, supernatants were collected, and pellets were discarded.

Samples underwent cleanup and LC-MS/MS analysis as described in sections 3 and 4. The LC-MS/MS analysis determined that the purity of the peptide samples was unsatisfactory for the relative quantification of peptide abundance. For this reason, the ACN precipitation method was abandoned. The trichloroacetic acid (TCA) precipitation approach developed by Parker et al, described below, was adopted (107). Parker et al. demonstrated that TCA precipitation yields more peptides compared to ACN precipitation, acetone precipitation, and size-exclusion 10 kDa MWCO filtration.

## 2. Plasma peptide purification

To avoid systematic bias, the plasma samples were handled as four sample flights (flight 1-4), each composed of balanced proportions of all groups with the sample order interwoven into a randomized fashion. Total plasma peptides were purified by TCA precipitation based on Parker et al. (107). 100 µL PBS with K3 EDTA was added to 100 µL plasma. Samples were mixed and incubated at RT for 5 minutes. Samples were placed on ice, and 200 µL 20% w/v TCA (prechilled to 4 °C) were mixed into each sample. Samples were allowed to incubate for 1 hour on ice. Precipitate was pelleted by centrifugation at 16,000 × g for 10 minutes at 4 °C; pellets were discarded. Supernatant collection, centrifugation and discarding of pellets was repeated twice to ensure efficient removal of high molecular weight proteins.

## 3. Peptide sample cleanup and preparation for liquid chromatography and mass spectrometry

275 µL of each sample was desalted and concentrated using solid phase extraction (Waters Oasis HLB µElution 30 µm plate, part no. 186001828BA) as previously described by Keshishian, et al. (102). Solid phase extraction eluates were dried in a rotary evaporator, and dried peptides were resuspended in 25 µL 2% v/v ACN/ 0.1% v/v FA. Peptide concentrations were measured by absorbance at 250 nm.

### 4. Liquid chromatography and tandem mass spectrometry

A high mass accuracy approach was used for relative quantification of plasma peptides isolated from AH patients, AUD patients with and without liver injury, and healthy volunteers plasma samples using a label-free approach. Peptides were prepared to a concentration of 0.1 µg/µL in 2% v/v ACN/ 0.1% v/v FA. A commercial mixture of 11 synthetic peptides (iRT1-11, Biognosis USA, Beverly, MA) eluting across the chromatographic retention time spectrum were spiked into each sample following peptidome resuspension. Peptides were separated by reverse phase chromatography on a Proxeon EASY-nLC 1000 UHPLC system. 2 µL (0.2 µg) of each peptide sample was injected in random order. The trap column used was a 75µm i.d. x 2cm Acclaim PepMapTM 100 nanoViper cartridge packed with C18, 3µm, 100Å material(Thermo); the separating column used was a 75µm i.d. x 50cm Acclaim PepMap RSLC nanoViper column packed with C18, 2µm, 100Å material (Thermo). The separation was performed with a gradient of solvent A = 2% v/v ACN / 0.1% v/v FA and solvent B = 80% v/v ACN / 0.1% v/v FA. After loading the sample onto the trap for 6min at 2µL/min in solvent A, the sample was eluted and separated at 250nL/min with a gradient from 0% to 55% solvent B over 165min. Following the gradient, the columns were washed at 300nL/min for 10min with 95% solvent B and then returned to initial conditions.

Liquid chromatography eluate was analyzed with an Orbitrap Elite mass spectrometer with nanoelectrospray ionization. An Nth Order Double Play was created in Xcalibur v2.2. Scan event one of the method obtained an FTMS MS1

scan (normal mass range; 240,000 resolution, full scan type, positive polarity, profile data type) for the range 300-2000m/z. Scan event two obtained ITMS MS2 scans (normal mass range, rapid scan rate, centroid data type) on up to twenty peaks that had a minimum signal threshold of 5,000 counts from scan event one. The lock mass option was enabled (0% lock mass abundance) using the 371.101236m/z polysiloxane peak as an internal calibrant.

## I. Informatics

### 1. Liver ECM proteomic data analysis

Hepatic protein enrichment was quantified using total ion current (TIC). Within Scaffold, proteins were filtered for extracellular GO annotation. The NaCl, SDS, GnHCl, and pellet fractions contained 89, 63, 84, and 46 extracellular proteins, respectively. Additional analysis was only performed on these proteins that were classified as extracellular by GO annotation. The extracellular proteins were further categorized into four classes based on their role in the extracellular space as determined by a comprehensive literature search. These four ECM groups include class 1) glycoproteins and proteoglycans, class 2) other ECM-associated proteins, class 3) proteases and protease inhibitors, and class 4) collagens. If no record could be found supporting the hypothesis that a protein was associated with the ECM, the protein was placed into (5), other proteins.

### 2. Renal cortex proteomic data analysis

Renal cortex data were filtered by BH corrected ANOVA p-value <0.05 and fold change (FC) ≥ 1.2. Ingenuity Pathways Analysis (IPA) was used to identify pathways changed by EtOH, LPS, and/or the combination. The PANTHER web application was used to identify statistically overrepresented GO cellular compartments in groups of proteins that were significantly regulated by EtOH, LPS, and EtOH + LPS compared to control. The statistical overrepresentation test was carried out for (A) GO cellular component complete, (B) within each cellular compartment, and (C) for GO biological process complete and with Bonferroni correction using default settings.

### 3. Multivariate analysis of renal cortex proteomic and transcriptomic data sets

Hierarchical clustering of the top-20 GO biological process terms for the proteomic and the transcriptomic data sets were conducted using the Heatmapper web application (www.heatmapper.ca). Data were clustered using an average linkage method and a Spearman Rank Correlation distance measurement method.

### 4. AH plasma peptidome data analysis

Peptide spectra collected in a data dependent fashion were interpreted using a de novo spectrum assignment approach that enabled shotgun analysis of peptide post-translational modification. The AUC for high resolution extracted ion chromatograms were used as a label-free relative quantification of the peptide

abundances. Quantitative and qualitative feature data were extracted and analyzed using PEAKS Studio (v8.5). Data were normalized to TIC. The following data analysis was done in collaboration with Dr. Shesh Rai and Dr. Sudhir Srivastava. There were 1730 peptides initially. In each group, a peptide was discarded if all observations were missing. Therefore, peptides having at least one observation across all samples in each group were retained for further analysis. After this filtering, 1273 peptides remained. Data were normalized by taking log base 2 of raw data followed by quantile normalization using "normalize.quantiles" function (108) available in R package "preprocessors". Missing values were imputed using the "SVD" (109) method under the assumption of MAR. The R package "imputeLCMD" was used for imputing the missing values. We used the imputed data for further analysis (see section J2).

## J. Statistics

### 1. Statistical analysis of liver ECM proteomic data

Heat maps were compiled in the Arteel laboratory by Dr. Shanice Hudson in the open-source statistical programming language R (R Development Core Team. R: A language and environment for statistical computing.Vienna, Austria: R Foundation for Statistical Computing, 2008.). ECM proteome output as $Log_2$ FC of control was analyzed with the *heatmap.2* function of the *gplots* package, using the methods described by Key et al. (110) Pearson's correlation coefficient was used to measure distance, and the Ward method (*ward.D*) was the agglomeration method for row and column clustering. In addition, protein

distribution patterns across the four treatment groups were clustered using hierarchical clustering (function *hclust* within R package cluster) (Cluster analysis basics and extensions: R package version [computer program]. Version 1.15.3 2014). Patterns were clustered separately for each fraction, and the optimal number of clusters was determined using a combination of statistical measures (R package *clValid*) (Brock G, Pihur V, Datta S, Datta S. clValid: An R package for cluster validation. Journal of Statistical Software 2008;25:1-22.) and biological interpretability. Since interest was in the pattern of abundance across the treatment groups, abundance values for each protein were standardized to mean zero and standard deviation one for each protein prior to clustering.

**2. Statistical analysis of alcoholic hepatitis plasma peptidomic data**

Statistical analyses of the peptidomic data were carried out in collaboration with Dr. Shesh Rai and Dr. Sudhir Srivastava. A non-discriminant data reduction method termed principal components analysis (PCA) was used to evaluate the data at the patient level and determine the ability of the data to 'self-sort' into discrete groups. To evaluate the data more discretely at the peptide level, a multivariate analysis approach using hierarchical clustering and heat-map annotation was used incorporating linear mixed modeling of the data to control for fixed and random variables. Lastly, univariate (pair-wise t-tests with Benjamini-Hochberg correction for multiple comparisons) were used to establish differences in peptide groups and individual peptides across patient cohorts. Peptide abundance differences were plotted as $\log_2$FC versus $-\log_{10}$ BH-

corrected p-value. Peptides with BH-corrected p-value < 0.05 and $log_2FC \geq 1$ were considered significantly upregulated, and peptides with BH-corrected p-value <0.05 and $log_2FC \leq -1$ were considered significantly downregulated. The Tukey's HSD test was used for all pairwise comparisons. Pairwise comparisons were illustrated for the major comparators of: A. Healthy vs. Mild-A, B. Healthy vs. Mild-B, C. Healthy vs. Moderate, D. Healthy vs. Severe, E. Mild-A vs Mild-B, F. Moderate vs. Severe. Prior to statistical comparisons, these data were adjusted for (a) random effects by correcting in a sample dependent fashion to iRT peptide AUCs and sample flight number and (b) fixed effects by correcting for age and sex. The peptides demonstrating differential abundance (regulated) in the pair-wise t-testing (BH-corrected p-value <0.05) were aggregated and filtered using the Matrix Annotator (http://matrisomeproject.mit.edu/analytical-tools/matrisome-annotator/) by GO assignment for ECM. The identification of regulated ECM peptides common to all or unique between AH, AUD, and healthy control groups were determined graphically (regulated ECM peptidome).

**3. Statistical analysis of renal cortex proteomic and transcriptomic data**

Statistical analyses of proteomic and transcriptomic data used one-way ANOVA and post-hoc t-tests corrected for multiple comparisons by the method of Benjamini-Hochberg, and a corrected p-value (q-value) of less than 0.05 was considered significant. Analysis of immunoblot data used two-way ANOVA to determine interaction effects of diet (EtOH) and treatment (LPS) with post-hoc t-test to determine significance of differences between group means with a p-value

≤ 0.05 considered significant. Statistical analyses used to determine significance of proteins or genes with canonical pathways, gene ontological associations, and pathway clustering were as embedded within Ingenuity Pathways Analyses (analysis.ingenuity.com), MetaCore (genego.com), Gene Ontology/GO (patherdb.org) and Heatmapper (heatmapper.ca).

CHAPTER III

# THE HEPATIC “MATRISOME” RESPONDS DYNAMICALLY TO INJURY: CHARACTERIZATION OF TRANSITIONAL CHANGES TO THE EXTRACELLULAR MATRIX IN MICE[1]

## A. Introduction

Although the structural role of the ECM is well known, this compartment contains a diverse range of components that work bidirectionally with surrounding cells to create a dynamic and responsive microenvironment. This microenvironment, in turn, regulates cell and tissue homeostasis. ECM components are directly involved in signaling through interactions with cell-surface receptors. The ECM also indirectly impacts cell-to-cell communication by binding and retaining soluble mediators, including cytokines, chemokines, and growth factors (18). Proteases and protease inhibitors interact with the ECM to maintain homeostasis or respond to stress or injury.(21) A broader definition of the ECM proteome (i.e., “‘matrisome”‘) has been established to encompass not

[1] Published in 93. Massey VL, Dolin CE, Poole LG, Hudson SV, Siow DL, Brock GN, Merchant ML, Wilkey DW, Arteel GE. The hepatic "matrisome" responds dynamically to injury: Characterization of transitional changes to the extracellular matrix in mice. Hepatology. 2017;65(3):969-82. Epub 2016/12/31. doi: 10.1002/hep.28918. PubMed PMID: 28035785; PMCID: PMC5319876. Reprint with permission.

only fibrillar ECM proteins, but also the proteins that contribute to the homeostasis of the ECM proteome.(18)

In some contexts, changes to the ECM are well recognized and understood; for example, the formation of collagenous scars in tissue is almost a canonical response to unresolved chronic injury. Hepatic fibrosis (HF) is a well-known example of this scarring process,(45) given that fibrotic livers develop easily detectable collagenous scars. Given the dominance of these changes in the hepatic ECM during fibrogenesis, many studies have focused on the mechanisms that underlie the increases in collagen deposition. However, the alterations of the hepatic ECM during fibrosis are much more diverse than simply an increase in collagen. Indeed, fibrosis is characterized by changes in the deposition and distribution of a myriad of other ECM proteins (e.g., laminin and vitronectin).(111) Whereas many of these changes are described, there are still gaps in our understanding. Specifically, the magnitude and impact of these changes on overall liver (dys)function are incompletely understood at this time.

ECM remodeling limited to chronic fibrogenesis, but also plays a role in early injury responses; the wound-healing response is a well-known example of this. The term “transitional tissue remodeling” describes changes to the ECM that do not alter the overall architecture of the organ (Fig. 3.1A). For example, changes in the hepatic abundance of ECM proteins, such as fibronectin(90) and fibrin,(89, 112) have been observed in models of hepatic inflammation. Importantly, blocking these ECM changes blunts, at least in part, hepatic injury in these models. Therefore, transitional changes to the ECM may contribute to early

disease initiation and/or progression before the onset of fibrogenesis (Fig. 3.1A). The nature, breadth, and magnitude of these ECM changes are currently poorly understood. A better understanding could forward new mechanisms and/or biomarkers for diseases.

Although previous studies have shown that subtle changes in the ECM may contribute to the development of inflammatory liver injury, the research in this area has generally been restricted to study of single ECM proteins (e.g., fibrin). (89, 112) A proteomic approach was hindered by the challenges of low abundance and insolubility of many ECM proteins, until the recent development of a new method. This method involves a sequential protein extraction using increasingly rigorous solubilization buffers along with LC-MS/MS analysis.(92, 99, 113) The sequential extraction was specifically designed to enrich and characterize ECM proteins in solid organs. This approach also potentially accounts for proteins that can exist in different solubility states, based on posttranslational modifications (e.g., cleavage, cross-linking, and degradation). The goals of the current study were 2-fold: (1) to characterize the sequential extraction method for hepatic matrisome and (2) to compare the impact of inflammatory liver injury (before fibrosis) on the hepatic matrisome.

## B. Experimental Procedures

### 1. Animals and exposures

Mice were exposed to $CCl_4$ as described in Chapter II. Mice were exposed to

**Figure 3.1: Scheme of transitional ECM changes and extraction methodology.**

Remodeling in response to chronic injury (i.e., fibrosis) is well known; however, the hepatic ECM also responses dynamically to acute stress. These acute responses can be viewed as an arm of the wound-healing response and facilitate recovery from damage, which resolves once the damage is repaired. However, under conditions of chronic injury, these changes contribute to activation of a significant remodeling response that leads to scar formation (i.e., fibrosis).

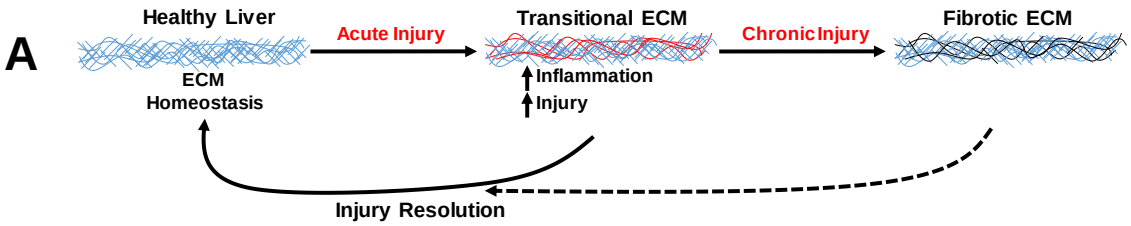
A
Healthy Liver
Acute Injury
Transitional ECM
Chronic Injury
Fibrotic ECM
ECM
Homeostasis
Inflammation
Injury
Injury Resolution

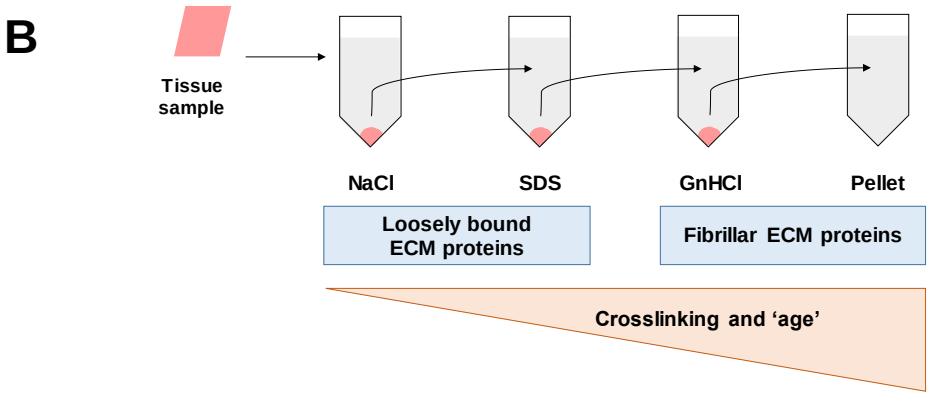
B
Tissue
sample
NaCl
SDS
GnHCl
Pellet
Loosely bound
ECM proteins
Fibrillar ECM proteins
Crosslinking and 'age'

ethanol and/or LPS also as described in Chapter II. 6 control mice, 5 ethanol mice, 6 24h LPS mice, and 4 ethanol+24h LPS mice were used for the hepatic matrisome analysis.

**2. Three-step ECM extraction**

Liver tissue was submitted to a 3-step extraction process that allows sequential isolation of loosely-bound extracellular proteins, cellular proteins, tightly bound extracellular proteins, and highly crosslinked, insoluble proteins to be differentially separated as described in Chapter II.

**3. Sample cleanup and preparation for liquid chromatography and mass spectrometry**

Liver tissue extracts were prepared for LC-MS/MS analysis as described in Chapter II.

**4. Liquid chromatography and mass spectrometry**

Liver tissue extracts underwent LC-MS/MS analysis as described in Chapter II.

**5. Data analysis**

LC-MS/MS data were analyzed as described in Chapter II.

**6. Statistical analysis**

Statistical analysis was performed as described in Chapter II.

## C. Results

### 1. Analysis of changes to the ECM proteome caused by $CCl_4$-induced hepatic fibrosis

Previous studies have investigated the matrisome profile for aortic vessel and cardiac tissue (99, 114). However, this method has never been employed for liver tissue. The first objective of this work was to validate this multi-step extraction and proteomic analysis of the hepatic matrisome; toward this end, a model that causes robust changes to the hepatic ECM (i.e., fibrosis) was used. Specifically, the impact of 4 weeks of $CCl_4$ exposure (see Experimental Procedures) on the ECM proteome was determined (Fig. 3.2). As expected,(96) $CCl_4$ exposure caused robust ECM deposition that was easily detected with standard collagen staining (Sirius Red/Fast Green; Fig. 3.2A), dot blot, and hydroxyproline content (Fig. 3.2B). The proteomic approach reinforced an increase in collagen 1α1 abundance with $CCl_4$ (Fig. 3.2C). Additionally, the proteomic approach demonstrated that $CCl_4$ exposure also increased abundance of collagens type III, IV, and V (Fig. 3.2C).

Proteomic analysis is typically carried out on total protein extracts, as opposed to extracts from multi-step fractionation. To simulate this approach, qualitative proteomic data from the different fractions (see Experimental Procedures) were pooled. The majority of ECM proteins were detected in extracts of livers of both naïve and $CCl_4$-exposed mice. Specifically, $CCl_4$

**Figure 3.2: Validation of extraction technique with $CCl_4$ model of fibrosis.**

Animals were injected with $CCl_4$ or vehicle for 4 weeks. Collagen type I accumulation was determined by Sirius Red staining (A) and by dot blot (control n=4, $CCl_4$ n=4) and hydroxyproline content (control n=4, $CCl_4$ n=6) (B). Quantitative changes in other collagens were also determined in the ECM extraction fractions (control n=1 pooled sample of 6, $CCl_4$, 1 pooled sample of 5) (C). Abbreviations: COL, collagen; GAPDH, glyceraldehyde 3-phosphate dehydrogenase.

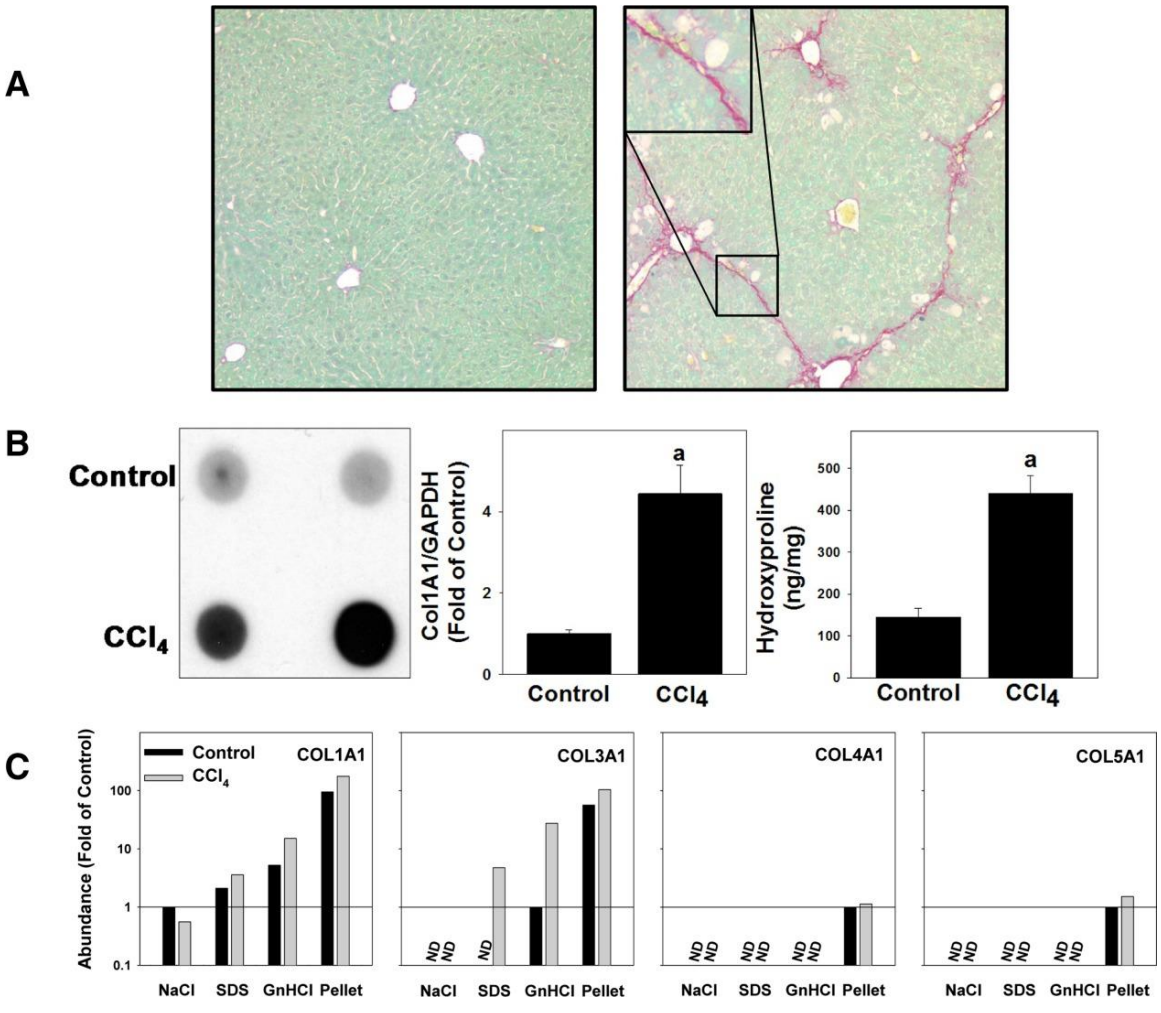
A
B
Control
CCl4
Col1A1/GAPDH (Fold of Control)
a
Control
CCl4
Hydroxyproline (ng/mg)
a
Control
CCl4
C
Abundance (Fold of Control)
Control
CCl4
COL1A1
COL3A1
COL4A1
COL5A1
NaCl
SDS
GnHCl
Pellet
ND

exposure increased the number of ECM proteins by 7, and only one protein was lost compared to the control group (data not shown). These data indicate that, when analyzed as a whole, there are few qualitative changes (i.e., disappearance or appearance of proteins) in the hepatic matrisome, even under conditions of significant histological ECM changes (e.g., fibrosis; Fig. 3.2A).

**2. Ethanol and LPS exposure cause global changes to the hepatic matrisome**

After validation of the multi-step extraction method with $CCl_4$-challenged livers (Fig. 3.2), a more detailed analysis of the effects of ethanol and LPS was carried out. Figure 3.3A shows a heatmap comparing the quantitative changes in the ECM proteome between the four exposure groups (±ethanol diet, ±LPS injection) after fractions were combined '*in silico*'; the most up-regulated or down-regulated ECM proteins were used to compare the groups. Heatmap visualization of the ECM proteomes demonstrates distinct segregation between the control group and exposure groups, with ethanol and LPS exposure groups producing varying patterns; ethanol + LPS produced patterns similar to both exposures alone, but also demonstrated unique patterns (Fig. 3.3A). However, similar to the $CCl_4$ qualitative analysis (see above and Fig. 3.2), ethanol and/or LPS caused only a small number of proteins to change qualitatively.

**3. Three-step serial extraction creates distinct protein profiles**

**Figure 3.3: Liver extracts have unique protein profiles based on fraction type and experimental group.**

A heatmap depicting quantitative changes to the total ECM proteome in response to ethanol or LPS is shown in (A). The number of proteins unique to, or shared by, all four extractions of pair-fed animals is shown (B). Bubble graphs are used to show presence of plasminogen, Annexin A1 and fibrin(ogen) gamma chain across the four extracts (x-axis) and the four experimental groups (y-axis; C).

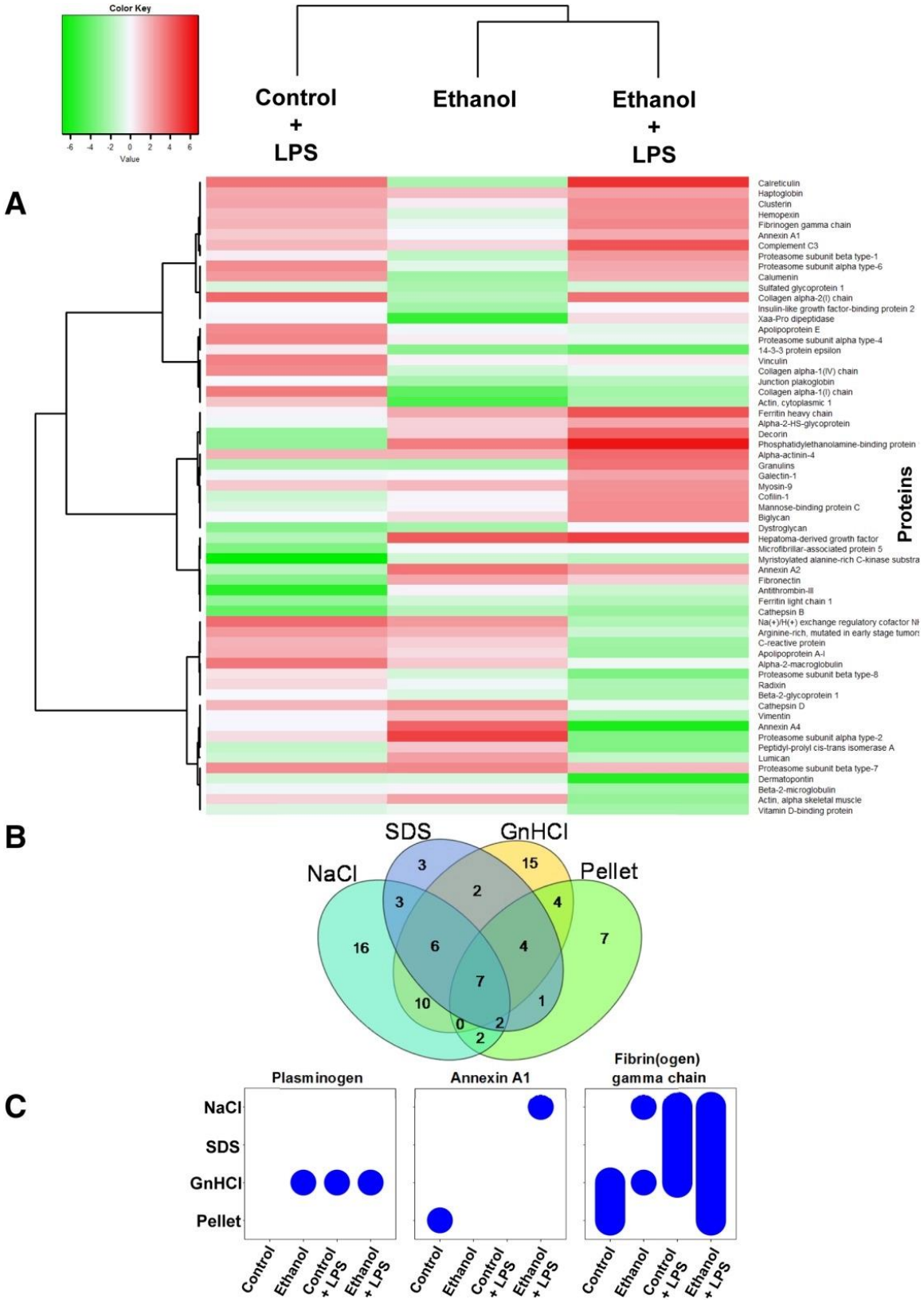
A
Color Key
-6 -4 -2 0 2 4 6
Value
Control + LPS
Ethanol
Ethanol + LPS
Proteins
Calreticulin
Haptoglobin
Clusterin
Hemopexin
Fibrinogen gamma chain
Annexin A1
Complement C3
Proteasome subunit beta type-1
Proteasome subunit alpha type-6
Calumenin
Sulfated glycoprotein 1
Collagen alpha-2(I) chain
Insulin-like growth factor-binding protein 2
Xaa-Pro dipeptidase
Apolipoprotein E
Proteasome subunit alpha type-4
14-3-3 protein epsilon
Vinculin
Collagen alpha-1(IV) chain
Junction plakoglobin
Collagen alpha-1(I) chain
Actin, cytoplasmic 1
Ferritin heavy chain
Alpha-2-HS-glycoprotein
Decorin
Phosphatidylethanolamine-binding protein
Alpha-actinin-4
Granulins
Galectin-1
Myosin-9
Cofilin-1
Mannose-binding protein C
Biglycan
Dystroglycan
Hepatoma-derived growth factor
Microfibrillar-associated protein 5
Myristoylated alanine-rich C-kinase substra
Annexin A2
Fibronectin
Antithrombin-III
Ferritin light chain 1
Cathepsin B
Na(+)/H(+) exchange regulatory cofactor NH
Arginine-rich, mutated in early stage tumors
C-reactive protein
Apolipoprotein A-I
Alpha-2-macroglobulin
Proteasome subunit beta type-8
Radixin
Beta-2-glycoprotein 1
Cathepsin D
Vimentin
Annexin A4
Proteasome subunit alpha type-2
Peptidyl-prolyl cis-trans isomerase A
Lumican
Proteasome subunit beta type-7
Dermatopontin
Beta-2-microglobulin
Actin, alpha skeletal muscle
Vitamin D-binding protein
B
SDS
GnHCl
NaCl
Pellet
3
15
2
3
4
16
6
4
7
7
10
1
0
2
2
C
Plasminogen
Annexin A1
Fibrin(ogen) gamma chain
NaCl
SDS
GnHCl
Pellet
Control
Ethanol
Control + LPS
Ethanol + LPS

ECM proteins are not only regulated at the level of *de novo* synthesis, but also at the level of enzymatic activation, degradation, and crosslinking. To gain insight into protein location and structure, previous studies have used a three-step ECM extraction method (Fig. 3.1B) in other organs. (99, 114) Here, that same approach was adapted for use with liver tissue. In the first step of this extraction, NaCl extraction solubilizes loosely bound proteins by displacing polyionic interactions. (115) Following NaCl extraction, the remaining liver tissue was decellularized using 1% sodium dodecyl sulfate (SDS). SDS solubilizes cytoplasmic and nuclear membranes, thereby releasing cellular proteins. Insoluble matter remaining after the decellularization then underwent extraction with a denaturing 4 M GnHCl buffer.(116) Following the denaturing extraction, an insoluble pellet enriched in heavily cross-linked matrix proteins remained.(114) Fig. 3.3B shows a qualitative comparison of the four extracts of ECM proteins from control animals. Each extract yielded a distinct ECM protein profile consisting of not only ECM proteins that were shared among all four extracts, but also proteins unique to specific extracts (Fig. 3.3B). Analysis of the $CCl_4$ extracts for collagen isoforms (Fig. 3.2C) indicated that, as expected, these proteins tended to accumulate in the later extraction fractions. These results indicate that the extraction approach effectively separated ECM proteins.

When ECM proteins were compared between experimental groups, interesting patterns of distribution across the extracts were revealed (Table 3.1); representative examples of some of these patterns are shown in Fig. 3.3C. For example, some proteins (e.g., plasminogen) changed in overall “presence” or

## Table 3.1: Qualitative presence of ECM proteins in sample extracts

| Protein name | Accession Number | MW (kDa) | ECM function | Ref | Presence of protein | Con | EtOH | LPS | EtOH +LPS |
|---|---|---|---|---|---|---|---|---|---|
| **Proteoglycans and glycoproteins** | | | | | | | | | |
| **Alpha-1-acid glycoprotein 1** | A1AG1_MOUSE | 24 | Acute phase serum protein | (201) | NaCl | | | | |
| | | | | | SDS | | | | |
| | | | | | GnHCl | | | | |
| | | | | | Pellet | | | | |
| **Alpha-2-HS-glycoprotein** | FETUA_MOUSE | 37 | Inhibitor of ECM mineralization | (202) | NaCl | ■ | ■ | ■ | ■ |
| | | | | | SDS | | | | |
| | | | | | GnHCl | ■ | ■ | ■ | ■ |
| | | | | | Pellet | | | | |
| **Arylsulfatase A** | ARSA_MOUSE | 54 | ECM structure | (203) | NaCl | | ■ | | |
| | | | | | SDS | | | | |
| | | | | | GnHCl | | | | |
| | | | | | Pellet | | | | |
| **Beta-2-glycoprotein** | APOH_MOUSE | 39 | Coagulation, phospholipid binding | (204) | NaCl | | | | |
| | | | | | SDS | | | | |
| | | | | | GnHCl | ■ | ■ | ■ | ■ |
| | | | | | Pellet | | | | |
| **Biglycan** | PGS1_MOUSE | 42 | Regulation of collagen fibril formation, ECM-cell interactions | (205) | NaCl | | | | |
| | | | | | SDS | | | | |
| | | | | | GnHCl | ■ | ■ | ■ | ■ |
| | | | | | Pellet | | | | |
| **Corneodesmosin** | CDSN_MOUSE | 54 | Adhesive protein | (206) | NaCl | | | | |
| | | | | | SDS | | | | |
| | | | | | GnHCl | | | | |
| | | | | | Pellet | ■ | | ■ | |
| **Cysteine-rich with EGF-like domain protein 2** | CREL2_MOUSE | 38 | Extracellular protein heavily glycosylated. ECM function unknown | (207) | NaCl | ■ | ■ | ■ | ■ |
| | | | | | SDS | | | | |
| | | | | | GnHCl | ■ | ■ | ■ | ■ |
| | | | | | Pellet | | | | |

| | | | | | | | | | | |
|---|---|---|---|---|---|---|---|---|---|---|
| **Decorin** | PGS2_MOUSE | 40 | ECM-cell interactions, ECM assembly | (208) | NaCl | | | | | |
| | | | | | SDS | | | | | |
| | | | | | GnHCl | ■ | ■ | ■ | ■ | |
| | | | | | Pellet | | | | | |
| **Dermatopontin** | DERM_MOUSE | 24 | ECM-cell interactions, ECM assembly | (209) | NaCl | | | | | |
| | | | | | SDS | | | | | |
| | | | | | GnHCl | ■ | ■ | ■ | ■ | |
| | | | | | Pellet | | | | | |
| **Dystroglycan** | DAG1_MOUSE | 97 | Matrix organization, basement membrane assembly | (210) | NaCl | ■ | ■ | ■ | ■ | |
| | | | | | SDS | | | | | |
| | | | | | GnHCl | ■ | ■ | ■ | | |
| | | | | | Pellet | | | | | |
| **Fibrinogen alpha chain** | E9PV24_MOUSE | 87 | Hemostasis, cell signaling (fibrin(ogen) alpha chain) | (211) | NaCl | | | ■ | ■ | |
| | | | | | SDS | | | ■ | ■ | |
| | | | | | GnHCl | | ■ | ■ | ■ | |
| | | | | | Pellet | | | | ■ | |
| **Fibrinogen beta chain** | FIBB_MOUSE | 55 | Hemostasis, cell signaling | (211) | NaCl | | ■ | ■ | ■ | |
| | | | | | SDS | | | | | |
| | | | | | GnHCl | | | | | |
| | | | | | Pellet | | | | | |
| **Fibrinogen gamma chain** | FIBG_MOUSE | 49 | Hemostasis, fibrinogen polymerization | (212) | NaCl | | ■ | ■ | ■ | |
| | | | | | SDS | | | ■ | ■ | |
| | | | | | GnHCl | ■ | ■ | ■ | ■ | |
| | | | | | Pellet | ■ | | | ■ | |
| **Fibronectin** | FINC_MOUSE | 273 | Scaffolding, ECM organization, regulation of ECM-cell interactions | (213) | NaCl | | | | | |
| | | | | | SDS | | | | | |
| | | | | | GnHCl | ■ | ■ | ■ | ■ | |
| | | | | | Pellet | | | | | |
| **Galectin-1** | LEG1_MOUSE | 15 | Matrix crosslinking, matrix organization | (214) | NaCl | ■ | ■ | ■ | | |
| | | | | | SDS | | | ■ | | |
| | | | | | GnHCl | ■ | ■ | ■ | ■ | |
| | | | | | Pellet | | | | | |
| **Galectin-3-binding protein** | LG3BP_MOUSE | 64 | Cell-matrix adhesion | (215) | NaCl | ■ | ■ | ■ | ■ | |
| | | | | | SDS | | ■ | ■ | ■ | |
| | | | | | GnHCl | ■ | | ■ | ■ | |
| | | | | | Pellet | | | | | |

| | | | | | | | | | | |
|---|---|---|---|---|---|---|---|---|---|---|
| **Granulins** | GRN_MOUSE | 63 | Cell-matrix signaling | (216) | NaCl | ■ | ■ | ■ | ■ |
| | | | | | SDS | ■ | ■ | ■ | ■ |
| | | | | | GnHCl | ■ | ■ | ■ | ■ |
| | | | | | Pellet | | | | |
| **Haptoglobin** | HPT_MOUSE | 39 | Inhibition of collagen degradation, cell migration | (217) | NaCl | ■ | ■ | ■ | ■ |
| | | | | | SDS | ■ | ■ | ■ | ■ |
| | | | | | GnHCl | ■ | ■ | ■ | ■ |
| | | | | | Pellet | | ■ | ■ | ■ |
| **Insulin-like growth factor-binding protein 2** | IBP2_MOUSE | 33 | Binding/retainment of ILGF in the extracellular space | (218) | NaCl | | | | |
| | | | | | SDS | | | | |
| | | | | | GnHCl | ■ | ■ | | |
| | | | | | Pellet | | | | |
| **Insulin-like growth factor-binding protein 4** | IBP4_MOUSE | 28 | Binding/retainment of ILGF in the extracellular space | (218) | NaCl | | | | |
| | | | | | SDS | | | | |
| | | | | | GnHCl | ■ | ■ | | |
| | | | | | Pellet | | | | |
| **Keratin, type I cytoskeletal 13** | K1C13_MOUSE | 48 | Cell-matrix adhesion, cell migration | (219) | NaCl | | ■ | | ■ |
| | | | | | SDS | | | | |
| | | | | | GnHCl | | | | |
| | | | | | Pellet | | | ■ | |
| **Leucine-rich HEV glycoprotein** | Q91XL1_MOUSE | 37 | Cell-matrix adhesion | (220) | NaCl | | | ■ | ■ |
| | | | | | SDS | | | | |
| | | | | | GnHCl | | | | |
| | | | | | Pellet | | | | |
| **Lumican** | LUM_MOUSE | 38 | Regulation of collagen fibril formation | (221) | NaCl | | | | |
| | | | | | SDS | | | | |
| | | | | | GnHCl | ■ | ■ | ■ | ■ |
| | | | | | Pellet | ■ | ■ | | ■ |
| **Microfibrillar-associated protein 5** | MFAP5_MOUSE | 18 | Elastic fiber assembly, binding of fibrillin-1 and fibrillin-2 | (222) | NaCl | | | | |
| | | | | | SDS | | | | |
| | | | | | GnHCl | ■ | | | ■ |
| | | | | | Pellet | | | | |
| **Fibrinogen alpha chain** | E9PV24_MOUSE | 87 | Hemostasis, cell signaling (fibrin(ogen) alpha chain) | (211) | NaCl | | | ■ | ■ |
| | | | | | SDS | | | ■ | ■ |
| | | | | | GnHCl | | ■ | ■ | ■ |
| | | | | | Pellet | | | | ■ |

| | | | | | | Con | EtOH | LPS | EtOH +LPS |
|---|---|---|---|---|---|---|---|---|---|
| **Ribonuclease inhibitor** | RINI_MOUSE | 50 | Extracellular inhibitor of angiogenin which can degrade BM | (223) | NaCl | | | | ■ |
| | | | | | SDS | | | | |
| | | | | | GnHCl | | | | |
| | | | | | Pellet | | | | |
| **Sulfated glycoprotein 1** | SAP_MOUSE | 61 | Cell survival, cell signaling | (224, 225) | NaCl | | | | |
| | | | | | SDS | ■ | ■ | ■ | ■ |
| | | | | | GnHCl | ■ | ■ | ■ | ■ |
| | | | | | Pellet | ■ | ■ | ■ | ■ |
| **Syndecan-4** | SDC4_MOUSE | 21 | ECM organization, signal transduction, cell adhesion | (226) | NaCl | | ■ | ■ | ■ |
| | | | | | SDS | ■ | ■ | ■ | ■ |
| | | | | | GnHCl | ■ | ■ | ■ | ■ |
| | | | | | Pellet | | | | |
| **Tubulointerstitial nephritis antigen-like** | TINAL_MOUSE | 52 | Protein binding - fibronectins, collagens | (227) | NaCl | ■ | ■ | ■ | ■ |
| | | | | | SDS | | | | |
| | | | | | GnHCl | ■ | ■ | | ■ |
| | | | | | Pellet | | | | |
| **Vitronectin** | VTNC_MOUSE | 55 | ECM-cell signal transduction, cell adhesion | (228) | NaCl | ■ | ■ | ■ | ■ |
| | | | | | SDS | | | | |
| | | | | | GnHCl | | ■ | ■ | ■ |
| | | | | | Pellet | | | | |
| **Other ECM-associated proteins** | | | | | | **Con** | **EtOH** | **LPS** | **EtOH +LPS** |
| **14-3-3 protein epsilon** | 1433E_MOUSE | 29 | Protein binding | (229) | NaCl | ■ | ■ | ■ | ■ |
| | | | | | SDS | | | | |
| | | | | | GnHCl | | | | |
| | | | | | Pellet | | | ■ | |
| **14-3-3 protein gamma** | 1433G_MOUSE | 28 | Protein binding | (229) | NaCl | ■ | ■ | ■ | ■ |
| | | | | | SDS | | | | |
| | | | | | GnHCl | | ■ | ■ | ■ |
| | | | | | Pellet | | | | |
| **14-3-3 protein sigma** | 1433S_MOUSE | 28 | Protein binding | (229) | NaCl | | | | |
| | | | | | SDS | | | | |
| | | | | | GnHCl | | | | |
| | | | | | Pellet | ■ | | ■ | |

| | | | | | | | | | | |
|---|---|---|---|---|---|---|---|---|---|---|
| **14-3-3 protein zeta/delta** | 1433Z_MOUSE | 28 | Protein binding | (229) | NaCl<br>SDS<br>GnHCl<br>Pellet | ■<br>■<br><br><br> | <br>■<br><br><br> | ■<br>■<br><br>■ | ■<br>■<br><br><br> |
| **Actin, cytoplasmic 1** | ACTB_MOUSE | 42 | Cortical cytoskeleton | (230, 231) | NaCl<br>SDS<br>GnHCl<br>Pellet | ■<br>■<br><br>■ | ■<br>■<br><br>■ | ■<br>■<br><br>■ | ■<br>■<br><br>■ |
| **Actin, cytoplasmic 2** | ACTG_MOUSE | 42 | Cortical cytoskeleton | (230, 231) | NaCl<br>SDS<br>GnHCl<br>Pellet | <br><br>■<br> | <br><br>■<br> | <br><br>■<br> | <br><br>■<br> |
| **Alpha-2-macroglobulin receptor-associated protein** | AMRP_MOUSE | 42 | Protein binding, soluble mediator internalization | (232) | NaCl<br>SDS<br>GnHCl<br>Pellet | ■<br><br>■<br> | ■<br>■<br>■<br> | ■<br>■<br>■<br> | <br>■<br>■<br> |
| **Alpha-actinin-4** | ACTN4_MOUSE | 105 | Focal adhesion, cell adhesion | (233, 234) | NaCl<br>SDS<br>GnHCl<br>Pellet | ■<br><br><br> | ■<br><br><br> | ■<br><br><br>■ | ■<br><br><br> |
| **Annexin A1** | ANXA1_MOUSE | 39 | ECM binding, fibrinolysis | (235) | NaCl<br>SDS<br>GnHCl<br>Pellet | <br><br>■<br> | <br><br><br> | <br><br><br> | ■<br><br><br> |
| **Annexin A2** | ANXA2_MOUSE | 39 | ECM binding, fibrinolysis | (236) | NaCl<br>SDS<br>GnHCl<br>Pellet | ■<br>■<br><br>■ | ■<br>■<br><br>■ | ■<br><br><br>■ | ■<br><br><br>■ |
| **Annexin A5** | ANXA5_MOUSE | 36 | ECM binding (collagen) | (237) | NaCl<br>SDS<br>GnHCl<br>Pellet | ■<br><br><br> | ■<br><br><br> | ■<br><br><br> | ■<br><br><br> |
| **Apolipoprotein A-I** | APOA1_MOUSE | 31 | ECM binding (collagen, fibronectin) | (238) | NaCl<br>SDS<br>GnHCl<br>Pellet | ■<br>■<br>■<br>■ | ■<br>■<br>■<br>■ | ■<br>■<br>■<br>■ | ■<br>■<br>■<br>■ |

| | | | | | | | | | | |
|---|---|---|---|---|---|---|---|---|---|---|
| **Apolipoprotein A-IV** | APOA4_MOUSE | 45 | Lipid metabolism | (239) | NaCl | ■ | ■ | ■ | ■ |
| | | | | | SDS | | | ■ | ■ |
| | | | | | GnHCl | ■ | | ■ | ■ |
| | | | | | Pellet | ■ | ■ | | ■ |
| **Apolipoprotein E** | APOE_MOUSE | 36 | Lipid metabolism, cell signaling | (240) | NaCl | ■ | ■ | ■ | ■ |
| | | | | | SDS | | | | |
| | | | | | GnHCl | ■ | ■ | | ■ |
| | | | | | Pellet | | | | |
| **Apolipoprotein O-like** | APOOL_MOUSE | 29 | | | NaCl | ■ | ■ | ■ | ■ |
| | | | | | SDS | | ■ | ■ | ■ |
| | | | | | GnHCl | | | | |
| | | | | | Pellet | | | | |
| **Beta-2-microglobulin** | B2MG_MOUSE | 14 | Protein binding, cell-ECM interaction | (241) | NaCl | | | | |
| | | | | | SDS | ■ | ■ | ■ | ■ |
| | | | | | GnHCl | ■ | ■ | ■ | ■ |
| | | | | | Pellet | | | | |
| **Calreticulin** | CALR_MOUSE | 48 | Protein binding (collagens, laminin) | (242) | NaCl | ■ | ■ | ■ | ■ |
| | | | | | SDS | ■ | ■ | ■ | ■ |
| | | | | | GnHCl | ■ | ■ | ■ | ■ |
| | | | | | Pellet | | | | |
| **Calumenin** | CALU_MOUSE | 37 | Pprotein binding, stabilization of fibulin-1 | (243) | NaCl | ■ | ■ | ■ | ■ |
| | | | | | SDS | | | | |
| | | | | | GnHCl | | | | |
| | | | | | Pellet | ■ | ■ | | ■ |
| **Carbonic anhydrase 2** | CAH2_MOUSE | 29 | pH regulation of ECM (other isozymes) | (244) | NaCl | ■ | ■ | ■ | ■ |
| | | | | | SDS | | | | |
| | | | | | GnHCl | | | | |
| | | | | | Pellet | | | | |
| **Ceruloplasmin** | CERU_MOUSE | 121 | Iron, copper binding | (245) | NaCl | | ■ | ■ | ■ |
| | | | | | SDS | | | | |
| | | | | | GnHCl | | | | |
| | | | | | Pellet | | | | |
| **Chitinase-like protein 3** | CHIL3_MOUSE | 44 | ECM turnover | (246) | NaCl | | | ■ | ■ |
| | | | | | SDS | | | | |
| | | | | | GnHCl | | | | |
| | | | | | Pellet | | | | |

| | | | | | | | | | | |
|---|---|---|---|---|---|---|---|---|---|---|
| **Clusterin** | CLUS_MOUSE | 52 | Extracellular protein chaperone | (247) | NaCl<br>SDS<br>GnHCl<br>Pellet | | | ■<br>■ | ■<br>■ | ■<br>■ |
| **Cofilin-1** | COF1_MOUSE | 19 | Cortical cytoskeleton, cell motility | (248) | NaCl<br>SDS<br>GnHCl<br>Pellet | ■ | ■ | ■ | ■ | |
| **C-reactive protein** | CRP_MOUSE | 25 | Protein binding (fibronectin) | (249) | NaCl<br>SDS<br>GnHCl<br>Pellet | ■ | ■<br>■ | ■<br>■ | ■ | |
| **C-X-C motif chemokine 9** | CXCL9_MOUSE | 14 | Soluble mediator (angiostatic cytokine) | (250, 251) | NaCl<br>SDS<br>GnHCl<br>Pellet | ■ | ■ | ■<br>■ | ■ | |
| **Endoplasmin** | ENPL_MOUSE | 92 | Soluble mediator (TLR signaling) | (252) | NaCl<br>SDS<br>GnHCl<br>Pellet | ■<br>■ | ■<br>■ | ■<br>■ | ■<br>■ | |
| **Estradiol 17-beta-dehydrogenase 12** | DHB12_MOUSE | 35 | Protein binding (heparin, fibronectin, collagen) | (253) | NaCl<br>SDS<br>GnHCl<br>Pellet | ■ | ■ | | | |
| **Ferritin heavy chain** | FRIH_MOUSE | 21 | Cell migration | (254) | NaCl<br>SDS<br>GnHCl<br>Pellet | ■<br>■ | ■<br>■<br>■ | ■<br>■<br>■ | ■<br>■<br>■ | |
| **Ferritin light chain 1** | FRIL1_MOUSE | 21 | Cell migration | (254) | NaCl<br>SDS<br>GnHCl<br>Pellet | ■<br>■<br>■ | ■<br>■<br>■ | ■<br>■<br>■ | ■<br>■<br>■ | |
| **Glucose-6-phosphate isomerase** | G6PI_MOUSE | 63 | Cell motility | (255) | NaCl<br>SDS<br>GnHCl<br>Pellet | ■ | ■ | ■ | ■ | |

| | | | | | | | | | | |
|---|---|---|---|---|---|---|---|---|---|---|
| **Hepatoma-derived growth factor** | HDGF_MOUSE | 26 | Decreted heparin-binding growth factor | (256) | NaCl<br>SDS<br>GnHCl<br>Pellet | ■<br><br>■<br>■ | ■<br><br>■<br>■ | ■<br><br>■<br>■ | ■<br><br>■<br>■ |
| **High mobility group protein B1** | HMGB1_MOUSE | 25 | Heparin binding, cytokine | (257, 258) | NaCl<br>SDS<br>GnHCl<br>Pellet | ■<br><br>■<br>■ | ■<br><br>■<br>■ | ■<br><br>■<br>■ | ■<br><br>■<br>■ |
| **High mobility group protein B2** | HMGB2_MOUSE | 24 | Heparin binding, cytokine | (257, 258) | NaCl<br>SDS<br>GnHCl<br>Pellet | <br><br><br> | ■<br><br><br> | ■<br><br><br> | ■<br><br><br> |
| **Lumican** | LUM_MOUSE | 38 | Regulation of collagen fibril formation | (221) | NaCl<br>SDS<br>GnHCl<br>Pellet | <br><br><br> | <br><br><br> | ■<br><br><br> | ■<br><br><br> |
| **Moesin** | MOES_MOUSE | 68 | Cell cortex organization | (259) | NaCl<br>SDS<br>GnHCl<br>Pellet | ■<br><br><br> | ■<br><br><br> | ■<br><br><br> | ■<br><br><br> |
| **Myosin-9** | MYH9_MOUSE | 226 | Cell migration, cortical actin organization | (260) | NaCl<br>SDS<br>GnHCl<br>Pellet | <br>■<br>■<br> | <br>■<br>■<br> | ■<br>■<br>■<br> | ■<br>■<br>■<br> |
| **Neutrophil gelatinase-associated lipocalin** | NGAL_MOUSE | 23 | ECM remodeling (modulation of MMP9 activity) | (261) | NaCl<br>SDS<br>GnHCl<br>Pellet | <br><br><br> | <br><br><br> | ■<br><br>■<br> | ■<br><br>■<br> |
| **Nucleobindin-2** | NUCB2_MOUSE | 50 | Matrix maturation | (262) | NaCl<br>SDS<br>GnHCl<br>Pellet | <br><br><br> | <br><br><br> | <br><br><br> | <br><br>■<br> |
| **Peptidyl-prolyl cis-trans isomerase A** | PPIA_MOUSE | 18 | Matrix assembly of hensin | (263) | NaCl<br>SDS<br>GnHCl<br>Pellet | ■<br>■<br>■<br>■ | ■<br>■<br>■<br> | ■<br>■<br>■<br>■ | ■<br>■<br>■<br> |

| | | | | | | | | | | |
|---|---|---|---|---|---|---|---|---|---|---|
| **Pro-cathepsin H** | CATH_MOUSE | 37 | Matrix degradation | (264) | NaCl<br>SDS<br>GnHCl<br>Pellet | | | | |
| **S100-A13** | S10AD_MOUSE | 11 | Calcium binding | (265) | NaCl<br>SDS<br>GnHCl<br>Pellet | | | | |
| **S100-A9** | | | | | NaCl<br>SDS<br>GnHCl<br>Pellet | | | | |
| **Serum amyloid A-1** | SAA1_MOUSE | 14 | Cell adhesion | (266) | NaCl<br>SDS<br>GnHCl<br>Pellet | | | | |
| **Serum amyloid A-2** | SAA2_MOUSE | 14 | Cell adhesion | (266) | NaCl<br>SDS<br>GnHCl<br>Pellet | | | | |
| **Serum amyloid A-3** | SAA3_MOUSE | 14 | Cell adhesion | (266) | NaCl<br>SDS<br>GnHCl<br>Pellet | | | | |
| **Serum amyloid P-component** | SAMP_MOUSE | 26 | Protein binding (type IV collagen, laminin) | (267, 268) | NaCl<br>SDS<br>GnHCl<br>Pellet | | | | |
| **Superoxide dismutase [Cu-Zn]** | SODC_MOUSE | 16 | Protein binding (heparin/heparan sulfate, type 1 collage) | (269) | NaCl<br>SDS<br>GnHCl<br>Pellet | | | | |
| **Thioredoxin** | THIO_MOUSE | 12 | Soluble mediator (immunomodulatory cytokine) | (258) | NaCl<br>SDS<br>GnHCl<br>Pellet | | | | |

| | | | | | | Con | EtOH | LPS | EtOH +LPS |
|---|---|---|---|---|---|---|---|---|---|
| **Tubulin beta-5 chain** | TBB5_MOUSE | 50 | Microtubule formation, modified via ECM interactions | (231) | NaCl | | | | |
| | | | | | SDS | | | | |
| | | | | | GnHCl | ■ | ■ | ■ | ■ |
| | | | | | Pellet | | | | |
| **UPF0556 protein C19orf10 homolog** | CS010_MOUSE | 18 | Soluble mediator (cytokine) | (270) | NaCl | ■ | ■ | ■ | ■ |
| | | | | | SDS | | | | |
| | | | | | GnHCl | | | | |
| | | | | | Pellet | | | | |
| **Vimentin** | VIME_MOUSE | 54 | Microtubule formation | (271) | NaCl | ■ | ■ | ■ | ■ |
| | | | | | SDS | | | | |
| | | | | | GnHCl | ■ | ■ | ■ | ■ |
| | | | | | Pellet | ■ | ■ | | ■ |
| **Vitamin D-binding protein** | VTDB_MOUSE | 54 | Vitamin D binding | (272) | NaCl | ■ | ■ | ■ | ■ |
| | | | | | SDS | ■ | ■ | ■ | ■ |
| | | | | | GnHCl | ■ | ■ | ■ | ■ |
| | | | | | Pellet | | | | |
| **Proteases and protease inhibitors** | | | | | | | | | |
| **Alpha-1-antitrypsin 1-1** | A1AT1_MOUSE | 46 | Inhibition of ECM proteases; inhibition of trypsin | (273) | NaCl | ■ | ■ | ■ | |
| | | | | | SDS | | | | |
| | | | | | GnHCl | | ■ | ■ | ■ |
| | | | | | Pellet | ■ | ■ | | ■ |
| **Alpha-1-antitrypsin 1-4** | A1AT4_MOUSE | 46 | Inhibition of ECM proteases; inhibition of trypsin | (273) | NaCl | ■ | ■ | ■ | ■ |
| | | | | | SDS | ■ | ■ | ■ | ■ |
| | | | | | GnHCl | | | | |
| | | | | | Pellet | | | | |
| **AMBP** | AMBP_MOUSE | 39 | Precursor of protein HC (protein-ECM interactions) & bikunin (protease inhibitor), | (274-276) | NaCl | | | ■ | ■ |
| | | | | | SDS | | | | |
| | | | | | GnHCl | ■ | ■ | ■ | ■ |
| | | | | | Pellet | | | | |
| **Alpha-2-macroglobulin** | A2M_MOUSE | 166 | Inhibition of ECM proteases, inhibition of ADAMTS-7 and ADAMTS-12 | (277) | NaCl | ■ | ■ | | ■ |
| | | | | | SDS | | | | |
| | | | | | GnHCl | | | | |
| | | | | | Pellet | | | | |

| | | | | | | | |
|---|---|---|---|---|---|---|---|
| **Antithrombin-III** | ANT3_MOUSE | 52 | Inhibition of ECM proteases, inhibition of thrombin | (278) | NaCl<br>SDS<br>GnHCl<br>Pellet | 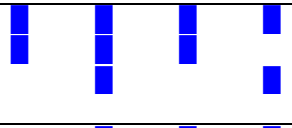 | |
| **Cathelin-related antimicrobial peptide** | CRAMP_MOUSE | 20 | Inhibition of ECM proteases, inhibition of cathepsin L-cysteine protease activity | (279) | NaCl<br>SDS<br>GnHCl<br>Pellet | 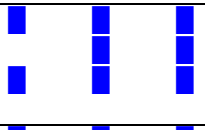 | |
| **Cathepsin B** | CATB_MOUSE | 37 | ECM degradation | (264) | NaCl<br>SDS<br>GnHCl<br>Pellet | 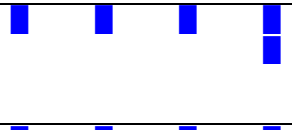 | |
| **Cathepsin D** | CATD_MOUSE | 45 | ECM degradation, activation of cathepsin B | (280) | NaCl<br>SDS<br>GnHCl<br>Pellet | 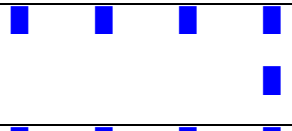 | |
| **Cathepsin Z** | CATZ_MOUSE | 34 | ECM degradation, integrin signaling | (281, 282) | NaCl<br>SDS<br>GnHCl<br>Pellet | 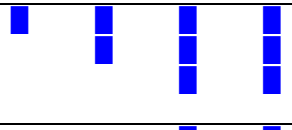 | |
| **Complement C3** | CO3_MOUSE | 186 | Activation of complement system | (283) | NaCl<br>SDS<br>GnHCl<br>Pellet | 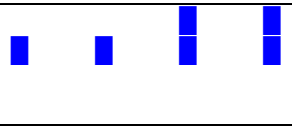 | |
| **Dipeptidyl peptidase 4** | DPP4_MOUSE | 87 | Protein cleavage (cytokines, chemokines), protein binding (collagen) | (284) | NaCl<br>SDS<br>GnHCl<br>Pellet | 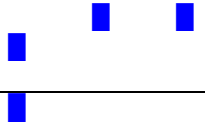 | |
| **Ectonucleoside triphosphate diphosphohydrolase 5** | ENTP5_MOUSE | 47 | Hydrolysis of extracellular ATP | (285) | NaCl<br>SDS<br>GnHCl<br>Pellet | 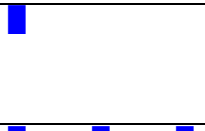 | |
| **Fetuin-B** | FETUB_MOUSE | 43 | Cysteine protease inhibitor, metalloprotease inhibitor, matrix mineralization | (286, 287) | NaCl<br>SDS<br>GnHCl<br>Pellet | | |

| | | | | | | | | | | |
|---|---|---|---|---|---|---|---|---|---|---|
| **Gelsolin** | GELS_MOUSE | 86 | Actin filament capping | (288) | NaCl<br>SDS<br>GnHCl<br>Pellet | ■ | ■ | ■<br><br>■ | ■<br><br>■ |
| **Ectonucleoside triphosphate diphosphohydrolase 5** | ENTP5_MOUSE | 47 | Hydrolysis of extracellular ATP/ADP (signaling) | (286) | NaCl<br>SDS<br>GnHCl<br>Pellet | | ■ | | ■ |
| **Hemopexin** | HEMO_MOUSE | 51 | Heme binding | (289) | NaCl<br>SDS<br>GnHCl<br>Pellet | ■<br><br>■ | ■<br><br>■ | ■<br><br>■ | ■<br><br>■ |
| **Insulin-degrading enzyme** | IDE_MOUSE | 118 | Metalloendopeptidase | (290) | NaCl<br>SDS<br>GnHCl<br>Pellet | | | ■ | |
| **Inter alpha-trypsin inhibitor, heavy chain 4** | ITIH4_MOUSE | 100 | Chain of ITI (protease inhibitor) | (291) | NaCl<br>SDS<br>GnHCl<br>Pellet | | | ■ | |
| **Lysozyme C-1** | LYZ1_MOUSE | 17 | Antibacterial, hydrolysis of β-1, 4-glycosidic linkages | (292) | NaCl<br>SDS<br>GnHCl<br>Pellet | ■ | ■ | ■ | ■ |
| **Lysozyme C-2** | LYZ2_MOUSE | 17 | Antibacterial, hydrolysis of β-1, 4-glycosidic linkages | (292) | NaCl<br>SDS<br>GnHCl<br>Pellet | | ■ | ■ | ■ |
| **Murinoglobulin-1** | MUG1_MOUSE | 165 | Protease inhibitor | (293, 294) | NaCl<br>SDS<br>GnHCl<br>Pellet | ■<br><br>■ | ■<br><br>■ | ■<br><br>■ | ■<br><br>■ |
| **Myeloid bactenecin (F1)** | O08692_MOUSE | 19 | Cysteine protease inhibitor | (295) | NaCl<br>SDS<br>GnHCl<br>Pellet | | ■<br>■<br>■ | ■<br>■<br>■ | ■<br>■<br>■ |

| | | | | | | | | | | |
|---|---|---|---|---|---|---|---|---|---|---|
| **Phosphatidylethanolamine-binding protein 1** | PEBP1_MOUSE | 21 | Serine protease inhibitor | (296) | NaCl<br>SDS<br>GnHCl<br>Pellet | ■<br><br>■ | ■<br>■<br>■ | ■<br>■<br>■ | ■<br>■<br>■ |
| **Plasminogen** | PLMN_MOUSE | 91 | Precursor of plasmin (serine protease) | (297) | NaCl<br>SDS<br>GnHCl<br>Pellet | <br><br><br> | <br><br>■<br> | <br><br>■<br> | <br><br>■<br> |
| **Probable carboxypeptidase PM20D1** | P20D1_MOUSE | 56 | | | NaCl<br>SDS<br>GnHCl<br>Pellet | ■<br><br><br> | ■<br>■<br><br> | ■<br>■<br><br> | ■<br>■<br><br> |
| **Serpinb9** | O08797_MOUSE | 42 | Serine protease inhibitor, granzyme inhibitor) | (298) | NaCl<br>SDS<br>GnHCl<br>Pellet | <br><br><br> | <br><br><br> | <br><br><br> | ■<br><br><br> |
| **Serine protease inhibitor A3K** | SPA3K_MOUSE | 47 | Serine protease inhibitor, chymotrypsin inhibitor | (299) | NaCl<br>SDS<br>GnHCl<br>Pellet | ■<br><br><br> | ■<br><br><br> | ■<br>■<br><br> | ■<br>■<br><br> |
| **Serine protease inhibitor A3N** | SPA3N_MOUSE | 47 | Serine protease inhibitor, chymotrypsin inhibitor | (299) | NaCl<br>SDS<br>GnHCl<br>Pellet | <br><br><br> | <br><br><br> | ■<br><br><br> | ■<br><br><br> |
| **Serpin B5** | SPB5_MOUSE | 42 | Serine protease inhibitor, | (299) | NaCl<br>SDS<br>GnHCl<br>Pellet | <br><br><br> | <br><br><br> | <br><br>■<br> | <br><br><br> |
| **Thioredoxin** | THIO_MOUSE | 12 | Activation of transglutaminase | (300) | NaCl<br>SDS<br>GnHCl<br>Pellet | <br>■<br><br> | <br>■<br><br> | <br>■<br><br> | <br>■<br><br> |
| **Transthyretin** | TTHY_MOUSE | 16 | Hormone binding protein, cryptic protease, peptidase | (301)<br>(302) | NaCl<br>SDS<br>GnHCl<br>Pellet | <br>■<br>■<br> | <br>■<br>■<br> | <br>■<br>■<br> | <br>■<br>■<br> |

| Collagens | | | | | | Con | EtOH | LPS | EtOH +LPS |
|---|---|---|---|---|---|---|---|---|---|
| **Adiponectin** | ADIPO_MOUSE | 27 | Inhibition of vascular matrix degradation (contains collagen-like domain) | (303, 304) | NaCl<br>SDS<br>GnHCl<br>Pellet | | | | |
| **Collagen alpha-1(I) chain** | CO1A1_MOUSE | 138 | Component of collagen fibrins | (303) | NaCl<br>SDS<br>GnHCl<br>Pellet | | | | |
| **Collagen alpha-1(III) chain** | CO3A1_MOUSE | 139 | Component of collagen fibrils | (303) | NaCl<br>SDS<br>GnHCl<br>Pellet | | | | |
| **Collagen alpha-1(IV) chain** | CO4A1_MOUSE | 161 | Component of collagen network | (303) | NaCl<br>SDS<br>GnHCl<br>Pellet | | | | |
| **Collagen alpha-1(V) chain** | CO5A1_MOUSE | 184 | Fibrillogenesis, crosslinking | (303) | NaCl<br>SDS<br>GnHCl<br>Pellet | | | | |
| **Collagen alpha-2(I) chain** | CO1A2_MOUSE | 130 | Component of collagen fibrils (contains collage-like domain) | (303) | NaCl<br>SDS<br>GnHCl<br>Pellet | | | | |
| **Collagen alpha-2(IV) chain** | CO4A2_MOUSE | 167 | Component of collagen network | (303) | NaCl<br>SDS<br>GnHCl<br>Pellet | | | | |
| **Collagen alpha-2(V) chain** | CO5A2_MOUSE | 145 | Fibrillogenesis, crosslinking | (303) | NaCl<br>SDS<br>GnHCl<br>Pellet | | | | |
| **Mannose binding protein** | MBL2_MOUSE | 26 | soluble pattern recognition receptor | (305) | NaCl<br>SDS<br>GnHCl<br>Pellet | | | | |

**Extracellular - ECM interactions unknown**

| | | |
|---|---|---|
| **60 heat shock protein, mitochondrial** | CH60_MOUSE | 61 |
| **78 glucose-regulated protein** | GRP78_MOUSE | 72 |
| **Aminoacyl tRNA synthase complex-interacting multifunctional protein 1** | AIMP1_MOUSE | 34 |
| **Arginase-1** | ARGI1_MOUSE | 35 |
| **BolA-like protein 1** | BOLA1_MOUSE | 14 |
| **BolA-like protein 3** | BOLA3_MOUSE | 12 |
| **Carboxylesterase 1C** | EST1C_MOUSE | 61 |
| **Clathrin heavy chain 1** | CLH1_MOUSE | 192 |
| **Epididymal secretory protein E1** | NPC2_MOUSE | 16 |
| **Group XIIB secretory phospholipase A2-like protein** | Q8VC81_MOUSE | 22 |
| **Heat shock cognate 71 protein** | HSP7C_MOUSE | 71 |
| **Hepcidin** | HEPC_MOUSE | 9 |
| **Hypoxia up-regulated protein 1** | HYOU1_MOUSE | 111 |

| | | |
|---|---|---|
| **Interferon-inducible GTPase 1** | IIGP1_MOUSE | 48 |
| **Lactotransferrin** | TRFL_MOUSE | 78 |
| **Macrophage migration inhibitory factor** | MIF_MOUSE | 13 |
| **Major urinary protein 12** | A2CEK7_MOUSE | 21 |
| **Major urinary protein 17** | MUP17_MOUSE | 21 |
| **Major urinary protein 20** | MUP20_MOUSE | 21 |
| **Major urinary protein 3** | MUP3_MOUSE | 21 |
| **Major vault protein** | MVP_MOUSE | 96 |
| **Monocyte differentiation antigen CD14** | CD14_MOUSE | 39 |
| **Multiple coagulation factor deficiency protein 2 homolog** | MCFD2_MOUSE | 16 |
| **Myeloperoxidase** | PERM_MOUSE | 81 |
| **Nuclease-sensitive element-binding protein 1** | YBOX1_MOUSE | 36 |
| **Polymeric immunoglobulin receptor** | PIGR_MOUSE | 85 |
| **Profilin-1** | PROF1_MOUSE | 15 |

| | | |
|---|---|---|
| **Protein CREG1** | CREG1_MOUSE | 24 |
| **Protein Gm20425** | E9Q035_MOUSE | 108 |
| **Pyruvate kinase PKM** | KPYM_MOUSE | 58 |
| **RNA binding motif protein, X-linked-like-1** | RMXL1_MOUSE | 42 |
| **Serotransferrin** | TRFE_MOUSE | 77 |
| **Serum albumin** | ALBU_MOUSE | 69 |
| **Serum paraoxonase/arylesterase 1** | PON1_MOUSE | 40 |
| **Translationally-controlled tumor protein** | TCTP_MOUSE | 19 |
| **UPF0369 protein C6orf57 homolog** | CF057_MOUSE | 12 |
| **Xanthine dehydrogenase/oxidase** | XDH_MOUSE | 147 |

“absence” in response to exposures, but localized consistently to the same fraction when present. Ethanol and/or LPS exposure caused other proteins to appear in different extracts in simple or complex patterns. For example, whereas Annexin A1 was found in the insoluble pellet from control animals, it was not detected in any fraction from animals exposed to ethanol or LPS alone; however, the combination of ethanol and LPS caused this protein to accumulate in the NaCl fraction. Similarly, fibrin(ogen) gamma chain was found in all experimental groups, but its fractionation pattern was unique to each exposure condition. These patterns likely represent differences in the synthesis, degradation, and/or maturity of the ECM proteins.

**4. Qualitative changes to the ECM proteome in response to stress**

Figure 3.4 summarizes the abundance of ECM proteins, organized by category (i.e., glycoproteins and proteoglycans (Fig. 3.4A), ECM-associated proteins (Fig. 3.4B), proteases and inhibitors (Fig 3.4C), and collagens (Fig. 3.4D)) across the four extraction conditions. The majority of the proteins in the NaCl and SDS extracts were ECM-associated proteins (Fig. 3.4A); this was unsurprising, given that proteins in this category are generally loosely associated with the ECM and are therefore easily solubilized. Additionally, the low abundance of collagens in the NaCl and SDS fractions (Fig. 3.4D) was not surprising, given that collagens are often tightly cross-linked and require denaturing conditions for solubilization. As expected, the denaturing conditions

**Figure 3.4: Ethanol and LPS cause dynamic changes in the matrisome.** The impact of ethanol diet (left panels) and 24-hour LPS (right panels) on the types of proteins found in the ECM proteome are shown. Proteins are categorized by class (A-D) and organized by extraction fraction (NaCl, SDS, GnHCl, and pellet). Red proteins indicate those that appeared with exposure, whereas green proteins indicate those that were lost with exposure, compared to control.

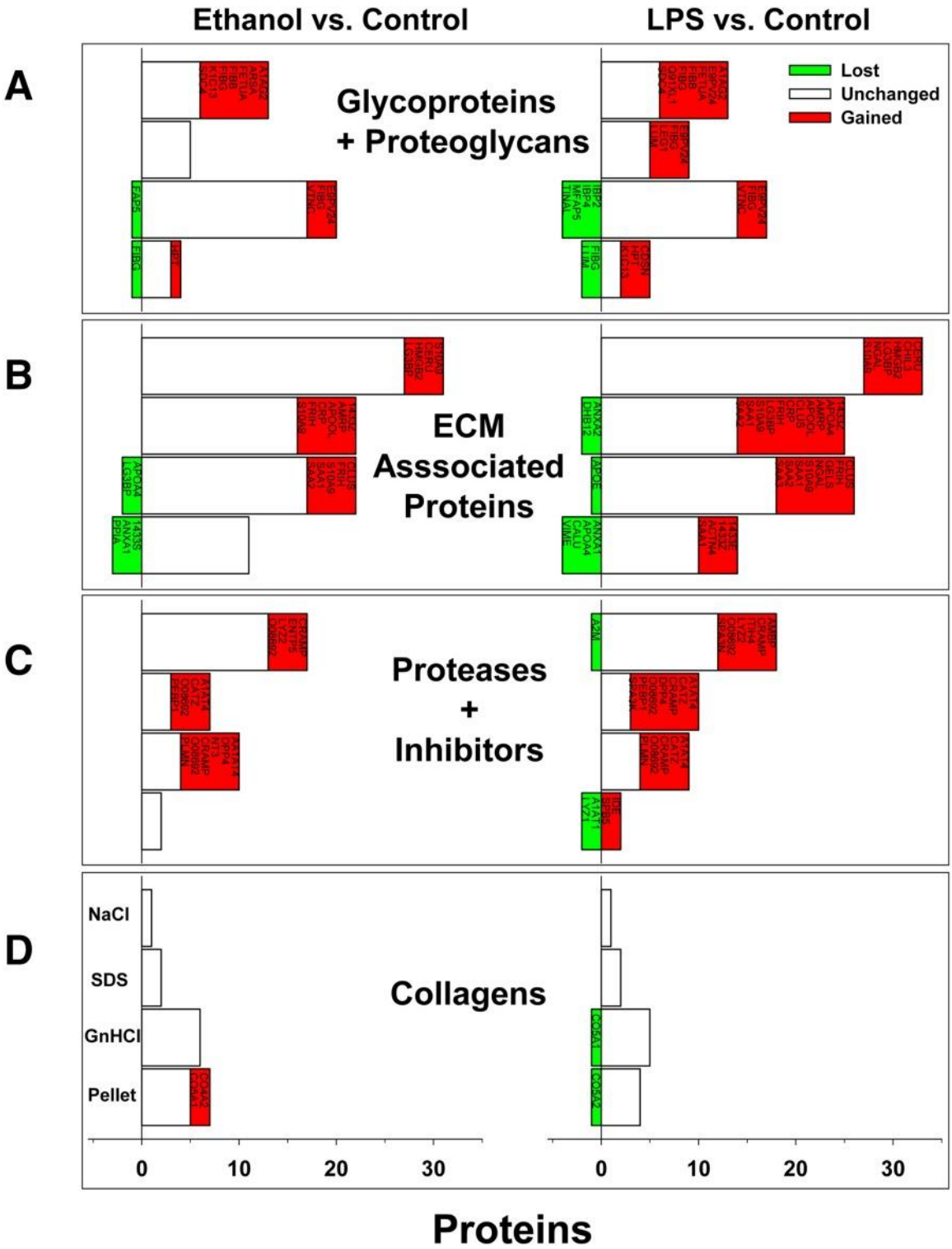
Ethanol vs. Control
LPS vs. Control
A
Glycoproteins
+ Proteoglycans
Lost
Unchanged
Gained
B
ECM
Asssociated
Proteins
C
Proteases
+
Inhibitors
D
Collagens
NaCl
SDS
GnHCl
Pellet
0
10
20
30
Proteins

created by GnHCl more than doubled the number of proteoglycans and glycoproteins in that extract compared to the NaCl and SDS fractions. The number of collagens in the GnHCl extract was also dramatically increased compared to the NaCl and SDS fractions. The pellet fraction contained the fewest proteins of all four extracts but contained the greatest number of collagens.

Ethanol and/or LPS exposure did not change the general pattern of proteins found in the various extracts (Fig. 3.4), but both tended to increase the total number of ECM proteins in the fractions combined. For example, ethanol exposure caused a net increase in the number of ECM proteins by ~25%. These changes were predominantly spread across the first three protein classes, with the NaCl, SDS, and GnHCl extracts all increasing evenly. The pellet fraction responded the least dynamically to ethanol or LPS exposure and actually showed a net loss in total proteins. Likewise, collagens were the least responsive protein class (Fig. 3.4D). Figure 3.5 (left panels) shows the distribution of the proteins in the various extracts between all four exposure groups.

In addition to proteins that changed in their extraction pattern in response to ethanol (e.g., see Fig. 3.3C), there were several proteins that were uniquely detected with ethanol exposure compared to control (Figs. 3.4 and 3.5); these include fibrin(ogen) α and β chains, cytokeratin 13, vitronectin, plasminogen, high mobility group protein B2, and collagens IVα2 and Vα2 (see Table 3.1). Similarly, LPS exposure caused the appearance of several proteins that were unique

**Figure 3.5: Shared and unique changes to the hepatic matrisome.**

Venn diagrams (left column) show all ECM proteins within each of the four extracts and indicate the number that are shared between, or that are unique to, the four experimental groups. Bubble plots (right column) show quantitative changes in abundance of proteins that were shared by all four experimental groups. The bubble plots show fold of control in protein abundance caused by LPS (y-axis), ethanol (x-axis), and the combination of ethanol + LPS (bubble size). Each bubble represents a protein; bubble color indicates the protein's class.

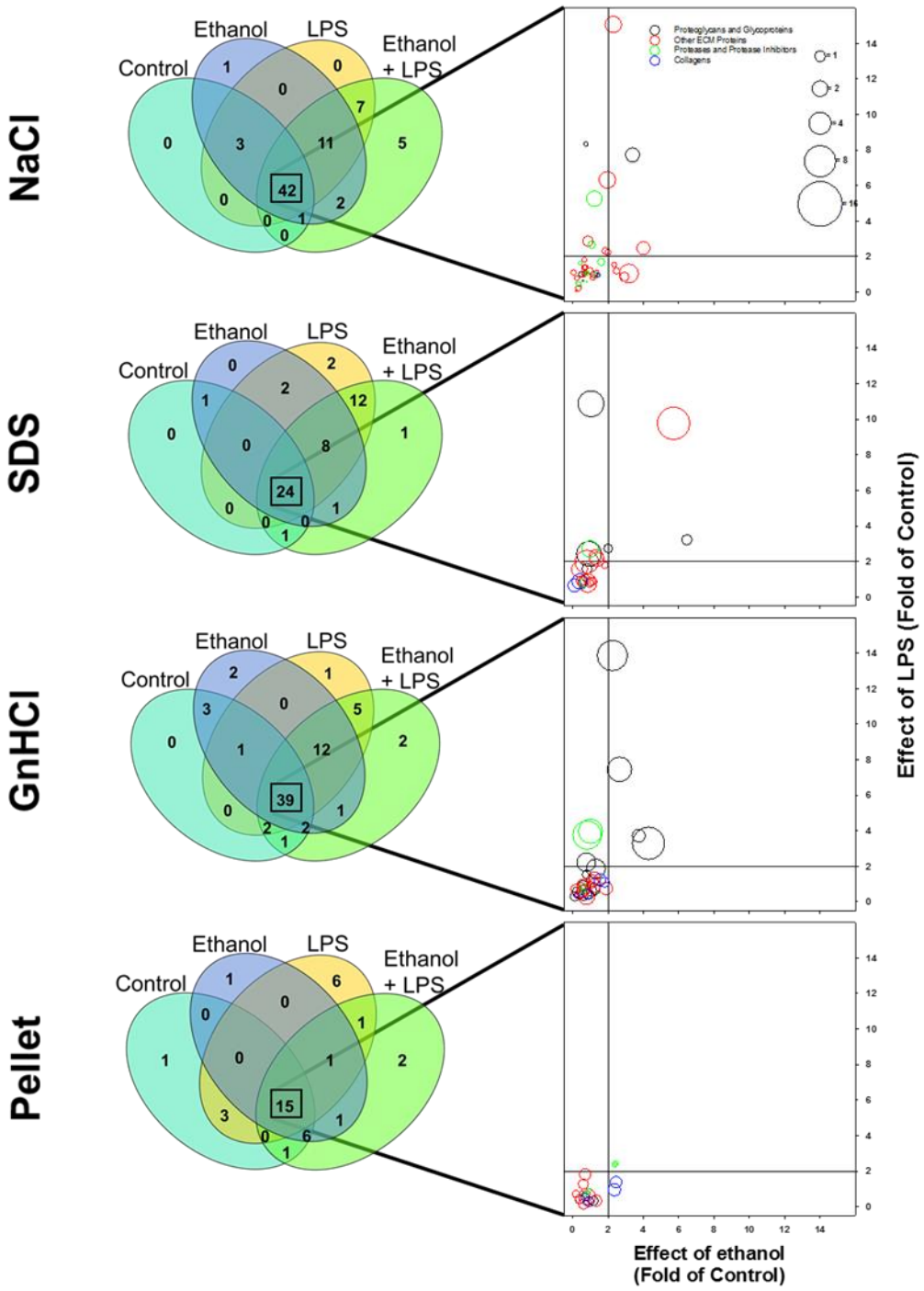
NaCl
SDS
GnHCl
Pellet
Control
Ethanol
LPS
Ethanol + LPS
Proteoglycans and Glycoproteins
Other ECM Proteins
Proteases and Protease Inhibitors
Collagens
Effect of LPS (Fold of Control)
Effect of ethanol (Fold of Control)

compared to control (Figs. 3.4 and 3.5). Several of these proteins were the same as those detected with ethanol exposure, but several were unique to LPS, including serpine B5 (maspin), serine protease inhibitor A3N, and CXC motif chemokine ligand 9 (see Fig. 3.5; Table 3.1).

Previous work has shown that ethanol preexposure sensitizes the liver to inflammatory injury caused by a second insult (i.e., LPS) (26, 117). Furthermore, previous studies have suggested that changes in ECM composition can contribute to the sensitizing effect of ethanol preexposure (89). In this study, the combination of chronic ethanol exposure and a second hit of LPS caused unique changes in the ECM protein profile of the liver. The combination of EtOH+LPS resulted in the appearance of four unique proteins that were not detected in livers from animals exposed to either ethanol or LPS alone, including serum amyloid P and serpine B9.

**5. Quantitative changes to the ECM proteome in response to stress**

Dramatic changes to the ECM (i.e., “lost” or “gained” proteins) can significantly affect overall organ function; it is not surprising that the majority of the matrisome did not change at the qualitative level. However, several of these proteins did change in relative abundance in response to ethanol and/or LPS compared to control (Figs. 3.5 and 3.6). Figs. 3.7-3.10 provide results of the clustering analysis of the protein abundances for each fraction. Based on this analysis, six clusters were identified as the best visual representation of the data. Table 3.2 identifies the membership of each protein within each cluster. Notable

**Figure 3.6: Quantitative changes to the matrisome.**

Heatmap analysis of the quantitative changes in abundance of proteins that were shared by all four experimental groups (see Fig. 3.5) are shown for the NaCl (A), SDS (B), GnHCl (C), and pellet (D) extraction fractions.

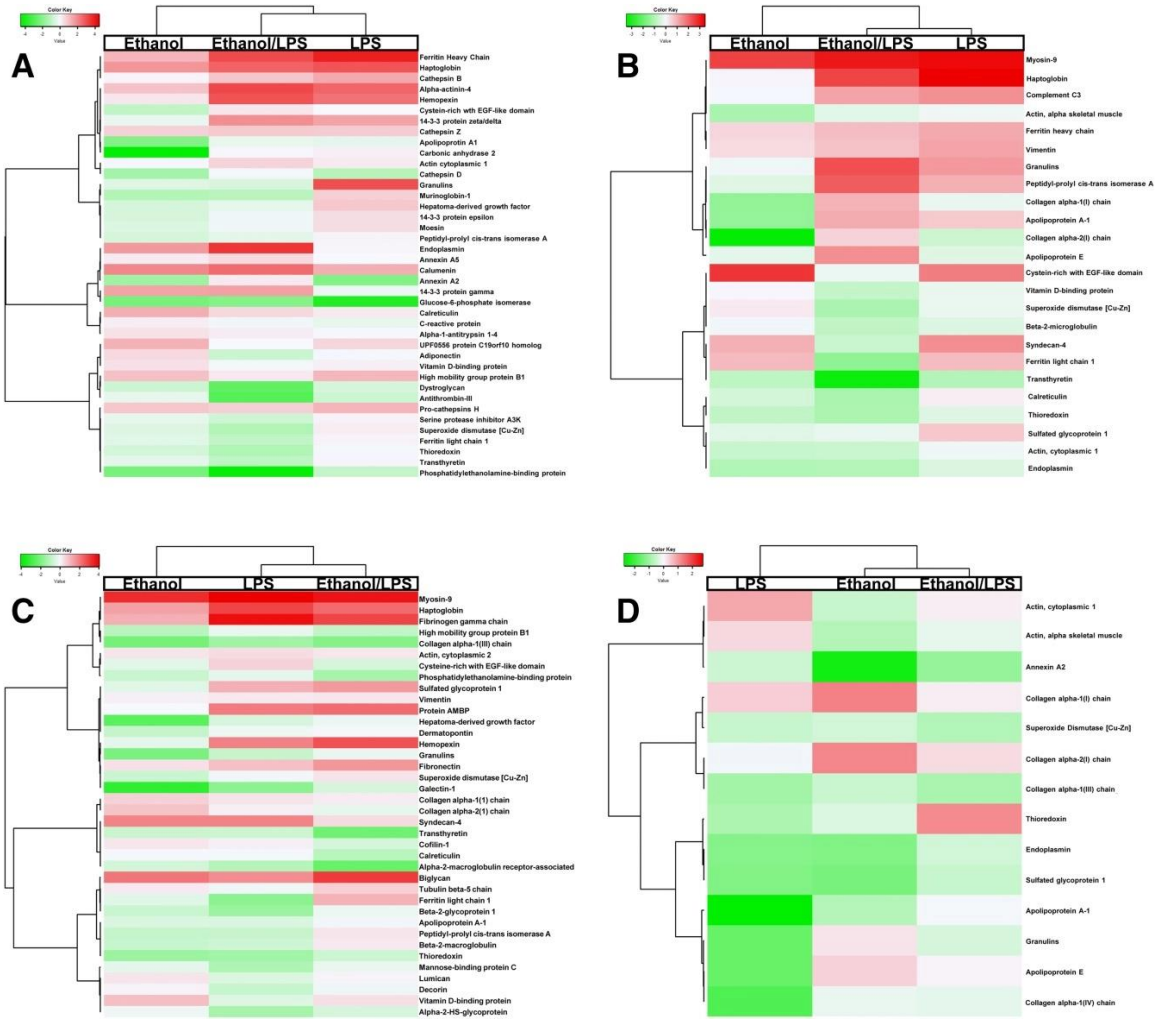
A
Ethanol
Ethanol//LPS
LPS
Ferritin Heavy Chain
Haptoglobin
Cathepsin B
Alpha-actinin-4
Hemopexin
Cystein-rich wth EGF-like domain
14-3-3 protein zeta/delta
Cathepsin Z
Apolipoprotin A1
Carbonic anhydrase 2
Actin cytoplasmic 1
Cathepsin D
Granulins
Murinoglobin-1
Hepatoma-derived growth factor
14-3-3 protein epsilon
Moesin
Peptidyl-prolyl cis-trans isomerase A
Endoplasmin
Annexin A5
Calumenin
Annexin A2
14-3-3 protein gamma
Glucose-6-phosphate isomerase
Calreticulin
C-reactive protein
Alpha-1-antitrypsin 1-4
UPF0556 protein C19orf10 homolog
Adiponectin
Vitamin D-binding protein
High mobility group protein B1
Dystroglycan
Antithrombin-III
Pro-cathepsins H
Serine protease inhibitor A3K
Superoxide dismutase [Cu-Zn]
Ferritin light chain 1
Thioredoxin
Transthyretin
Phosphatidylethanolamine-binding protein
B
Ethanol
Ethanol/LPS
LPS
Myosin-9
Haptoglobin
Complement C3
Actin, alpha skeletal muscle
Ferritin heavy chain
Vimentin
Granulins
Peptidyl-prolyl cis-trans isomerase A
Collagen alpha-1(I) chain
Apolipoprotein A-1
Collagen alpha-2(I) chain
Apolipoprotein E
Cystein-rich with EGF-like domain
Vitamin D-binding protein
Superoxide dismutase [Cu-Zn]
Beta-2-microglobulin
Syndecan-4
Ferritin light chain 1
Transthyretin
Calreticulin
Thioredoxin
Sulfated glycoprotein 1
Actin, cytoplasmic 1
Endoplasmin
C
Ethanol
LPS
Ethanol//LPS
Myosin-9
Haptoglobin
Fibrinogen gamma chain
High mobility group protein B1
Collagen alpha-1(III) chain
Actin, cytoplasmic 2
Cysteine-rich with EGF-like domain
Phosphatidylethanolamine-binding protein
Sulfated glycoprotein 1
Vimentin
Protein AMBP
Hepatoma-derived growth factor
Dermatopontin
Hemopexin
Granulins
Fibronectin
Superoxide dismutase [Cu-Zn]
Galectin-1
Collagen alpha-1(1) chain
Collagen alpha-2(1) chain
Syndecan-4
Transthyretin
Cofilin-1
Calreticulin
Alpha-2-macroglobulin receptor-associated
Biglycan
Tubulin beta-5 chain
Ferritin light chain 1
Beta-2-glycoprotein 1
Apolipoprotein A-1
Peptidyl-prolyl cis-trans isomerase A
Beta-2-macroglobulin
Thioredoxin
Mannose-binding protein C
Lumican
Decorin
Vitamin D-binding protein
Alpha-2-HS-glycoprotein
D
LPS
Ethanol
Ethanol//LPS
Actin, cytoplasmic 1
Actin, alpha skeletal muscle
Annexin A2
Collagen alpha-1(I) chain
Superoxide Dismutase [Cu-Zn]
Collagen alpha-2(I) chain
Collagen alpha-1(III) chain
Thioredoxin
Endoplasmin
Sulfated glycoprotein 1
Apolipoprotein A-1
Granulins
Apolipoprotein E
Collagen alpha-1(IV) chain

**Figure 3.7: Clustered profiles of protein abundances for proteins identified in the NaCl fraction.**

Abundance values for each protein were first standardized to a mean of zero and a standard deviation of one prior to clustering. See also Table 3.2.

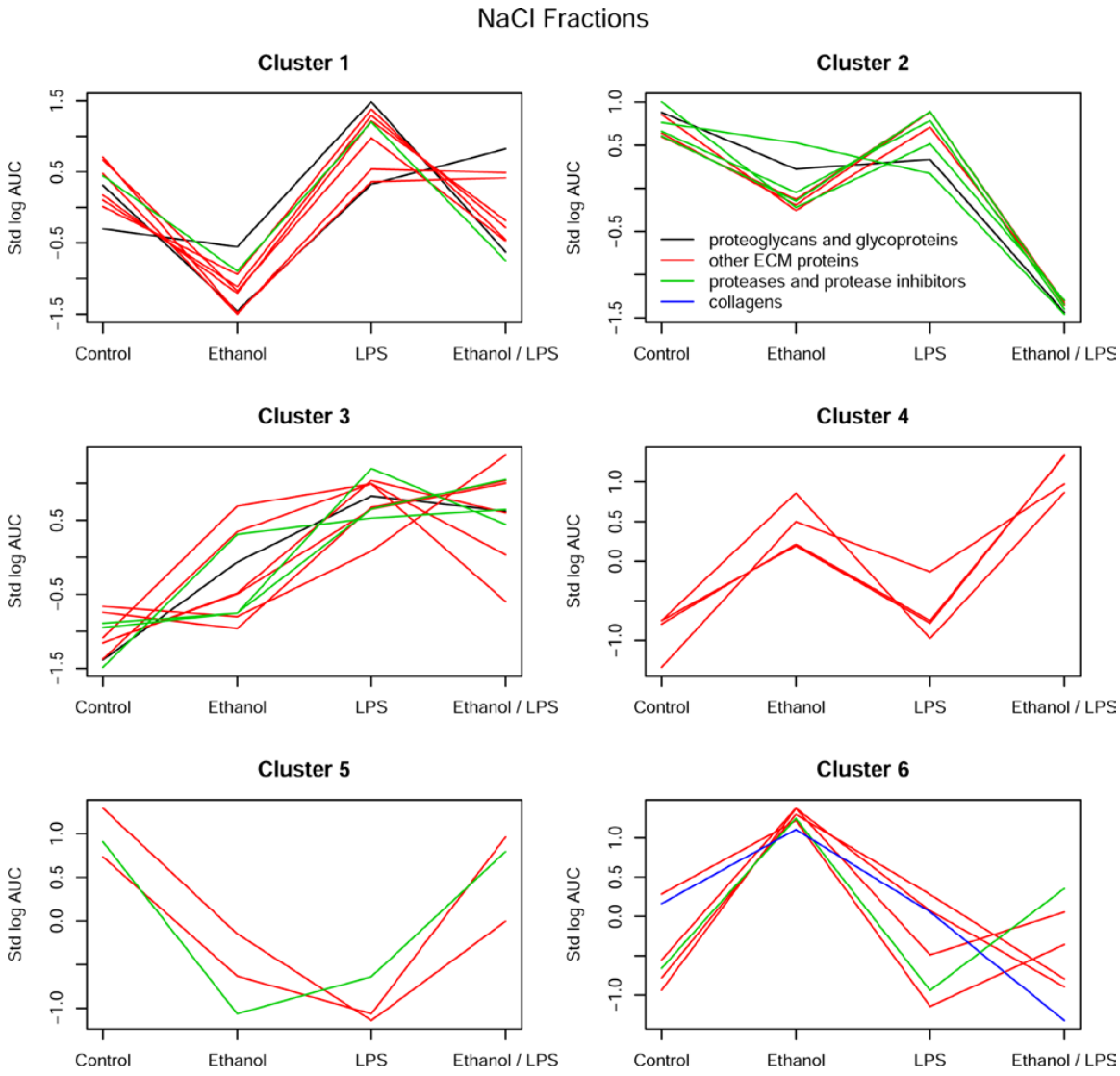
NaCl Fractions
Cluster 1
Cluster 2
Cluster 3
Cluster 4
Cluster 5
Cluster 6
Std log AUC
Control
Ethanol
LPS
Ethanol / LPS
proteoglycans and glycoproteins
other ECM proteins
proteases and protease inhibitors
collagens

**Figure 3.8: Clustered profiles of protein abundances for proteins identified in the SDS fraction.**

Abundance values for each protein were first standardized to a mean of zero and a standard deviation of one prior to clustering. See also Table 3.2.

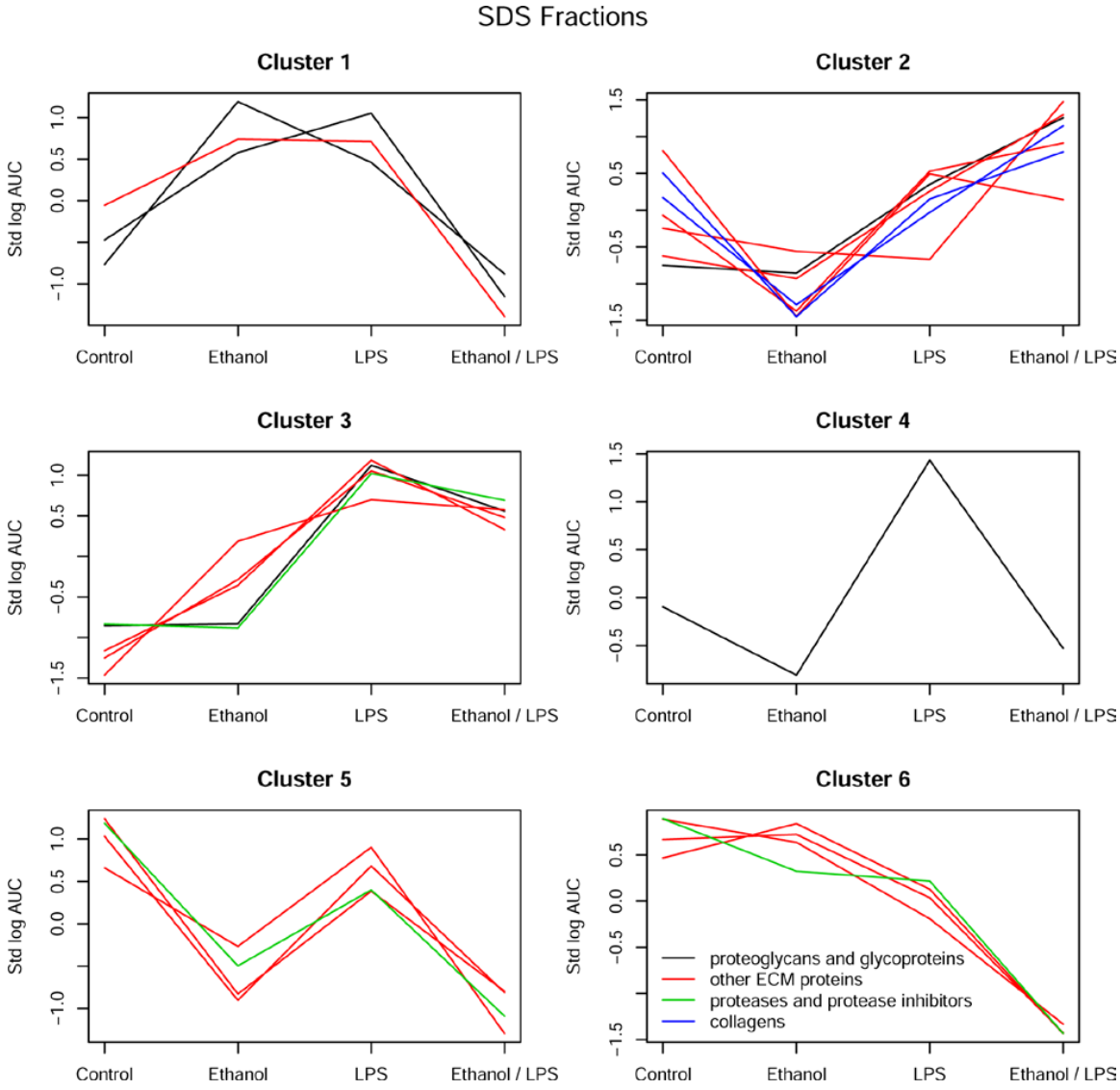
SDS Fractions
Cluster 1
Cluster 2
Cluster 3
Cluster 4
Cluster 5
Cluster 6
Std log AUC
Control
Ethanol
LPS
Ethanol / LPS
proteoglycans and glycoproteins
other ECM proteins
proteases and protease inhibitors
collagens

**Figure 3.9: Clustered profiles of protein abundances for proteins identified in the GnHCl fraction.**

Protein abundances were first standardized to a mean zero and a standard deviation one for each protein prior to clustering. See also Table 3.2.

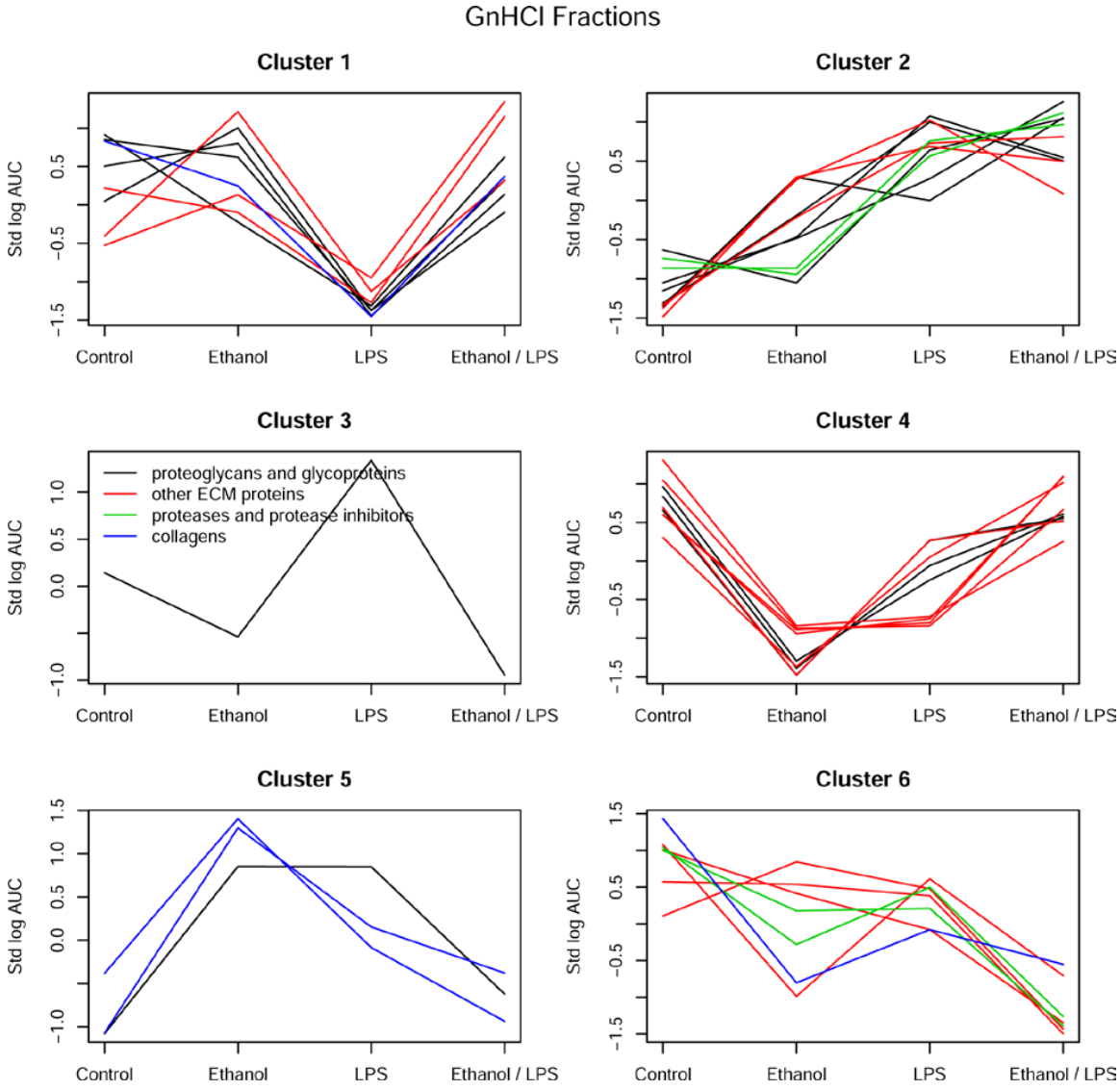
GnHCl Fractions
Cluster 1
Cluster 2
Cluster 3
Cluster 4
Cluster 5
Cluster 6
Std log AUC
Control
Ethanol
LPS
Ethanol / LPS
proteoglycans and glycoproteins
other ECM proteins
proteases and protease inhibitors
collagens

**Figure 3.10: Clustered profiles of protein concentrations for proteins identified in the pellet.**

Abundance values for each protein were standardized to a mean of zero and a standard deviation of one prior to clustering. See also Table 3.2.

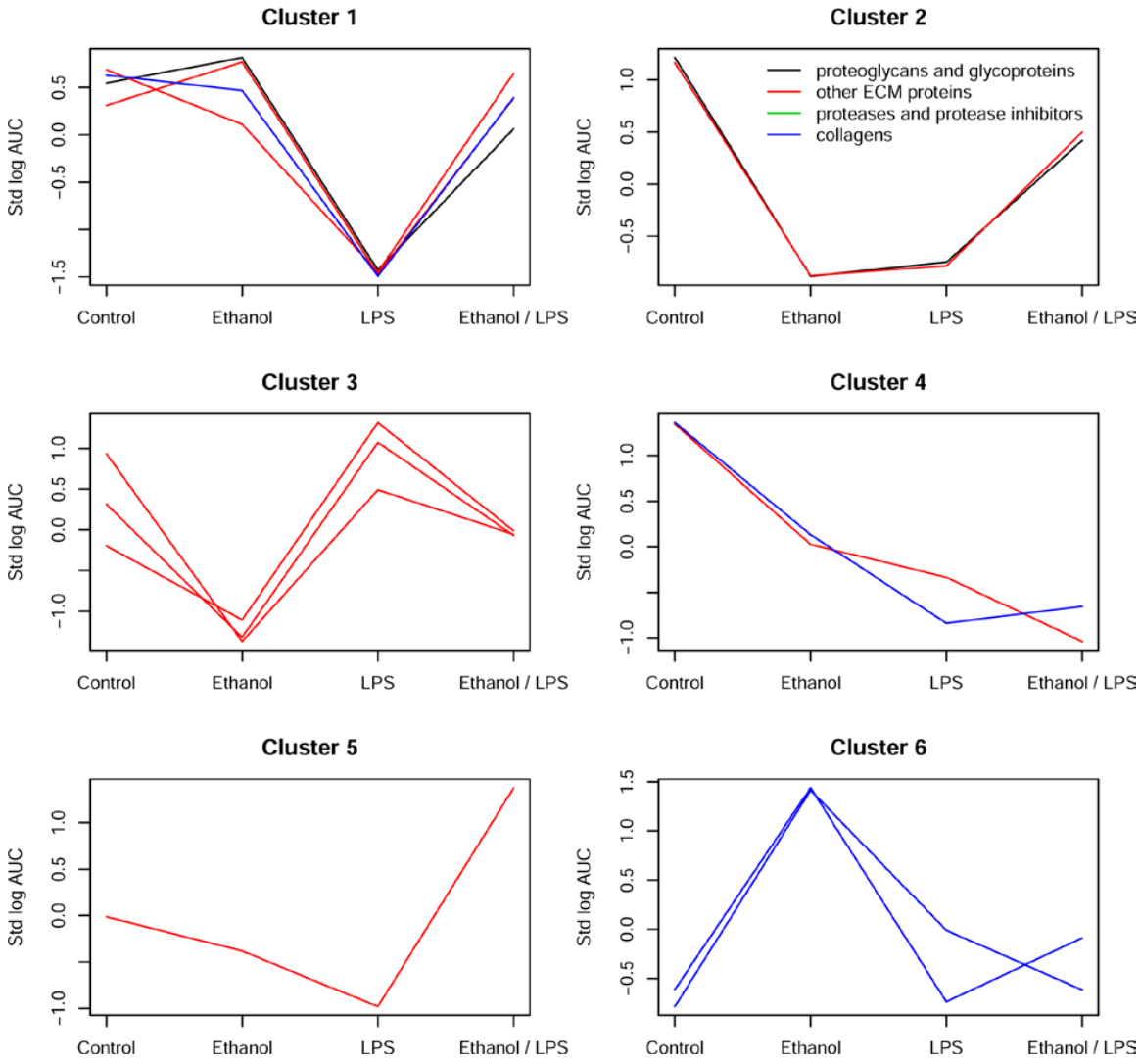
Pellet Fractions
Cluster 1
Cluster 2
Cluster 3
Cluster 4
Cluster 5
Cluster 6
Std log AUC
Control
Ethanol
LPS
Ethanol / LPS
proteoglycans and glycoproteins
other ECM proteins
proteases and protease inhibitors
collagens

## Table 3.2: Clustering of proteins in response to ethanol and/or LPS

| NaCl fraction | | |
|---|---|---|
| **Protein** | **Class** | **Cluster** |
| 14-3-3 protein epsilon | other ECM proteins | 1 |
| Apolipoprotein A-I | other ECM proteins | 1 |
| Carbonic anhydrase 2 | other ECM proteins | 1 |
| Cysteine-rich with EGF-like domain protein | proteoglycans and glycoproteins | 1 |
| Granulins | proteoglycans and glycoproteins | 1 |
| Hepatoma-derived growth factor | other ECM proteins | 1 |
| Moesin | other ECM proteins | 1 |
| Murinoglobulin-1 | proteases and protease inhibitors | 1 |
| Peptidyl-prolyl cis-trans isomerase A | other ECM proteins | 1 |
| Antithrombin-III | proteases and protease inhibitors | 2 |
| Dystroglycan | proteoglycans and glycoproteins | 2 |
| Ferritin light chain 1 | other ECM proteins | 2 |
| Phosphatidylethanolamine-binding protein 1 | proteases and protease inhibitors | 2 |
| Serine protease inhibitor A3K | proteases and protease inhibitors | 2 |
| Superoxide dismutase [Cu-Zn] | other ECM proteins | 2 |
| Thioredoxin | other ECM proteins | 2 |
| Transthyretin | proteases and protease inhibitors | 2 |
| 14-3-3 protein zeta/delta | other ECM proteins | 3 |
| Actin, cytoplasmic 1 | other ECM proteins | 3 |
| Alpha-actinin-4 | other ECM proteins | 3 |
| Cathepsin B | proteases and protease inhibitors | 3 |
| Cathepsin Z | proteases and protease inhibitors | 3 |
| Ferritin heavy chain | other ECM proteins | 3 |

| | | |
|---|---|---|
| Haptoglobin | proteoglycans and glycoproteins | 3 |
| Hemopexin | proteases and protease inhibitors | 3 |
| High mobility group protein B1 | other ECM proteins | 3 |
| Pro-cathepsin H | other ECM proteins | 3 |
| 14-3-3 protein gamma | other ECM proteins | 4 |
| Annexin A5 | other ECM proteins | 4 |
| Calumenin | other ECM proteins | 4 |
| Endoplasmin | other ECM proteins | 4 |
| Annexin A2 | other ECM proteins | 5 |
| Cathepsin D | proteases and protease inhibitors | 5 |
| Glucose-6-phosphate isomerase | other ECM proteins | 5 |
| Alpha-1-antitrypsin 1-4 | proteases and protease inhibitors | 6 |
| Calreticulin | other ECM proteins | 6 |
| C-reactive protein | other ECM proteins | 6 |
| UPF0556 protein C19orf10 homolog | other ECM proteins | 6 |
| Vitamin D-binding protein | other ECM proteins | 6 |
| Adiponectin | collagens | 6 |
| **SDS fraction** | | |
| Cysteine-rich with EGF-like domain protein 2 | proteoglycans and glycoproteins | 1 |
| Ferritin light chain 1 | other ECM proteins | 1 |
| Syndecan-4 | proteoglycans and glycoproteins other ECM proteins | 1 |
| Actin, alpha skeletal muscle | | 2 |
| Apolipoprotein A-I | other ECM proteins | 2 |
| Apolipoprotein E | other ECM proteins | 2 |
| Collagen alpha-1(I) chain | collagens | 2 |
| Collagen alpha-2(I) chain | collagens | 2 |
| Granulins | proteoglycans and glycoproteins | 2 |
| Peptidyl-prolyl cis-trans isomerase A other ECM proteins 2 Complement C3 proteases and protease inhibitors 3 | | |
| Ferritin heavy chain | other ECM proteins | 3 |
| Haptoglobin | proteoglycans and glycoproteins | 3 |
| Myosin-9 | other ECM proteins | 3 |

| | | |
|---|---|---|
| Vimentin | other ECM proteins | 3 |
| Sulfated glycoprotein 1 | proteoglycans and glycoproteins | 4 |
| Actin, cytoplasmic 1 | other ECM proteins | 5 |
| Calreticulin | other ECM proteins | 5 |
| Endoplasmin | other ECM proteins | 5 |
| Thioredoxin | proteases and protease inhibitors | 5 |
| Beta-2-microglobulin | other ECM proteins | 6 |
| Superoxide dismutase [Cu-Zn] | other ECM proteins | 6 |
| Transthyretin | proteases and protease inhibitors | 6 |
| Vitamin D-binding protein | other ECM proteins | 6 |
| **GnHCl fraction** | | |
| Alpha-2-HS-glycoprotein | proteoglycans and glycoproteins | 1 |
| Beta-2-glycoprotein 1 | proteoglycans and glycoproteins | 1 |
| Decorin | proteoglycans and glycoproteins | 1 |
| Ferritin light chain 1 | other ECM proteins | 1 |
| Lumican | proteoglycans and glycoproteins | 1 |
| Mannose-binding protein C | collagens | 1 |
| Tubulin beta-5 chain | other ECM proteins | 1 |
| Vitamin D-binding protein | other ECM proteins | 1 |
| Actin, cytoplasmic 2 | other ECM proteins | 2 |
| Biglycan | proteoglycans and glycoproteins | 2 |
| Fibrinogen gamma chain | proteoglycans and glycoproteins | 2 |
| Fibronectin | proteoglycans and glycoproteins | 2 |
| Haptoglobin | proteoglycans and glycoproteins | 2 |
| Hemopexin | proteases and protease inhibitors | 2 |
| Myosin-9 | other ECM proteins | 2 |
| Protein AMBP | proteases and protease inhibitors | 2 |
| Sulfated glycoprotein 1 | proteoglycans and glycoproteins | 2 |
| Vimentin | other ECM proteins | 2 |
| Cysteine-rich with EGF-like domain protein 2 | proteoglycans and glycoproteins | 3 |
| Apolipoprotein A-I | other ECM proteins | 4 |
| Beta-2-microglobulin | other ECM proteins | 4 |
| Dermatopontin | proteoglycans and glycoproteins | 4 |
| Galectin-1 | proteoglycans and glycoproteins | 4 |
| Granulins | proteoglycans and glycoproteins | 4 |
| Hepatoma-derived growth factor | other ECM proteins | 4 |

| | | |
|---|---|---|
| Peptidyl-prolyl cis-trans isomerase A | other ECM proteins | 4 |
| Superoxide dismutase [Cu-Zn] | other ECM proteins | 4 |
| Thioredoxin | other ECM proteins | 4 |
| Collagen alpha-1(I) chain | collagens | 5 |
| Collagen alpha-2(I) chain | collagens | 5 |
| Syndecan-4 | proteoglycans and glycoproteins | 5 |
| Alpha-2-macroglobulin receptor-associated protein | other ECM proteins | 6 |
| Calreticulin | other ECM proteins | 6 |
| Cofilin-1 | other ECM proteins | 6 |
| Collagen alpha-1(III) chain | collagens | 6 |
| High mobility group protein B1 | other ECM proteins | 6 |
| Phosphatidylethanolamine-binding protein 1 | proteases and protease inhibitors | 6 |
| Transthyretin | proteases and protease inhibitors | 6 |
| **Pellet fraction** | | |
| Apolipoprotein A-I | other ECM proteins | 1 |
| Apolipoprotein E | other ECM proteins | 1 |
| Collagen alpha-1(IV) chain | collagens | 1 |
| Granulins | proteoglycans and glycoproteins | 1 |
| Endoplasmin | other ECM proteins | 2 |
| Sulfated glycoprotein 1 | proteoglycans and glycoproteins | 2 |
| Actin, alpha skeletal muscle | other ECM proteins | 3 |
| Actin, cytoplasmic 1 | other ECM proteins | 3 |
| Annexin A2 | other ECM proteins | 3 |
| Collagen alpha-1(III) chain | collagens | 4 |

| | | |
|---|---|---|
| Superoxide dismutase [Cu-Zn] | other ECM proteins | 4 |
| Thioredoxin other ECM proteins 5 Collagen alpha-1(I) chain collagens 6 | | |
| Collagen alpha-2(I) chain | collagens | 6 |

(>4-fold increase) changes caused by LPS included ferritin heavy chain (15-fold increase) in the NaCl fraction, haptoglobin and myosin-9 (11- and 9-fold, respectively) in the SDS fraction, and fibrinogen γ chain and haptoglobin (14- and 7-fold, respectively) in the GnHCl fraction. Likewise, ethanol exposure increased the abundance of several proteins, including myosin-9 (6-fold) and cysteine-rich with EGF-like domain protein 2 (CREDL2; 6-fold) in the SDS fraction. As was observed for qualitative analysis (Fig. 3.4), ethanol and/or LPS affected proteins in the pellet fraction the least of all fractions.

While ethanol alone and LPS alone each changed the abundance of certain proteins, the combination of the two exposures caused its own unique effects on the matrisome (Figs. 3.7-3.10). For example, although LPS alone did not change endoplasmin abundance compared to control, and ethanol only increased it 3-fold, the combination of ethanol and LPS increased this endoplasmin abundance 11-fold in the NaCl fraction (Figs. 3.5 and 3.6). Similarly, the combination of ethanol and LPS increased granulin abundance 5-fold in the SDS fraction, despite no effect by ethanol alone and only a 2-fold increase by LPS (Figs. 3.5 and 3.6). Additionally, although both ethanol alone and LPS alone increased CRELD2, the combination of ethanol and LPS decreased CRELD2 abundance in the SDS fraction. Proteins that were differentially regulated by the combination of ethanol and LPS in the GnHCl fraction include hemopexin and alpha-1-microglobulin/bikunin precursor.

## D. DISCUSSION

This work had two primary goals: (1) to characterize and validate an extraction and analysis method for the hepatic matrisome that would provide both the sensitivity to identify low-abundance proteins and the power to observe global changes and (2) to use this method to explore transitional (i.e., prefibrotic) changes to the hepatic matrisome caused by ethanol diet and/or LPS exposure. As discussed in the Introduction, the study of the hepatic ECM has largely been "collagenocentric" and "fibrosocentric"—that is, centered on the dramatic increase in collagen deposition during fibrosis, a quasi-permanent scarring of the organ. However, the matrisome of both healthy and diseased liver is exceedingly more diverse than collagen ECM. Indeed, studies have revealed that in addition to collagen, laminin (118) and vitronectin (119, 120) are also increased during fibrogenesis. Furthermore, proteomic studies in other organs have shown that matrisome composition responds dynamically after insult well before organ fibrosis.(99, 114, 121) Previously, this group showed that fibrin ECM accumulation correlates with inflammatory liver injury in several models and may play a causal role in hepatic damage.(89) Additionally, Gillis et al. (90) have demonstrated a similar role for fibronectin ECM in experimental ALD. However, global changes in the hepatic ECM during inflammatory liver injury have not yet been characterized. The models herein employed (Lieber-DeCarli ethanol diet and acute LPS) are well known to cause significant liver damage, but do not result in histologically detectable changes to the ECM.

Global ECM changes may affect tissue function through three general types of mechanisms: physical, biochemical, and signaling. Physical properties of the

ECM include the matrix topography, cross-linking, and organization.(21) These physical properties are not only essential to the structural role of the ECM, but also allow the ECM to either obstruct or facilitate cell migration.(49) Fibrin matrices have been demonstrated to be permissive to monocyte and leukocyte chemotaxis and activation.(122, 123) Physical alterations in the ECM can cause tissue rigidity, resulting in decreased organ function. Although such physical changes to the ECM can indirectly affect the biochemistry of the liver (e.g., hemostasis-induced hypoxia), matrisome changes can also directly cause biochemical changes that are independent of structural changes. For example, ECM components can facilitate ligand-receptor interactions, (124) bind and retain chemokines,(18) and regulate activation of growth factors (i.e., transforming growth factor beta). (18) ECM molecules can also directly serve as signaling molecules through interactions with cell-surface receptors, including integrins. (125) Because of the multifaceted roles of many ECM molecules, any single change in the ECM can, in principle, trigger a cascade of dependent changes that influence the composition and properties of the ECM. For example, biglycan acts as a structural component that regulates collagen fiber assembly, but, upon release from the matrix, can act as a signaling molecule binding to Toll-like receptor 4 (TLR4) receptors.(126)

The current study determined the individual and combined effects of two experimental exposures (ethanol and LPS) on the hepatic matrisome. LPS was selected because it induces robust hepatic inflammation. The liver is often exposed to LPS during several pathophysiologic states, including after alcohol

consumption.(127) Whereas inflammatory responses triggered by small doses of LPS are typically noninjurious, other stresses can synergistically enhance the hepatotoxic response to LPS. Indeed, ethanol not only increases circulating LPS, but also enhances inflammation and liver damage caused by acute LPS exposure.(117) This “two-hit” paradigm is common in fatty liver diseases. (64) In the current study, both stresses caused the hepatic matrisome to respond dynamically, not only increasing the number of matrisome proteins , but also differentially changing protein abundance (Fig. 3.5) and likely structure or location (Figs. 3.4 and 3.5).

Several of the protein changes reported here reiterate results of previous hypothesis-driven studies. For example, this work validated that LPS dramatically alters the fibrin(ogen) ECM, and that ethanol preexposure enhances this effect. In the current study, LPS exposure increased the relative abundance of fibrinogen gamma chain in the GnHCl extract. The fibrin(ogen) gamma chain is a major component of fibrin clots given that it is polymerized into insoluble fibrin fibers.(128) Therefore, the localization of this robust increase in fibrinogen gamma chain in the GnHCl fractions suggests that there was an increase in fibrin(ogen) gamma chain polymerization into a less-soluble, more highly cross-linked form. Furthermore, the combination of ethanol and LPS resulted in detection of the fibrin(ogen) gamma chain in the insoluble pellet, which suggests additional modifications that decreased solubility (e.g., cross-linking). The appearance of serum amyloid A-1 and A-2 proteins in response to LPS was also confirmed here. (129, 130) In fact, LPS exposure increased the abundance of

several other acute-phase proteins, including haptoglobin, complement C, and ceruloplasmin, which are all known to be increased by LPS exposure. (131-133) This work also validates previous studies which reported ethanol increased fibronectin deposition before the onset of fibrosis. (90)

The work herin also identified novel changes caused by ethanol and LPS. For example, previous studies have shown an association between vitronectin accumulation and HF/end-stage liver disease.(119, 120) The results of the current study suggest that more subtle changes in vitronectin abundance occur before the onset of fibrosis and hepatic decompensation. Ethanol exposure also resulted in the detection of galectin-1. Galectin-1 is a glycosaminoglycan-binding lectin associated with cell proliferation and adhesion through modulation of glycoprotein cross-linking. Galectin-1 may also play a role in hepatic inflammation and fibrinogenesis.(134) These data suggest that ethanol and/or LPS likely contribute to a multitude of changes in the ECM composition, many of which have not yet been fully investigated.

Changes in abundance of protease and protease inhibitors can also contribute to inflammatory liver injury and fibrogenesis. In the current study, several ECM-associated proteases were increased in response to stress, including plasmin(ogen), antithrombin III, dipeptidyl peptidase, and alpha-1-antitrypsin. Stress also resulted in the presence of protease inhibitors, such as serpine B5 (maspin) and plasminogen activator inhibitor-1 (PAI-1). Ethanol and/or LPS increased several other proteases and protease inhibitors that may be critical for ECM homeostasis (e.g., transthyretin, phosphatidylethanolamin-

binding protein-1 [PEBP1], and serine protease inhibitor A2K). These data support the notion that transitional remodeling of the hepatic matrisome is bidirectional, driven by both increased secretion of matrix proteins as well as altered ECM degradation.

As mentioned above, ethanol is well known to synergize liver damage caused by LPS exposure. In the current study, the combination of ethanol and LPS resulted in unique changes to the hepatic matrisome compared to either ethanol or LPS alone. Indeed, coexposure differentially increased fibronectin and biglycan abundance (Fig. 3.3; Table 3.1). Fibronectin accumulation caused by ethanol may contribute to hepatic inflammation through stimulation of Kupffer cells (KCs). (135) Biglycan is a small proteoglycan that was first recognized as a structural component and signaling molecule in the ECM (136). Biglycan has also been implicated in inflammation, (137) possibly by retaining proinflammatory cytokines,(138) and/or by activating TLR4 signaling.(138) These data suggest that biglycan abundance may be increased in prefibrotic stages of liver disease. In contrast, the combination of ethanol and LPS synergistically decreased PEBP1; this enzyme has been shown to inhibit trypsin-like serine proteases, including thrombin, but not trypsin or tissue-type plasminogen activator.(139) Multiple studies have identified PEBP1 as a critical player in metastasis (140) and have defined it as a metastasis suppressor gene.(141) These changes represent dynamic (and potentially unique) responses of hepatic ECM to stress that may serve as a basis for future biomarker and/or mechanistic studies.

Whereas it is well established that myofibroblast-like cells (e.g., hepatic stellate cells) are the primary source of fibrillar ECM during HF, most, if not all, hepatic cells contribute to overall matrisome homeostasis. For example, hepatic sinusoidal endothelial cells are almost solely responsible for the metabolism and degradation of hyaluronic acid. Furthermore, stress causes inflammatory cells (e.g., KCs) and hepatocytes release proteases and protease inhibitors (e.g., PAI-1) that can affect the ECM. Extrahepatic sources (e.g., the coagulation and complement cascades) can also affect the hepatic matrisome. The ECM not only serves as a physical structure, but also binds/interacts with several biomolecules that can directly or indirectly alter responses. For example, ECM/integrin interactions mediate rapid and dynamic responses to changes in the environment. It is known that fibrotic ECM is known to influence cell phenotype, inflammation, and metastasis in the liver.(142-144) The effects of the ECM changes observed here on earlier stages of liver injury should be investigated.

In summary, the results of this work demonstrate that the hepatic matrisome responds dynamically to both chronic (ethanol) and acute (LPS) stresses, preceding more-dramatic fibrotic changes to the liver. It is likely that these transitional changes to the hepatic ECM contribute to the pathological responses to these stresses. It is also interesting that several ECM proteins responded similarly to both stresses, suggesting a shared mechanism in both models. Protein changes that were unique to either ethanol or LPS exposure alone (or their combination) also represent potential new biomarkers or targets. These

results therefore serve as a foundation for future analyses in models of liver disease.

# CHAPTER IV

# NOVEL BIOMARKERS IN ALCOHOLIC HEPATITIS: ANALYSIS OF THE PLASMA PEPTIDOME/DEGRADOME

## A. Introduction

AH is an acute sequela of alcoholic liver disease with a high mortality rate of 30-50% at 3 months and 40% at 6 months.(72, 73) AH is characterized by jaundice and liver failure.(145) AH occurs in patients with heavy chronic alcohol consumption (80-100 g per day) and severe ASH with or without advanced fibrosis and/or cirrhosis.(145, 146) AH can be the first manifestation of clinically silent ALD or an exacerbation of pre-existing cirrhosis.(145)

Accurately predicting AH patient outcome is important for clinical decision-making. For example, AH patients with higher risk are better candidates for corticosteroid treatment, and patients with lower risk could be candidates for long-term clinical studies.(72, 145) While identifying AH patients at risk of liver inflammatory injury and failure is important, it is also difficult. Currently, the best approach for predicting outcome is combining static scores, such as the modified Maddrey's discriminant-function, MELD, ABIC (Age, Bilirubin, INR and Creatinine) and/or Glasgow with the dynamic Lille scoring system.(147) These

clinical scores are useful for predicting outcome in patients with severe disease, but are more limited in predicting outcome in patients with moderate AH.(84)

Our group recently demonstrated significant ECM remodeling during inflammatory liver injury (93). During such remodeling, peptide fragments of the degraded ECM increase in biologic fluids (e.g., plasma) (58). Peptidomic analysis of the degraded ECM (i.e., 'degradome') is a useful diagnostic/prognostic tool in metastatic cancers and other diseases of ECM remodeling (58).

It was hypothesized that the severe inflammatory liver injury caused by AH would yield a unique degradome profile in human patient plasma, and that ECM peptides would change between patient groups. The goals of this work are twofold: 1.) to identify novel candidate biomarkers for AH, and 2.) to develop new mechanistic hypotheses by predicting proteases that generated the observed degradome.

## B. Experimental procedures

### 1. Study participants and inclusion criteria

AH patients, AUD patients, and healthy volunteers were enrolled in the study as described in Chapter II.

### 2. Study paradigm

Relevant clinical data were collected as described in Chapter II. As provided in the workflow scheme in Figure 4.1, this study was designed to analyze plasma peptides for comparison between healthy volunteers, AUD patients ("mild", with

or without liver injury), patients with moderate AH, and patients with severe AH for potential associations between parameters.

### 3. Plasma collection

Plasma was collected from study participants as described in Chapter II.

### 4. Plasma peptide purification

Plasma peptide purification was optimized and carried out as described in Chapter II.

### 5. Liquid chromatography and tandem mass spectrometry

LC-MS/MS analysis was carried out as described in Chapter II

### 6. Data analysis

Peptidomic data analysis was performed as described in Chapter II.

### 7. Statistical analysis

Peptidomic data were $\log_2$ transformed prior to statistical analysis. Statistical analysis was performed as described in Chapter II.

## C. Results

### 1. Patient demographics

A total of 114 participants including healthy volunteers (n=7) and AH (n=107) patients stratified by MELD scores into three categories were studied. AH

**Figure 4.1: Scheme of peptidomic workflow.**

Plasma samples were handled randomly in balanced proportions between groups to avoid systematic bias. Plasma peptides were purified by TCA precipitation and underwent LC-MS/MS analysis with de novo spectrum assignment. We identified peptides significantly changing between MELD groups.

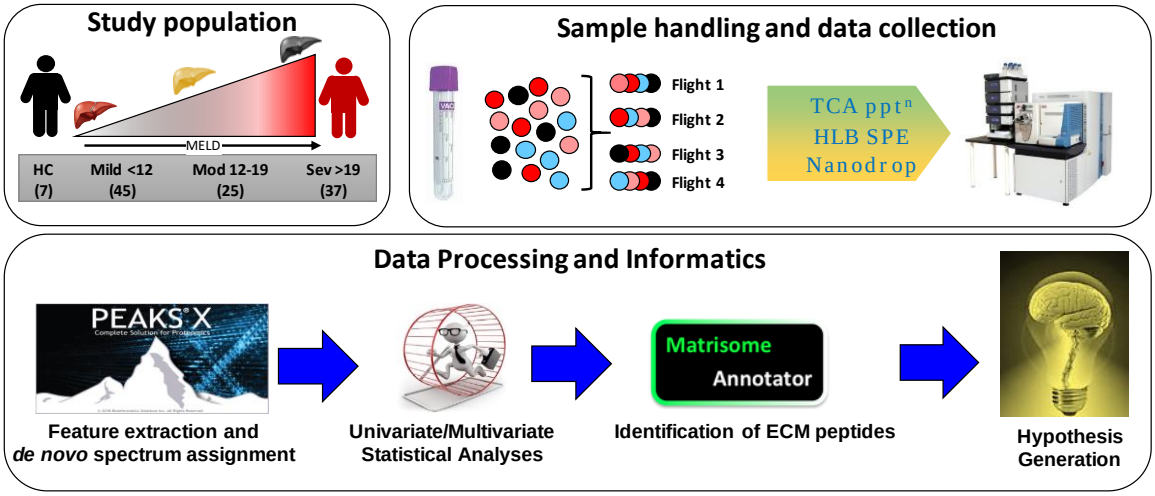
Study population
MELD
HC (7)
Mild <12 (45)
Mod 12-19 (25)
Sev >19 (37)
Sample handling and data collection
Flight 1
Flight 2
Flight 3
Flight 4
TCA ppt$^{n}$
HLB SPE
Nanodrop
Data Processing and Informatics
PEAKS X
Feature extraction and de novo spectrum assignment
Univariate/Multivariate Statistical Analyses
Matrisome Annotator
Identification of ECM peptides
Hypothesis Generation

patients with AUDs having a MELD score less than 12 were assigned to the mild category (n=45), patients having a MELD score between 12 and 19 were assigned to the moderate category (n=25), and patients having a MELD score greater than 19 were assigned to the severe category (n=37). The AUD/mild category was further subdivided into patients without liver injury (ALT<40, “Mild-A”, n= 14) with liver injury (ALT≥40, “Mild-B”, n=31). A variety of clinical data was gathered for these patients, including transaminases, alkaline phosphatase, and total bilirubin. Table 4.1 shows a list of demographics and clinical data for the healthy, AUD (‘mild’), moderate AH, and severe AH participants.

**2. Plasma peptides change between MELD groups**

To visualize differences in the patients based on the peptidomic data, PCA was carried out (Fig. 4.2). Principal components 1 and 2 accounted for 51.59% and 5.14% of the variability between the five peptidome cohorts. PCA1 was the component explaining the largest set of variability (51.59%) in the data as could be attributed to the differences between Mild-A + Mild-B versus Moderate + Severe peptidomes. PCA2 was the component explaining the second largest set of variability in the data (5.14%). This component was 10-fold less than PCA1 and could be attributed to the differences between Healthy Controls versus AH (Mild-A + Mild-B + Moderate + Severe). The hierarchical clustering of the peptidome as grouped patient samples by similar MELD scores (Healthy Control; Mild-A and Mild-B; Moderate and Severe) identified three primary clusters of

**Table 4.1: Patient demographics**

| | **Age** | | | | |
|---|---|---|---|---|---|
| **Groups** | **Healthy volunteer** | **Mild-A*** | **Mild-B**** | **Moderate***** | **Severe***** |
| # Samples | 7 | 14 | 31 | 25 | 37 |
| # Missing | 0 | 0 | 0 | 2 | 0 |
| Mean | 28.14 | 40.02 | 44.05 | 49.83 | 48.92 |
| Median | 26.00 | 37.30 | 44.00 | 51.00 | 50.00 |
| Std. Dev. | 4.74 | 11.74 | 10.26 | 9.97 | 10.67 |
| Min. | 25.00 | 25.30 | 23.19 | 31.00 | 27.00 |
| Max. | 38.00 | 62.90 | 67.00 | 63.00 | 66.00 |
| | | | | | |
| | **AST (SGOT) (IU/L)** | | | | |
| **Groups** | **Healthy volunteer** | **Mild-A$^{NS}$** | **Mild-B**** | **Moderate**** | **Severe**** |
| # Samples | 7 | 14 | 31 | 25 | 37 |
| # Missing | 2 | 0 | 0 | 2 | 0 |
| Mean | 24.40 | 36.00 | 131.55 | 135.30 | 141.08 |
| Median | 25.00 | 26.00 | 96.00 | 114.00 | 122.00 |
| Std. Dev. | 2.88 | 20.00 | 103.71 | 77.66 | 71.26 |
| Min. | 21.00 | 17.00 | 21.00 | 18.00 | 41.00 |
| Max. | 28.00 | 87.00 | 388.00 | 347.00 | 370.00 |
| | | | | | |
| | **ALT (SGPT) (IU/L)** | | | | |
| **Groups** | **Healthy volunteer** | **Mild-A$^{NS}$** | **Mild-B$^{****}$** | **Moderate$^{NS}$** | **Severe$^{NS}$** |
| # Samples | 7 | 14 | 31 | 25 | 37 |
| # Missing | 2 | 0 | 0 | 2 | 0 |
| Mean | 20.40 | 27.57 | 97.68 | 59.78 | 48.95 |
| Median | 17.00 | 27.00 | 83.00 | 46.00 | 40.00 |
| Std. Dev. | 5.18 | 8.05 | 59.31 | 45.63 | 30.11 |
| Min. | 16.00 | 14.00 | 40.00 | 15.00 | 12.00 |
| Max. | 27.00 | 39.00 | 312.00 | 194.00 | 159.00 |
| | | | | | |
| | **Alkaline phosphatase (IU/L)** | | | | |
| **Groups** | **Healthy volunteer** | **Mild-A$^{NS}$** | **Mild-B$^{NS}$** | **Moderate***** | **Severe***** |
| # Samples | 7 | 14 | 31 | 25 | 37 |
| # Missing | 2 | 0 | 0 | 2 | 0 |
| Mean | 48.80 | 68.50 | 93.52 | 175.91 | 180.65 |
| Median | 54.00 | 64.50 | 91.00 | 147.00 | 157.00 |
| Std. Dev. | 10.92 | 27.05 | 25.62 | 109.32 | 83.90 |
| Min. | 37.00 | 44.00 | 56.00 | 41.00 | 72.00 |
| Max. | 59.00 | 147.00 | 150.00 | 483.00 | 443.00 |

| | | | | | |
|---|---|---|---|---|---|
| | **Bilirubin (mg/dL)** | | | | |
| **Groups** | **Healthy volunteer** | **Mild-A$^{NS}$** | **Mild-B$^{NS}$** | **Moderate$^{*}$** | **Severe$^{****}$** |
| # Samples | 7 | 14 | 31 | 25 | 37 |
| # Missing | 2 | 0 | 0 | 2 | 0 |
| Mean | 0.52 | 0.86 | 0.74 | 7.22 | 18.31 |
| Median | 0.50 | 0.60 | 0.60 | 5.10 | 18.20 |
| Std. Dev. | 0.13 | 0.93 | 0.57 | 7.66 | 7.69 |
| Min. | 0.40 | 0.20 | 0.20 | 0.60 | 4.70 |
| Max. | 0.70 | 4.00 | 2.60 | 35.00 | 34.20 |
| | | | | | |
| | **Albumin (g/L)** | | | | |
| **Groups** | **Healthy volunteer** | **Mild-A$^{NS}$** | **Mild-B$^{NS}$** | **Moderate$^{****}$** | **Severe$^{****}$** |
| # Samples | 7 | 14 | 31 | 25 | 37 |
| # Missing | 2 | 0 | 0 | 2 | 0 |
| Mean | 4.06 | 4.03 | 4.17 | 2.77 | 2.51 |
| Median | 4.20 | 4.10 | 4.20 | 2.80 | 2.40 |
| Std. Dev. | 0.31 | 0.34 | 0.50 | 0.68 | 0.46 |
| Min. | 3.60 | 3.20 | 2.60 | 1.70 | 1.60 |
| Max. | 4.40 | 4.50 | 5.20 | 4.50 | 3.50 |
| | | | | | |
| **Sex** | | | | | |
| **Groups** | **Healthy volunteer** | **Mild-A$^{ND}$** | **Mild-B$^{ND}$** | **Moderate$^{ND}$** | **Severe$^{ND}$** |
| # Samples | 7 | 14 | 31 | 25 | 37 |
| # Missing | 0 | 0 | 0 | 2 | 0 |
| # Males | 1 | 7 | 26 | 15 | 24 |
| # Females | 6 | 7 | 5 | 8 | 13 |
| | | | | | |
| **Ascites** | | | | | |
| **Groups** | **Healthy volunteer** | **Mild-A$^{ND}$** | **Mild-B$^{ND}$** | **Moderate$^{ND}$** | **Severe$^{ND}$** |
| # Samples | 7 | 14 | 31 | 25 | 37 |
| # Missing | 0 | 0 | 0 | 3 | 0 |
| # None | 7 | 14 | 30 | 11 | 5 |
| # Mild/Moderate | 0 | 0 | 1 | 11 | 25 |
| # Severe | 0 | 0 | 0 | 0 | 7 |
| | | | | | |
| **Plasma color** | | | | | |
| **Groups** | **Healthy volunteer** | **Mild-A$^{ND}$** | **Mild-B$^{ND}$** | **Moderate$^{ND}$** | **Severe$^{ND}$** |
| # Samples | 7 | 14 | 31 | 25 | 37 |
| # Missing | 0 | 1 | 2 | 11 | 10 |
| # Light yellow | 5 | 12 | 26 | 1 | 0 |

| | | | | | |
|---|---|---|---|---|---|
| # Light orange | 0 | 0 | 2 | 0 | 0 |
| # Light red | 0 | 0 | 1 | 0 | 0 |
| # Dark yellow | 0 | 0 | 0 | 12 | 23 |
| # Orange | 2 | 0 | 0 | 1 | 3 |
| # Red orange | 0 | 0 | 0 | 0 | 1 |
| # Red | 0 | 1 | 0 | 0 | 0 |

**ND- not determined**

**NS- not significant**

***p<0.05**

****p<0.01**

*****p<0.001**

******p<0.0001**

**Figure 4.2: Multivariate analysis of the plasma peptidome using principal component analysis biplots and heat maps with hierarchical clustering.** Patient differences for different AH severity groups based on peptidome were visualized using (Fig 5A) PCA and heat maps with hierarchical clustering (Fig 5B). PCA was carried out for significantly changed peptides (BH corrected p-value <0.05) using a linear mixed model approach. “Age” and “Sex” were considered fixed variables, and “Flight” and iRT1-11 peptide standards were considered random variables.

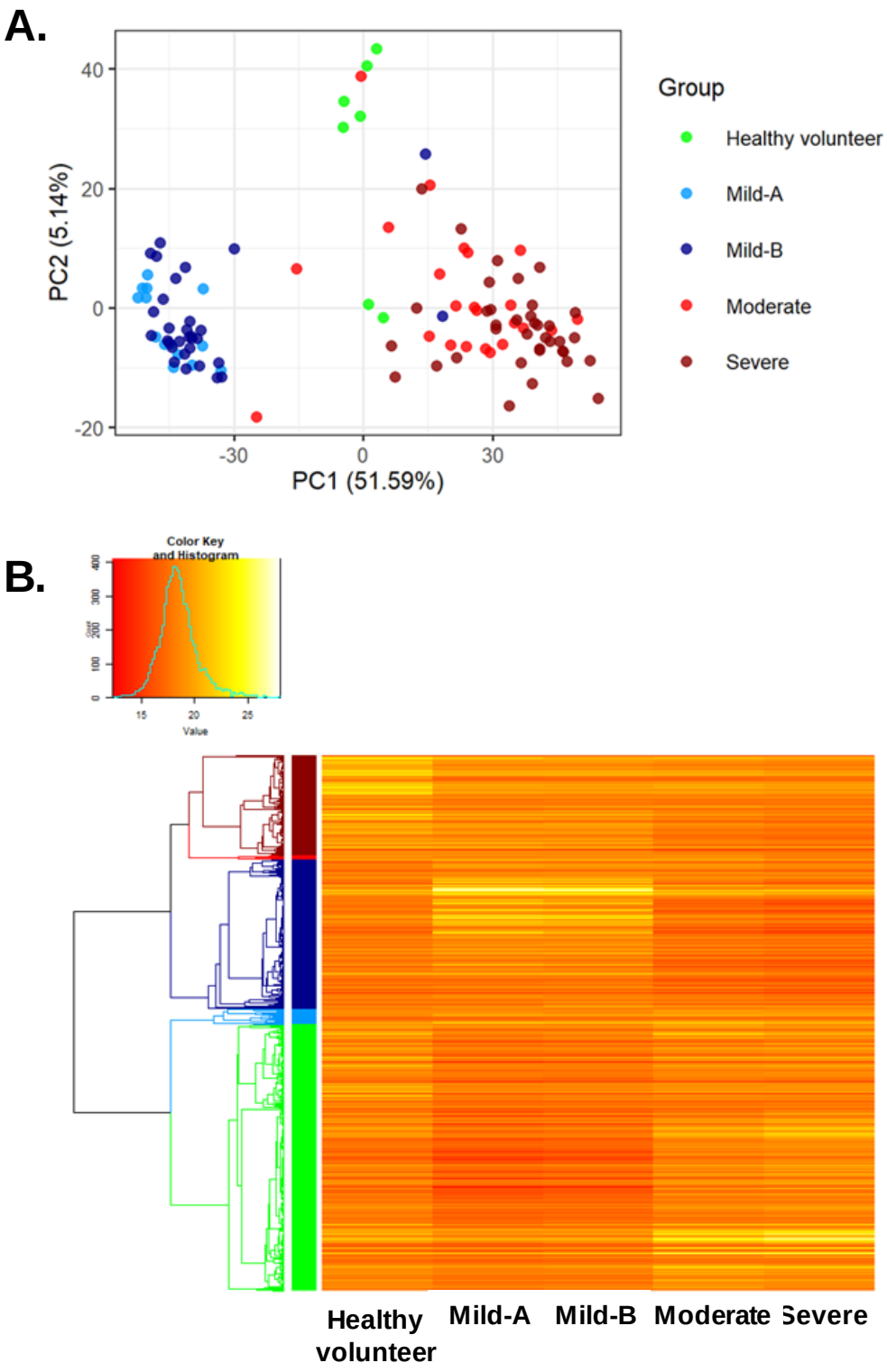
A.
PC2 (5.14%)
PC1 (51.59%)
40
20
0
-20
-30
0
30
Group
Healthy volunteer
Mild-A
Mild-B
Moderate
Severe
B.
Color Key and Histogram
Value
Healthy volunteer
Mild-A
Mild-B
Moderate
Severe

peptides . The first cluster was interpreted as peptide abundances in order of HC > Mild-A = Mild-B > Moderate = Severe. The second cluster was interpreted as peptides abundances in order of Mild-A = Mild-B > HC = Moderate = Severe. The third cluster was interpreted as peptide abundances in order of Moderate = Severe > HC > Mild-A = Mild-B; thus each disease severity stage yielded a unique peptidome pattern (Figure 4.3).

Linear discriminate modeling of the cohort peptide abundances following adjustment for age, sex, iRT internal standards, and sample analysis flight identified 12-497 differentially regulated peptides (Table 4.2). These pairwise differences were in agreement with PCA loading comparisons demonstrating very small numbers of significantly regulated peptides between Mild-A and Mild-B while large differences between HC and each AH cohort member. Individual pairwise comparisons by volcano plots were used to illustrate peptides that are differentially abundant by both statistical significance and fold change (Figure 4.3).

**3. ECM peptides change between MELD groups**

To address the working hypothesis that surrogate markers of AH would be associated with altered matrisome metabolism, the regulated peptides (q-value <0.05) identified from the iterative pairwise comparisons of Healthy Control (HC) versus AH cohort (Mild-A, Mild-B, Moderate and Severe) as well as the comparisons of Mild-A to Mild-B and of Moderate to Severe were assembled into

**Table 4.2: Pairwise comparisons of peptidomes.**

| Comparison | # Differentially expressed | # Up regulated | # Down regulated |
|---|---|---|---|
| Healthy volunteer vs. Mild-A | 497 | 130 | 301 |
| Healthy volunteer vs. Mild-B | 392 | 112 | 226 |
| Healthy volunteer vs. Moderate | 207 | 32 | 152 |
| Healthy volunteer vs. Severe | 344 | 109 | 205 |
| Mild-A vs Mild-B | 12 | 1 | 1 |
| Moderate vs. Severe | 94 | 37 | 11 |

**Figure 4.3: Pairwise comparison of the peptidomes of patients with different AH severity by volcano plots.**

Peptide abundance differences were plotted as $\log_2$ of the fold-change versus – $\log_{10}$ BH-corrected p-value. Peptides with BH-corrected p-value < 0.05 and $\log_2$FC ≥ 1 were considered significantly upregulated, and peptides with BH-corrected p-value <0.05 and $\log_2$FC ≤ -1 were considered significantly downregulated. The Tukey's HSD test was used for all pairwise comparisons. Pairwise comparisons were illustrated for the major comparators of: A. Healthy vs. Mild-A, B. Healthy vs. Mild-B, C. Healthy vs. Moderate, D. Healthy vs. Severe, E. Mild-A vs Mild-B, F. Moderate vs. Severe.

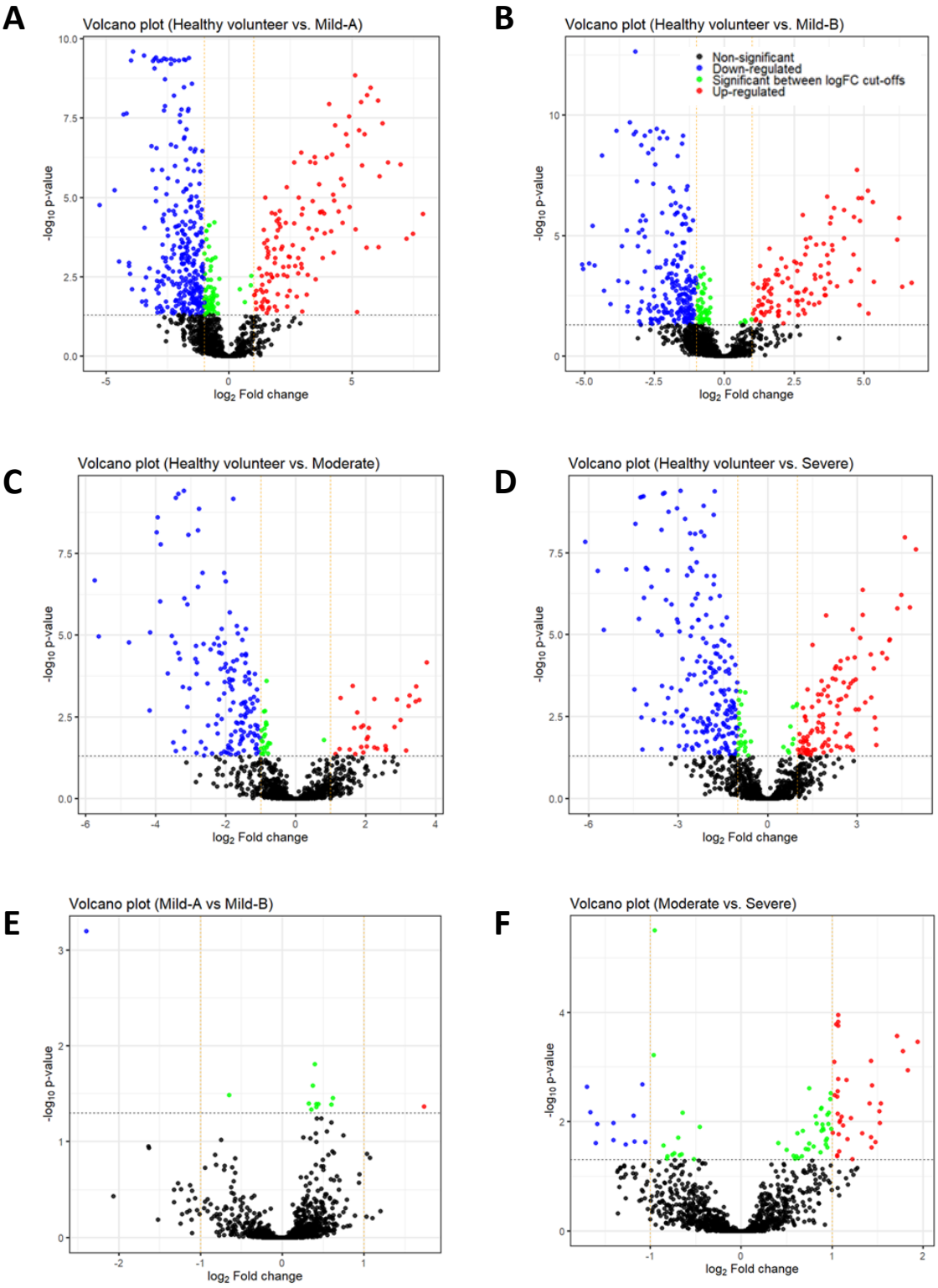
A
Volcano plot (Healthy volunteer vs. Mild-A)
B
Volcano plot (Healthy volunteer vs. Mild-B)
Non-significant
Down-regulated
Significant between logFC cut-offs
Up-regulated
C
Volcano plot (Healthy volunteer vs. Moderate)
D
Volcano plot (Healthy volunteer vs. Severe)
E
Volcano plot (Mild-A vs Mild-B)
F
Volcano plot (Moderate vs. Severe)
-log10 p-value
log2 Fold change

a spreadsheet. The gene names associated with each differentially regulated peptide were submitted for annotation by matrisome category and division using the matrix-annotator tool at the MIT Matrisome project website (http://matrisomeproject.mit.edu/analytical-tools/matrisome-annotator/). These gene names were annotated by the matrisome-annotator tool as a component of the core matrisome (collagen, ECM glycoprotein, proteoglycan) or the matrisome associated compartment (ECM regulators, ECM-affiliated proteins, secreted factors). The regulated ECM peptidome (Table 4.3) by absolute numbers were ranked in the following order: (HC versus Mild-A or Mild-B) >>> (HC versus Moderate or Severe) >>> (Moderate versus Severe) or (Mild-A versus Mild-B). These data suggest that the plasma peptidome may be able to discretely differentiate HC versus Mild AH and Moderate versus Severe AH.

The regulated ECM peptides for the HC versus AH cohorts (Mild-A, Mild-B, Moderate, and Severe) were compared by Venn Diagram (Fig. 4.4 inset) and regulated peptides to all four comparisons were identified. The annotation of these gene names by matrisome-annotator identified 4 ECM peptides out of 101. These four peptides included: one peptide derived from collagen (I) alpha 2 labeled as COL1A2-394 with the sequence $^{612}$SGP(OH)PGPDGNKGEP(OH)GVVGAVGTAGP$^{635}$, two peptides from fibrinogen alpha chain FGA-649 ($^{426}$REYHTEKLVTSKGDKEL$^{442}$), FGA-1238 ($^{581}$KQFTSSTSY$^{589}$), one peptide SRGN-392 from serglycin ($^{135}$SLDRNLPSDSQDLG$^{148}$), and one peptide from kininogen-1 (KNG1-123),

**Table 4.3: ECM-Matrisome Annotation for Pairwise Regulated Peptides.**

| Peptidome | Healthy Control versus Mild-A | Healthy Control versus Mild-A2 | Healthy Control versus Moderate | Healthy Control versus Severe | Mild-A versus Mild-B | Moderate versus Severe |
|---|---|---|---|---|---|---|
| Total Peptides | 497 | 392 | 207 | 344 | 12 | 94 |
| Non-ECM | 246 (49) | 207 (53) | 172 (83) | 204 (59) | 9 (75) | 23 (24) |
| ECM Peptides | 251 (45) | 185 (47) | 35 (17) | 140 (41) | 3 (25) | 71 (76) |
| Core Matrisome Peptides | 226 (45) | 169 (43) | 31 (15) | 127 (37) | 2 (17) | 67 (71) |
| -Collagens | 104 | 59 | 21 | 81 | 0 | 52 |
| -ECM Glycoproteins | 118 | 107 | 6 | 39 | 2 | 14 |
| -Proteoglycans | 4 | 3 | 4 | 7 | 0 | 1 |
| Matrisome-associated | 25 (5) | 16 (4) | 4 (2) | 13 (4) | 1 (8) | 4 (4) |
| -ECM Regulators | 24 | 16 | 4 | 11 | 1 | 4 |
| -ECM-affiliated Proteins | 1 | 0 | 0 | 1 | 0 | 0 |
| -Secreted Factors | 0 | 0 | 0 | 1 | 0 | 0 |
| | (percentage) | | | | | |

**Figure 4.4: Regulated peptides common to HC to AH pairwise comparisons include ECM peptides.**

Regulated peptides were identified using data from volcano plots of HC vs. Mild-A, HC vs. Mild-B, HC vs. Moderate, and HC vs. Severe were compared by Venn diagram analysis (inset). Peptides common to all comparisons (n=101) were annotated for GO and the relative fold difference of the HC to AH-cohort plotted for all ECM peptides.

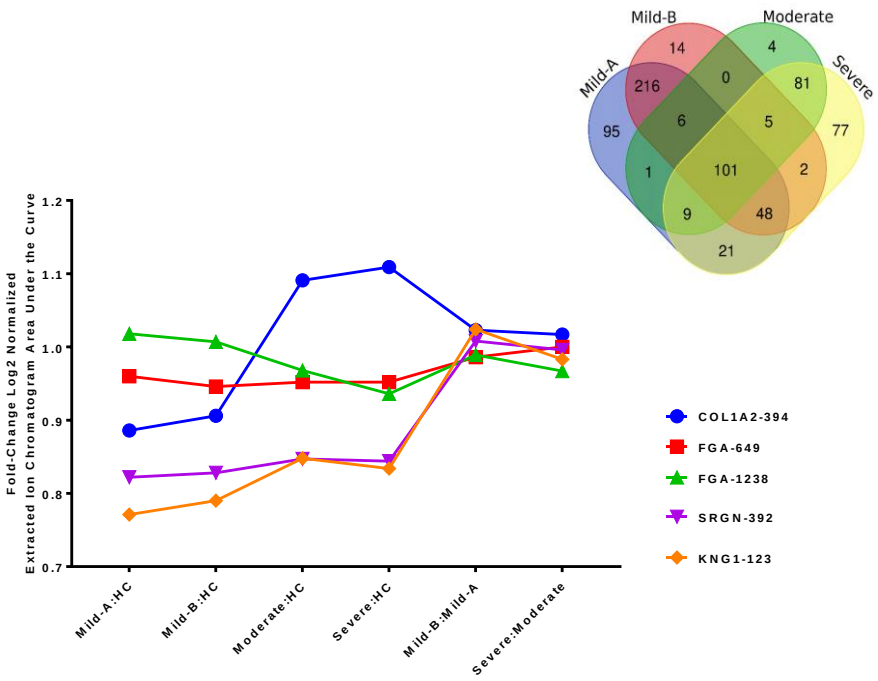
Mild-B
Moderate
Mild-A
Severe
14
4
0
216
81
95
6
5
77
1
101
2
9
48
21
Fold-Change Log2 Normalized
Extracted Ion Chromatogram Area Under the Curve
1.2
1.1
1.0
0.9
0.8
0.7
Mild-A:HC
Mild-B:HC
Moderate:HC
Severe:HC
Mild-B:Mild-A
Severe:Moderate
COL1A2-394
FGA-649
FGA-1238
SRGN-392
KNG1-123

$^{245}$RPPGFSP$^{251}$ (also known as bradykinin 1-7). As illustrated in Figure 4.4, two peptides (COL1A2-394, SRGN-392, and KNG1-123) increased with AH severity, one peptide (FGA-1238) decreased with AH severity and two peptides (FGA-649 and SRGN-392) were reduced across all AH cohorts and did not change with AH severity. These data demonstrate the response of select matrisome compartments across the AH spectrum.

## D. Discussion

AH is a diagnosis of acute hepatic inflammation and liver failure based on AST, AST/ALT, serum bilirubin, INR, neutrophilia, ascites, and history of AUD.(72) AH has a 3-month mortality rate of 30-50%.(73) Both AH diagnosis and prognosis could be impacted by the development of more sensitive and specific biomarkers. Our group previously demonstrated that inflammatory stress causes the hepatic ECM to undergo dynamic transitional remodeling.(93) Others have shown that ECM remodeling causes degradation products to be secreted into blood and that analysis of these peptides (i.e. the ECM degradome) is a useful prognostic tool in diseases that involve ECM remodeling.(58, 59) Therefore, the work in this pilot study aimed to test the hypothesis that the plasma ECM degradome changes with AH severity.

To this end, peptides were purified from AH patient plasma and analyzed using LC-MS/MS. Internal standards (non-human peptides, iRT, Biognosis USA, Beverly, MA) spiked into samples enabled normalizing of day-to-day instrument performance during the statistical modeling using linear mixed model approach.

Patients were divided into groups based on AH severity (MELD score) and the changes in the peptidome patterns across groups were examined with multivariate analyses, considering age and sex as fixed variables, and flight and the 11 peptide standards as random variables. The PCA approach to data analysis is based on data reduction and collapses all data points within a sample into a single x,y coordinate. This approach allowed for an unbiased self-sorting at the patient level, not the discrete peptide level, based on the intrinsic nature of the data. These data demonstrated that differences in the peptidome can separate patients by AH severity group. Principal component 1, which accounted for 51.59% of variability in the data, generally separated Mild-A and Mild B from Moderate and Severe, with the Healthy group in the middle. Principal component 2, which accounted for 5.14% of variability in the data, appeared to separate healthy patients from all AH patients. PCA showed little difference between Mild-A and Mild-B or between Moderate and Severe. The subsequent multivariate approach for modeling the peptidome data was hierarchical clustering with heap maps grouping the relative peptide abundances into unique patterns in the peptidome between AH severity groups. The hierarchical clustering of the complete dataset identified three strong groupings of peptide abundance patterns that reflected combinations of (A) increased peptide levels in healthy controls, (B) increased peptide levels in Moderate + Severe and (C) increased peptide levels in Mild-A + Mild-B AH cohorts. These data supported the justification to conduct pair-wise comparisons of the mean peptide differences between HC and AH cohorts. Post-hoc filtering of the differentially abundant peptides identified strong

relative abundance changes in ECM peptides with strong differences noted in the collagen and fibrinogen peptides. Consistent with the multivariate analysis, the largest changes in the peptidome were observed between mild vs. healthy and severe vs. healthy. While each pairwise comparison is heavily dominated by ECM fragments, the regulated peptides common to all HC to AH comparisons only contained 5 ECM peptides out of a possible 101. While these pilot data provide strong evidence that altered ECM turnover is associated with the AH spectrum additional research is required to confirm these findings.

While the sample handling, sample analysis and statistical modeling integrated methods for sample handling randomization, inclusion of internal standards and statistical modeling to account for random or fixed effect variables there are still several limitations to these studies that should be noted. The balance of HC to AH cohort is imbalances in “n” values and this may be insufficient to adequately power the study. Additionally, the potential for a “clinical site effect” is present. The HC plasma samples were recruited at the University of Louisville. The Mild-A and Mild-B plasma samples were recruited at the NIH-NIAAA. The Moderate and Severe plasma samples were recruited at the University of Louisville, the University of Massachusetts Medical School, the University of Texas-Southwestern and the Cleveland Clinic. Therefore, the potential for a “clinical site effect” is present. Despite these study limitations the statistical modeling and informatics filtering of the peptidomics data supports the hypothesis that the ECM plasma degradome is associated with the AH spectrum.

These patterns of select peptidome “features” can be investigated further in future studies as biomarkers for AH severity and outcome.

# CHAPTER V

# CHRONIC MODERATE ALCOHOL CONSUMPTION INFLUENCES RENAL CORTICAL OXIDANT RESPONSE PATHWAYS

## A. Introduction

Ethanol (EtOH) is arguably the most common substance voluntarily consumed at toxic doses by humans. Pharmacologically relevant concentrations of EtOH affect multiple organs,(148, 149) and EtOH consumption is a known risk factor in over 200 health conditions (9). Despite this knowledge, the ability to reverse EtOH-induced organ damage or predict at-risk individuals for EtOH-induced organ damage is limited even in well-known target organs (e.g. the liver) (150). In contrast to the liver, it is unclear if the kidney is a direct target of EtOH toxicity. Heavy EtOH consumption is well recognized to be associated with enhanced risk for renal failure secondary to hepatic cirrhosis, a phenomenon known as hepatorenal syndrome (HRS) (151). Renal failure associated with HRS is a complication in 14.4% of AH patients having MELD scores ≥22 (152). The widespread view that this renal failure is strictly secondary to hepatic cirrhosis with no role for direct EtOH nephrotoxicity may largely be an artifact of clinical charting, as was the case for alcoholic pancreatic damage (153). Moderate EtOH consumption is, however, absent from listed risk factors for chronic kidney

disease (154), and connections between alcohol use disorders and kidney damage are controversial (155). Studies on moderate EtOH consumption have shown EtOH to be (1) inversely associated with development or progression of chronic kidney disease (85, 95, 156, 157) and (2) associated with improved outcomes in renal transplant patient populations (158, 159). However, these studies were not specifically designed to address the question as to whether or not EtOH consumption damages the kidneys, and a mechanistic explanation for these observations has not been explored. Overall, a more in-depth investigation is justified to discern both the direct and indirect effects of EtOH on the kidney.

Rodent studies have identified detrimental effects of EtOH to kidney at the tissue and subcellular, including increased tissue markers of oxidative damage and myeloperoxidase expression in rats (87) and increased Cyp2e1 induction(88), and mitochondrial protein hyper-acetylation in mice (86). These investigations have been driven by the hypothesis that the effect of EtOH on the kidneys mirrors its effects on the liver. Confirmation of these parallel mechanisms between these two organs may be due to similarities in expression of EtOH metabolizing enzymes Cat and Cyp2e1. However, while the liver and kidney are the major organs for EtOH detoxification, significant differences in structure, function, and parenchymal composition exist.

We used discovery-based proteomic and transcriptomic approaches to study the effects of EtOH on the renal cortex and secondarily the effects of EtOH pre-exposure on the response (4h and 24h) to LPS (10mg/kg i.p.). Integrated IPA studies demonstrated significant EtOH-alone effects on multiple canonical

signaling pathways including decreased activation of the Nuclear factor (erythroid-derived 2)-like 2 (Nrf2) and increased activation of the aryl hydrocarbon receptor (Ahr) oxidative stress responses pathways. These studies suggested an EtOH-dependent, selective dysregulation of cortical oxidant response pathways.

## B. Experimental procedures

### 1. Animals and exposures

Mice were exposed to chronic ethanol and/or LPS as described in Chapter II. Mice were exposed to chronic ethanol and/or ethanol binge as described in Chapter II.

### 2. Histology and immunohistochemistry

Renal cortex tissue was stained with PAS as described in Chapter II. IHC for Mpo and Cat was conducted on renal cortex tissue as described in Chapter II.

### 4. Blood urea nitrogen analysis

BUN in mouse plasma was determined using a standard kit as described in Chapter II.

### 5. Proteomic sample handling

3 control mice, 3 ethanol mice, 3 4h LPS mice, and 3 ethanol+4h LPS mice were used for the renal cortex proteomic analysis. Proteins were extracted from

renal cortex tissue, digested, labeled, and prepared for LC-MS/MS analysis as described in Chapter II.

### 6. Liquid chromatography and tandem mass spectrometry

1D-LC-MS/MS analysis and subsequent data analysis were carried out as described in Chapter II

### 7. RNA seq analysis

3 control mice, 3 ethanol mice, 3 4h LPS mice, and 3 ethanol+4h LPS mice were used for the renal cortex transcriptomic analysis. The same mice were used for the renal cortex proteomics and transcriptomics, except for 1 4h LPS mouse and 1 ethanol+4h LPS mouse that were different. RNA was isolated from renal cortex sections and RNA Seq analysis was carried out as described in Chapter II. RNA Seq data were analyzed as described in Chapter II.

### 8. Multivariate analysis of proteomic and transcriptomic data

Multivariate analysis of proteomic and transcriptomic data was completed as described in Chapter II.

### 9. Immunoblot analysis

Western blot analysis was carried out on protein extracted from renal cortex tissue as described in Chapter II. Primary antibodies against Nqo1, Sod1, Sod2, Gclc, and Cat were used.

### 10. Statistical analyses

Statistical analyses of proteomic and transcriptomic data were carried out as described in Chapter II.

## C. Results

### 1. Ethanol, LPS, and the combination increase blood urea nitrogen

The Lieber-DeCarli model (Fig. 5.1A) of chronic moderate EtOH consumption was used to examine the effects of EtOH ± LPS on the kidneys of male mice. This is an established model that causes early alcohol-induced liver injury and sensitizes the liver to a subsequent inflammatory insult, such as LPS.(93). Ethanol consumption caused a small but significant increase in BUN levels ($p<0.05$) in mice in the absence of an LPS challenge (Fig. 5.1B). LPS injection significantly increased BUN levels ($p<0.005$) 24h after injection; ethanol exposure did not significantly alter the increase in BUN caused by LPS administration.

### 2. Ethanol alone contributes little-to-no morphological changes to mouse renal cortex

Analysis Hematoxylin and Eosin- (H&E, not shown) and PAS-stained (Fig. 5.2) tissue sections identified mild proximal tubular brush border loss with LPS and increased infiltration of polymorphonuclear leukocytes (PMNs, as noted by yellow arrows). However, little-to-no obvious histologic differences were detected

**Figure 5.1: Effects of chronic moderate EtOH feeding and low dose (10mg/kg intra-peritoneal (i.p.) lipopolysaccharide (LPS) on blood urea nitrogen (BUN).**

(A) To model chronic moderate EtOH consumption the Lieber DeCarli diet model of a four week escalation followed by a two week hold at 6% EtOH in the liquid diet was used. Control animals received a isocaloric substitute of maltose-dextrin in the liquid diet. A LPS (10mg/kg) LPS or saline injection given *i.p.* either 4h or 24h prior to sacrifice. (B) Baseline differences in BUN were observed with EtOH feeding as well as an LPS effect at 24h. Statistical differences were determined using students t-test or two-way ANOVA, *$p \leq 0.05$, **$p \leq 0.005$.

**A**

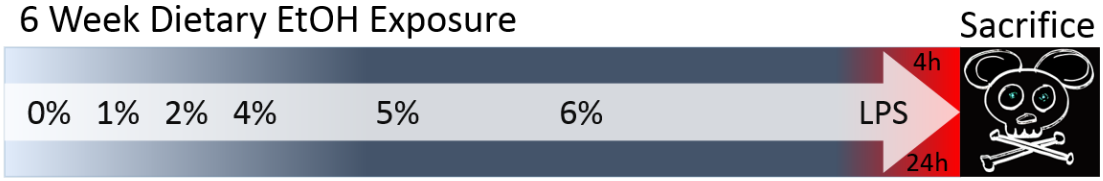
6 Week Dietary EtOH Exposure
Sacrifice
0%
1%
2%
4%
5%
6%
LPS
4h
24h

**B**

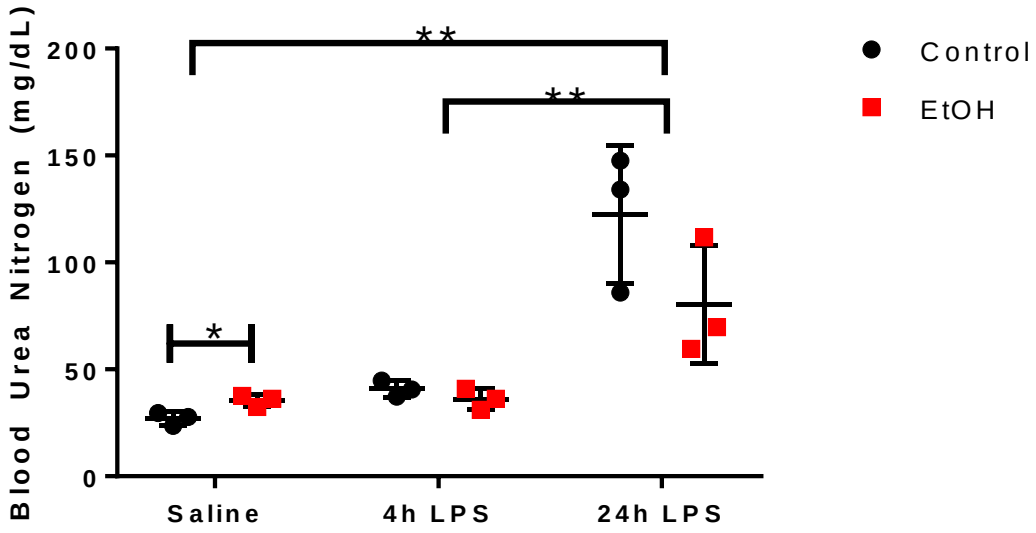
Blood Urea Nitrogen (mg/dL)
200
150
100
50
0
**
**
*
Saline
4h LPS
24h LPS
Control
EtOH

**Figure 5.2: Mild effects of EtOH and/or LPS on renal architecture.**

Histologic evaluation by periodic acid-shiff (PAS) stain (100x) demonstrates unremarkable effects on renal parenchymal architecture of control (left column, n=3) versus EtOH fed (right column, n=3) animals. Following low-dose (10mg/kg) i.p. LPS renal cortical sections demonstrate low to moderate levels of tubular dilation, vacuolization, brush border loss and PMN infiltration at 4h (middle row) and 24h (bottom row). Glomerular infiltration by polymorphonucleated cells is noted by yellow arrows (→).

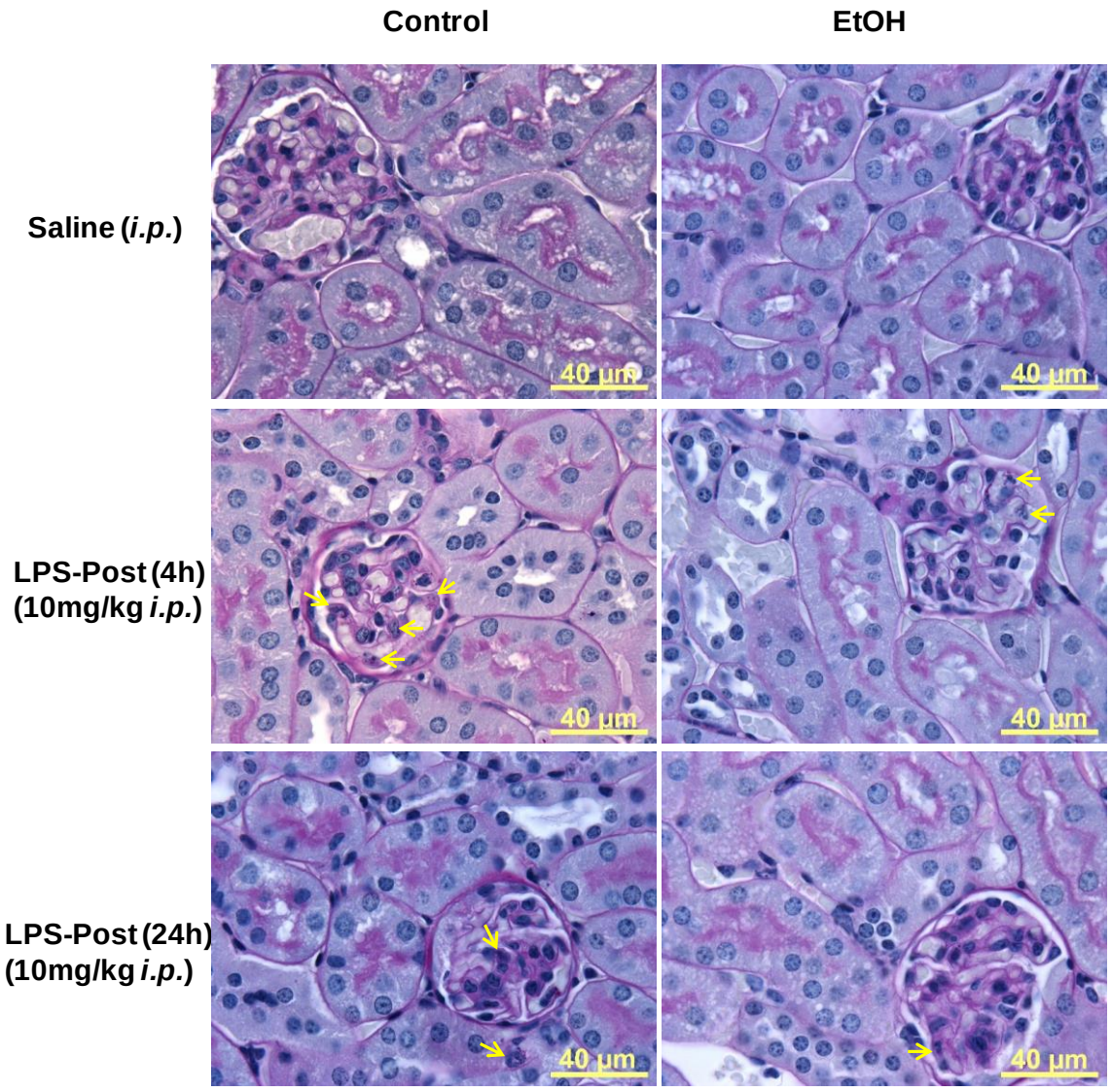
Control
EtOH
Saline (i.p.)
LPS-Post (4h) (10mg/kg i.p.)
LPS-Post (24h) (10mg/kg i.p.)
40 µm

in kidneys from mice exposed to EtOH versus control or EtOH + LPS versus LPS alone, suggesting at the gross level there was no need for tissue scoring of kidney histology.

### 3. Ethanol attenuates LPS-induced cortical recruitment of MPO-positive cells

Although gross histology was unaffected by exposure regimen, the PAS stain demonstrated that LPS exposure increased the number of infiltrating neutrophils and caused brush border loss both 4 and 24h after challenge in the EtOH and control cohorts. Based on quantitative IHC, control and EtOH-fed mouse kidneys were similar and unremarkably different for Mpo staining (Fig. 5.3). LPS induced a strong, significant recruitment of Mpo-positive cells into the cortex. Moreover, EtOH significantly attenuated the recruitment of Mpo-positive cells caused by LPS at 4h but not 24h post-injection (Fig. 5.3).

### 4. Ethanol and LPS each cause unique protein abundance patterns.

Proteomic analysis of TMT 10-plex labeled cortical digests (Fig. 5.4A) resulted in identification of over 2,400 proteins (Fig. 5.4B) by two or more peptides. Chronic, moderate EtOH consumption increased the abundance of 22 proteins and decreased the abundance of 70 proteins (Fig. 5.4C). Significant protein abundance changes in the LPS compared to control animals were greatest at 24h (108 increased, 10 decreased) compared to 4h-post LPS challenge (43 increased and 19 decreased) (Fig. 5.4D-E).

**Figure 5.3: LPS induced infiltration of myeloperoxidase (MPO) positive cells into the renal parenchyma.**

(A) Infiltration of MPO positive cells was quantified by IHC staining and counting of MPO-positive cells (40x) in glomerular (→) and tubular (→) compartments (33±4 visual fields per kidney section). (B) Infiltration was significantly increased at both 4h (n=3) and 24h after LPS (n=3), compared to baseline (n=3). There was significant difference between control (n=3) and EtOH fed animals (n=3) at 4h post low dose LPS i.p. challenge. Statistical differences were determined using students t-test or two-way ANOVA, *p≤0.01, **p≤0.005, @p≤0.0001.

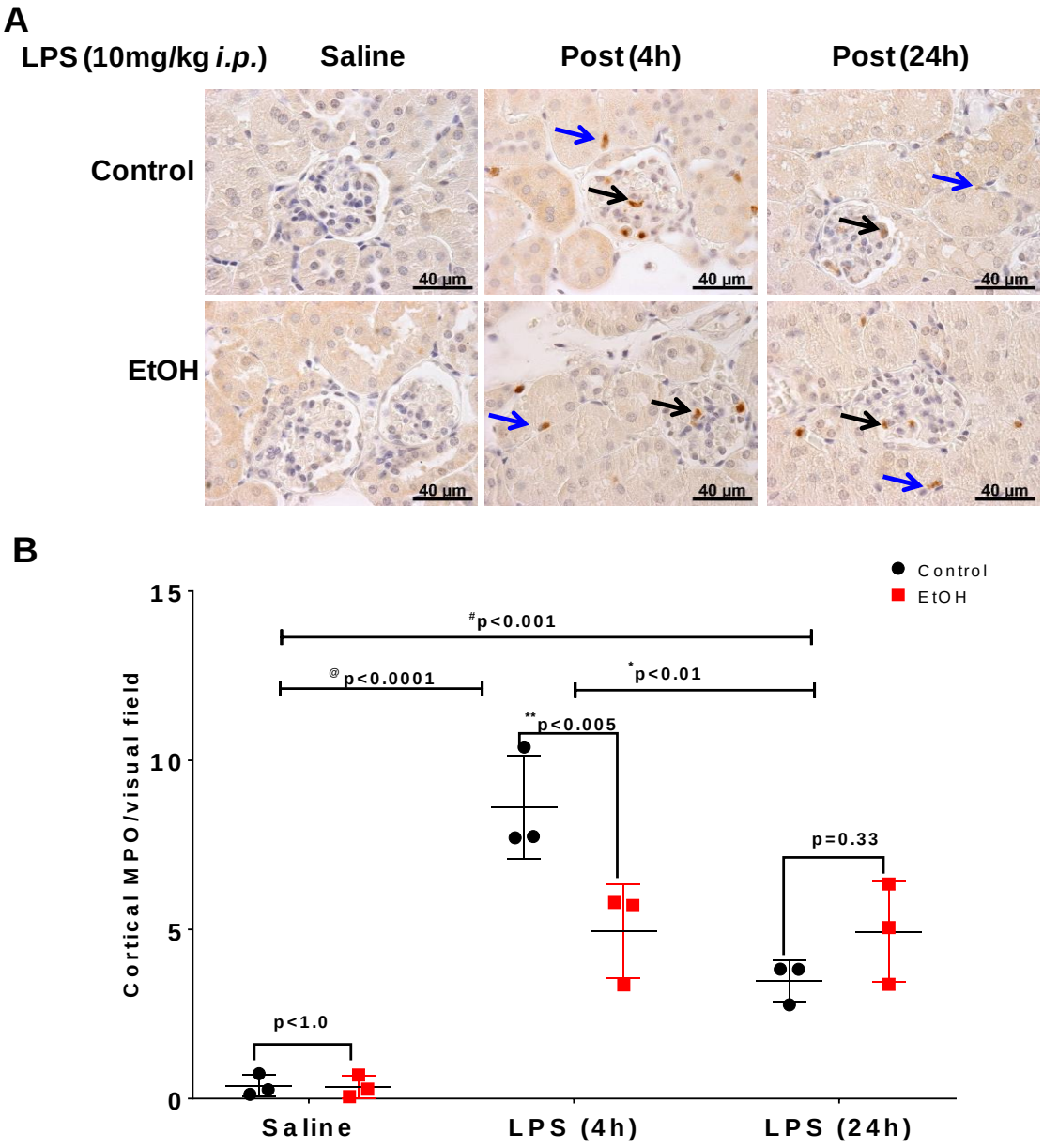
A
LPS (10mg/kg i.p.)
Saline
Post (4h)
Post (24h)
Control
EtOH
40 µm
B
Control
EtOH
Cortical MPO/visual field
15
10
5
0
#p<0.001
@p<0.0001
*p<0.01
**p<0.005
p=0.33
p<1.0
Saline
LPS (4h)
LPS (24h)

**Figure 5.4: Workflow and characterization of the global effect of EtOH and LPS on the cortical proteome.**

Using a TMT workflow (5.4A) the renal proteomic dataset included 2,487 proteins (>98% at ≥2-peptide level, (5.4B) detected with high confidence. Differences of relative abundance are shown as $Log_2$ fold change (FC) and are evaluated in volcano plots (5.4C-G) with a FC >1.2 and corrected ANOVA p-value<0.05 considered significant. As a primary hit, the effects of EtOH and LPS are comparable in magnitude. This time dependent effect was maintained (5.4F-G) with the two-hit comparison of EtOH on an LPS background (EtOH+LPS versus LPS) with smaller differences observed by $log_2$ FC (EtOH+4hLPS to 4hLPS) compared to $log_2$FC (EtOH+24hLPS to 24hLPS).

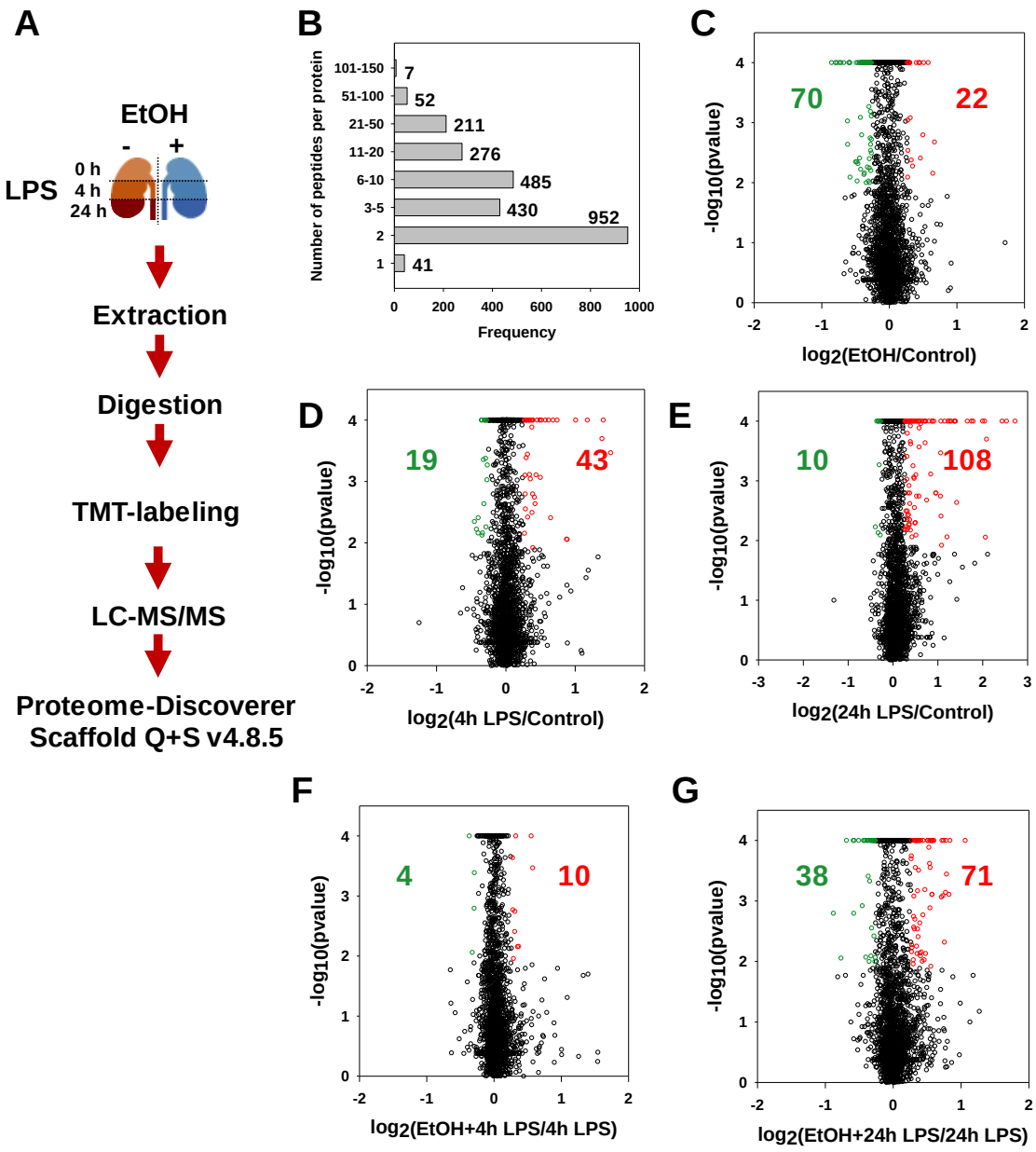
A
EtOH
-
+
LPS
0 h
4 h
24 h
Extraction
Digestion
TMT-labeling
LC-MS/MS
Proteome-Discoverer
Scaffold Q+S v4.8.5
B
Number of peptides per protein
101-150
51-100
21-50
11-20
6-10
3-5
2
1
7
52
211
276
485
430
952
41
0
200
400
600
800
1000
Frequency
C
70
22
-log10(pvalue)
log2(EtOH/Control)
D
19
43
-log10(pvalue)
log2(4h LPS/Control)
E
10
108
-log10(pvalue)
log2(24h LPS/Control)
F
4
10
-log10(pvalue)
log2(EtOH+4h LPS/4h LPS)
G
38
71
-log10(pvalue)
log2(EtOH+24h LPS/24h LPS)

value) <0.05) trends in protein abundance fold-changes ($Log_2FC>0.5$ or $Log_2FC<-0.5$) with larger fold changes between two or more conditions. A four protein grouping (Ehhadh, Acad11, Sqstm1, and Hnrnpc) had diminished abundance with EtOH versus control (Fig. 5.5A, dotted box) but the differences were normalized at 4h- and 24h-post LPS. A second grouping of ribosomal proteins (Rpl6, Rpl8, Rpl13a, and Rps15) had increased abundance in EtOH-fed animals on a background of 24h LPS (Fig. 5.5B, dotted box).

**5. RNA seq data support proteomic data for LPS effect.**

To study the early two-hit effects of EtOH ± LPS, the RNA were isolated from EtOH, control, 4h LPS and EtOH+4h LPS animals only. The RNA integrity number (RIN) values for RNA isolated from mouse kidneys averaged 7.8 ± 0.5. Following ribosomal depletion, RNA library preparation and high throughput sequencing, a total of 47,719 transcripts were observed including 24,405 detected in all samples. Of 47,719 detected transcripts, EtOH increased the expression of 88 and decreased the expression of 99 (Fig. 5.6D/Table 5.1A). LPS increased the expression of 1,468 and decreased the expression of 911 transcripts (Fig. 5.6E/Table 5.1A). Hence, 4h LPS, compared to EtOH, induced approximately a 10-fold increase of differentially abundant transcripts relative to the control animals (Fig. 5.6E-G). As shown in Table 1, EtOH significantly ($q \leq 0.05$; $Log_2FC \geq 1$) altered the expression of six (6) transcripts apparently independent of LPS.

**Figure 5.5: Quantitative cluster analysis reveals EtOH-regulated protein clusters.**

$Log_2$ FC values are plotted relative to the pooled internal standard reporter ions. (A) EtOH-dependent, LPS-independent protein abundance changes. Significant differences (q-value <0.05) were observed for a protein cluster in control versus EtOH (black dotted boxes). (B) EtOH-dependent and late (24h) low dose LPS protein abundance changes of ribosomal-related gene product cluster. Significant differences (q-value <0.05) were observed for LPS 24h versus EtOH +LPS 24h (black dotted boxes).

A

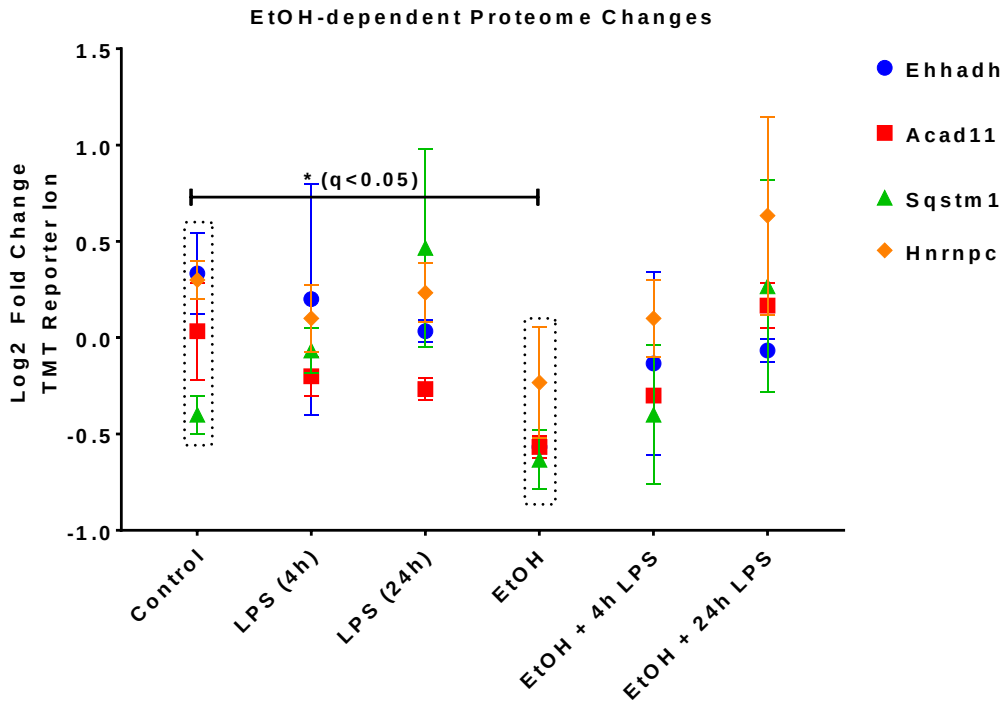
EtOH-dependent Proteome Changes
Log2 Fold Change
TMT Reporter Ion
1.5
1.0
0.5
0.0
-0.5
-1.0
*(q<0.05)
Control
LPS (4h)
LPS (24h)
EtOH
EtOH + 4h LPS
EtOH + 24h LPS
Ehhadh
Acad11
Sqstm1
Hnrnpc

B

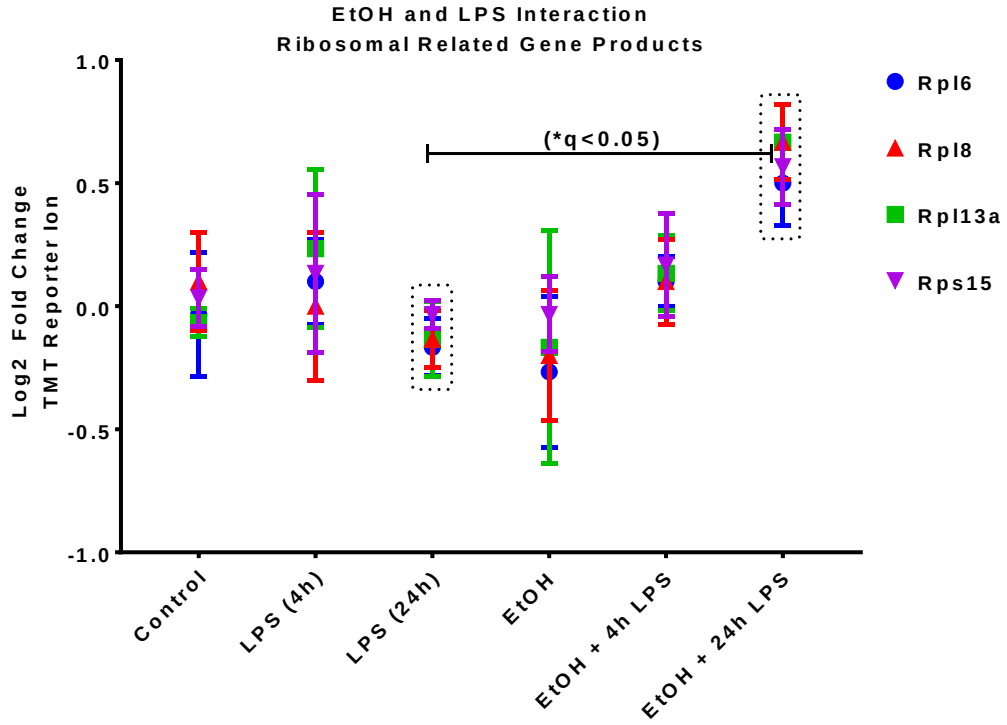
EtOH and LPS Interaction
Ribosomal Related Gene Products
Log2 Fold Change
TMT Reporter Ion
1.0
0.5
0.0
-0.5
-1.0
(*q<0.05)
Control
LPS (4h)
LPS (24h)
EtOH
EtOH + 4h LPS
EtOH + 24h LPS
Rpl6
Rpl8
Rpl13a
Rps15

### 6. Ethanol alone downregulates Nrf2-mediated oxidative stress response pathways at the protein level and transcript level.

A multivariate comparison by IPA of the top-20 canonical signaling pathways for the proteome and transcriptome by single-hit (EtOH compared to control, 4hLPS compared to control) and two-hit comparisons (EtOH + 4h LPS compared to 4h LPS; EtOH +4h LPS compared to EtOH) are shown in Fig. 5.5A. The effects of EtOH feeding ± LPS exposure on signaling pathways (Fig 5.5A) or individual protein abundance levels (Fig 5.5B) are illustrated as heat maps. Heat-map colors are assigned dichotomously to illustrate activation (positive Z-score, red/orange) or inactivation (negative Z-score, green/blue) based on the $Log_2$ relative abundance changes for proteins or transcripts within the pathway as previously discribed.(160, 161) Six overlapping canonical pathways (noted by asterisks) for EtOH alone include effects on cell-cell interactions, oxidant stress response, actin reorganization, protein unfolding stress response and protein translation.

In the EtOH vs. control comparison for both the proteomic and transcriptomic analyses, Ahr signaling had a positive z-score (i.e. overall pathway activation) largely due to decreased abundance of heat shock protein 90-α and –ß proteins, increased abundances Ahr-targets Nqo1, Aldh isoforms and Gst enzymes. Nrf2-mediated oxidative stress response canonical pathway had a negative z score (i.e. overall pathway deactivation, Fig. 5.7A-B) due to large decreases in Nrf2 targets such as Sod1, Sqstm1/p62, and Gclc. LPS caused overall strong positive z-scores for the acute phase response signaling pathway

**Figure 5.6: Workflow and characterization of the EtOH and 4h LPS regulated transcriptomes.**

Of 47,719 detected transcripts (36,571 in Venn Diagrams) after filtering for corrected p-value (Benjamini-Hochberg q-value <0.05), (D) EtOH increased the expression of 88 (red points) and decreased the expression of 99 (green points). (E) LPS increased the expression of 1,468 (red points) and decreased the expression of 911 (green points) transcripts. (F) EtOH on a background of 4h LPS increased the expression of 79 (red points) and decreased the expression of 68 (green points) transcripts.

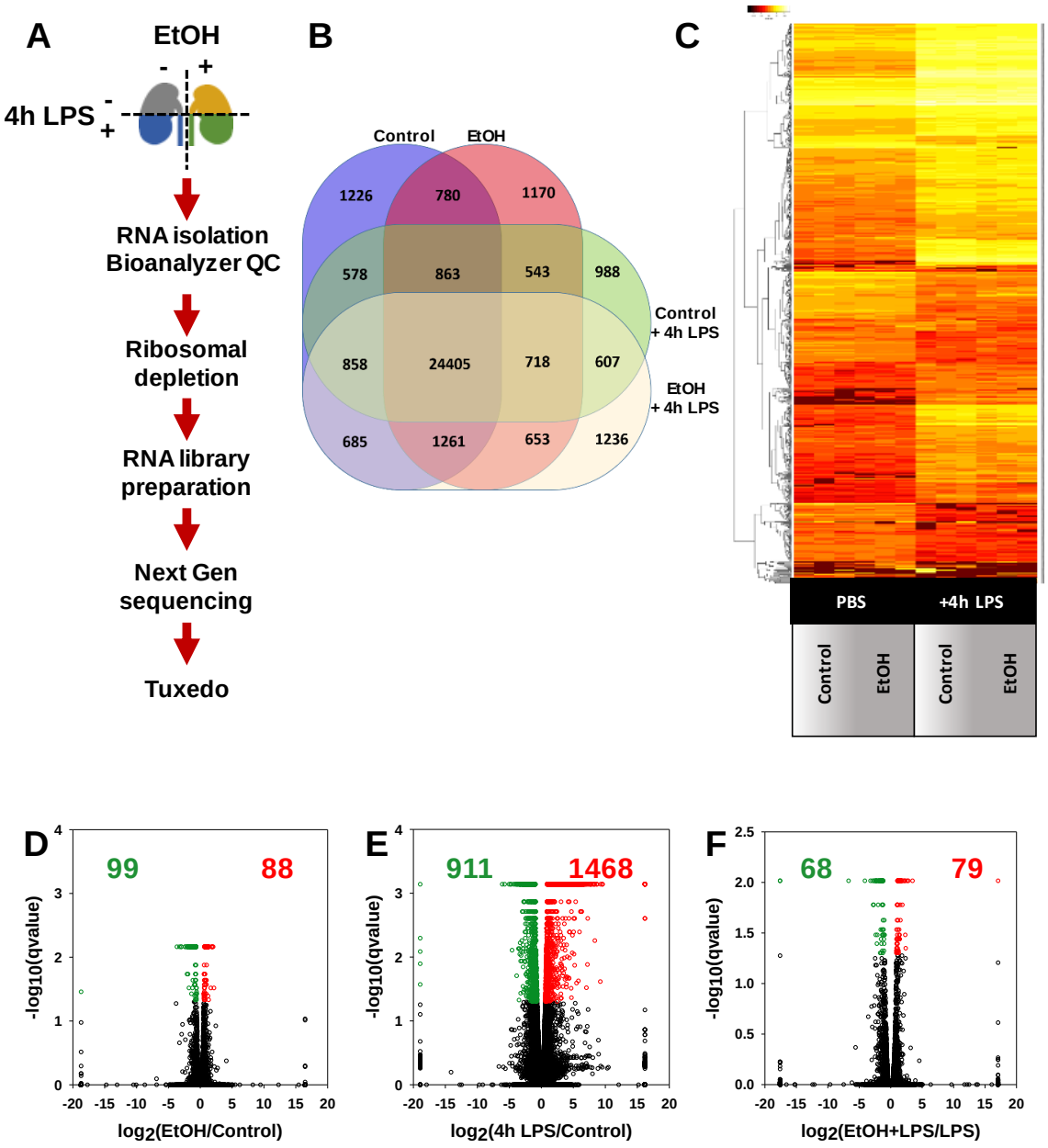
A
EtOH
-
+
4h LPS
-
+
RNA isolation
Bioanalyzer QC
Ribosomal
depletion
RNA library
preparation
Next Gen
sequencing
Tuxedo
B
Control
EtOH
1226
780
1170
578
863
543
988
858
24405
718
607
685
1261
653
1236
Control
+ 4h LPS
EtOH
+ 4h LPS
C
PBS
+4h LPS
Control
EtOH
Control
EtOH
D
99
88
-log10(qvalue)
log2(EtOH/Control)
E
911
1468
-log10(qvalue)
log2(4h LPS/Control)
F
68
79
-log10(qvalue)
log2(EtOH+LPS/LPS)

**Table 5.1: Effects of EtOH and LPS on differentially regulated cortical RNA transcripts, differentially regulated genes, and one-hit/two-hit associated Top-5 Gene Ontology (GO) terms.**

| Transcriptional Responses | | Differentially Expressed Genes (DEGs) | |
|---|---|---|---|
| Treatment | Comparator | Multiple Comparison Correction | Relative Fold-Change Filtered |
| | | $p \leq 0.05$ $q \leq 0.05$ | $p \leq 0.05$ $q \leq 0.05$; logFC≥1 |
| **EtOH** | **Control** | **187 (88↑, 99↓)** | 66 (22↑, **44↓**) |
| **4h LPS** | **Control** | **2379 (1468↑, 911↓)** | 1814 (1141↑, **673↓**) |
| **EtOH+4h LPS** | **EtOH** | 2695 (1538↑, **1157↓**) | 1842 (1114↑, **728↓**) |
| **EtOH + 4h LPS** | **4hLPS** | 147 (79↑, **68↓**) | 135 (68↑, **67↓**) |

| DEG Expression Regulation Trends ($q \leq 0.05$; logFC≥1) | | | | | | | |
|---|---|---|---|---|---|---|---|
| **mRNA Expression Changes by EtOH diet independent of 4h LPS exposure** | | | | | | | |
| Kynu ↑<br>Slc7a12a↑ | | | | Cntnap5↓<br>Cyp4a12a↓ | | Gm6300↓<br>Kif20b↓ | |
| **mRNA Expression Changes by 4h LPS exposure independent of EtOH diet** | | | | | | | |
| **Ifit1** ↑<br>**Ifit2**↑<br>**Saa2**↑ | **Lcn2**↑<br>Camp ↑<br>Cxcl1↑ | Cxcl10↑<br>Gm28347↑<br>Mx1↑ | Slfn4↑<br>Trem1↑ | Bsnd↓<br>Cd300lg↓<br>Cldn15↓ | Clec14a↓<br>Cyp26b1↓<br>Exoc3l2↓ | Myct1↓<br>Rasgrp3↓<br>Slc9a3r2↓ | Sox17↓ |

| Regulated Transcripts: Treatment versus Control (One-hit) | | | |
|---|---|---|---|
| **Treatment** | **GO Term Description** | **Genes** | ***q*-value** |
| **EtOH** | response to interferon-gamma | 2 | 0.011 |
| | skeletal muscle tissue development | 3 | 0.012 |
| | innate immune response | 5 | 0.012 |
| | regulation of body fluid levels | 4 | 0.014 |
| | skeletal muscle organ development | 3 | 0.014 |
| **4h LPS** | **innate immune response*** | 146 | 8.43E-50 |
| | **response to cytokine*** | 130 | 4.94E-36 |
| | **regulation of cytokine production*** | 128 | 1.96E-34 |
| | **defense response to other organism*** | 123 | 4.76E-34 |
| | positive regulation of cytokine production | 97 | 4.24E-31 |

| Regulated Transcripts: Treatment versus [EtOH + 4h LPS] (Two-hit) | | | |
|---|---|---|---|
| **Treatment** | **GO Term Description** | **Genes** | ***q*-value** |
| **EtOH** | **innate immune response*** | 149 | 4.34E-51 |
| | **response to cytokine*** | 140 | 6.71E-42 |
| | **defense response to other organism*** | 122 | 1.22E-32 |
| | **regulation of cytokine production*** | 126 | 2.18E-32 |
| | cellular response to cytokine stimulus | 107 | 1.08E-29 |
| **4h LPS** | positive regulation of smooth muscle cell proliferation | 6 | 6.24E-06 |
| | positive regulation of cell migration | 11 | 1.42E-05 |
| | positive regulation of cell motility | 11 | 1.91E-05 |
| | wound healing | 10 | 2.16E-05 |
| | positive regulation of cellular component movement | 11 | 2.37E-05 |

and the LXR/RXR activation pathway, whether or not mice were fed an EtOH diet.

**7. Effects of ethanol and LPS on catalase abundance.**

Cat IB analysis confirmed proteomic findings, demonstrating a significant (2-way ANOVA, *p-value<0.05) decrease of approximately 40-50% in the renal cortical tissue of EtOH fed mice with an insignificant LPS-effect (Fig. 5.10A-B). Additional Cat IB analyses lysates from a chronic-plus-binge study of alcohol feeding demonstrated similar effects on Cat abundance following 10-day EtOH feeding or, strikingly, 9h post-EtOH gavage (Fig. 5.10C). This data suggested the effect of EtOH on Cat abundance was not associated with the chronicity of EtOH feeding, IB.

**8. Data Sharing**

Proteomic files including acquired LCMS data (.RAW), search engine files (.mgf), and search results aggregated into a Scaffold3 (.sf3, ProteomeSoftware.com) have been deposited with MassIVE (http://massive.ucsd.edu/) data repository with the Center for Computational Mass Spectrometry at the University of California, San Diego (MSV000083053) and shared with the ProteomeXchange (www.proteomexchange.org) (PDX011429). Experimental details for NextGen sequencing and sequencing

**Figure 5.7: | Effects of EtOH feeding on Cat abundance in the renal cortex.** Cat immunoblot analysis (A) demonstrates a significant reduction of Cat protein with EtOH feeding (n=3) compared to control (n=3) without LPS administration (two-way ANOVA *p-value<0.001). IHC staining (10X) for Cat (B) demonstrated comparable EtOH-associated decreases in the cortical tissue (cortical/juxtamedullary boundary noted by red dashed line) of LPS-naïve (n=3) mice compared to control (n=3) and LPS-challenged mice (n=3) compared to LPS alone (n=3). (C) Similar EtOH effects on Cat abundance were observed using a separate more severe model of EtOH feeding (NIAAA chronic plus binge model; control n=3, chronic EtOH n=3, EtOH gavage n=3, chronic EtOH+EtOH gavage n=3).

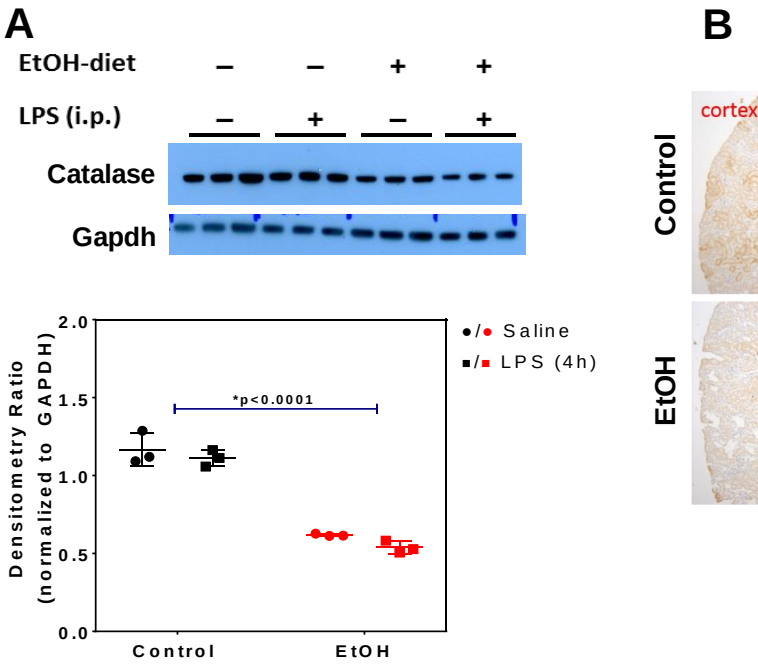
A
EtOH-diet
–
–
+
+
LPS (i.p.)
–
+
–
+
Catalase
Gapdh
Densitometry Ratio
(normalized to GAPDH)
2.0
1.5
1.0
0.5
0.0
*p<0.0001
●/● Saline
■/■ LPS (4h)
Control
EtOH

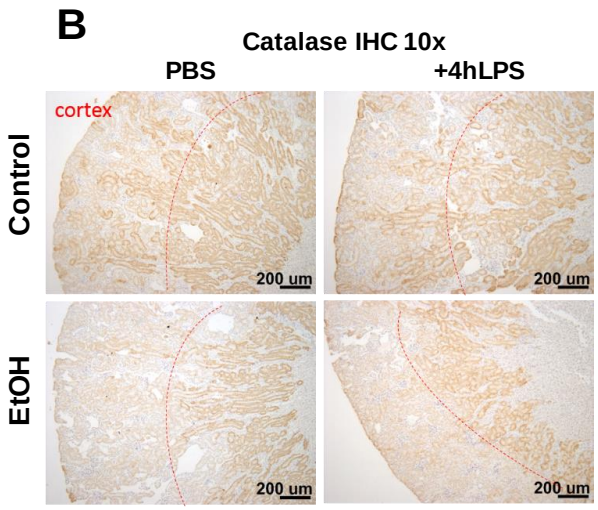
B
Catalase IHC 10x
PBS
+4hLPS
Control
EtOH
cortex
200 um
200 um
200 um
200 um

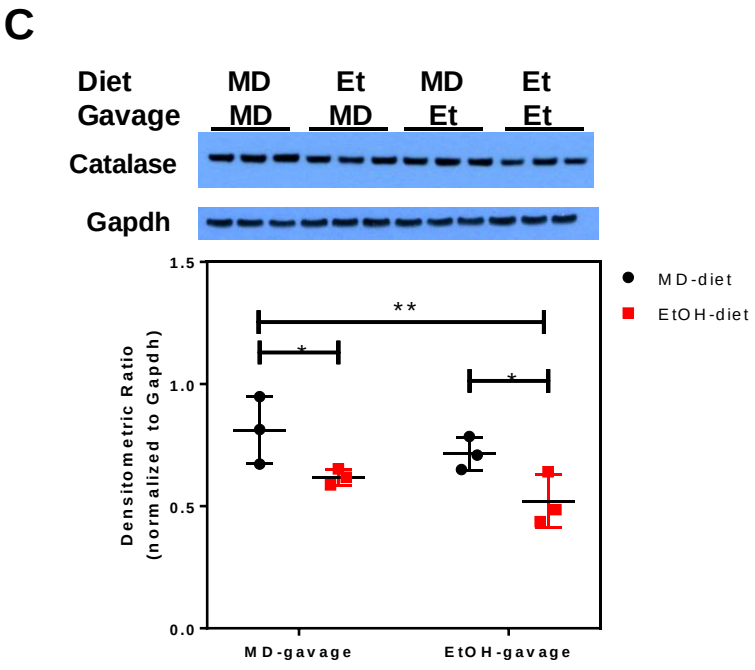
C
Diet
Gavage
MD
MD
Et
MD
MD
Et
Et
Et
Catalase
Gapdh
Densitometric Ratio
(normalized to Gapdh)
1.5
1.0
0.5
0.0
**
*
*
MD-diet
EtOH-diet
MD-gavage
EtOH-gavage

results have been deposited with the NCBI Gene Expression Omnibus (162) (https://www.ncbi.nlm.nih.gov/geo) as the study GSE81947.

## D. Discussion

Ethanol consumption is a risk factor in numerous health conditions, yet it is still unclear if the kidney is a direct target of EtOH toxicity. Hypothesis-driven studies on the effects of EtOH consumption on renal parenchyma are limited. We hypothesized that chronic, moderate EtOH consumption affects the kidney through pre- or post-translational regulation of protein abundance. Furthermore, these modifications contribute to the kidneys response to a second acute nephrotoxic event, such as experimental endotoxemia (163, 164). The current study addresses the hypothesis that chronic, moderate EtOH consumption significantly affects proteins, transcripts and canonical pathways in the kidney and the canonical response is modified by acute experimental endotoxemia (i.e. low dose LPS (10mg/kg) i.p.).

First, we examined the effects of EtOH and LPS on renal function and tissue structure. EtOH significantly increased BUN, a marker of kidney injury, as in a similar rodent model (87). LPS increased BUN (24h > 4h) in the presence or absence of EtOH, consistent with other studies of the same dose of LPS in mice (165). The effects of chronic, moderate EtOH consumption on the kidney at the tissue level were largely indiscernible, as shown by PAS histology. Our data show no significant effect of EtOH recruitment of MPO-positive cells into the kidney unlike differing reports in the rat Lieber-DeCarli model (87). The effect of

EtOH on LPS recruitment of MPO positive cells demonstrated a significant decrease at 4h post i.p. challenge that was lost at 24h. It is not clear if this difference was mitigated at the level of recruitment or clearance. However, EtOH is known to enhance neutrophil apoptosis, which suggests that our observations may result from increased neutrophil clearance in the EtOH fed mice (165).

Next, a discovery-based 'omics (Fig. 2A) approach was used to unbiasedly identify proteins, transcripts, and canonical signaling pathways affected by chronic, moderate EtOH consumption. EtOH significantly changed 92, 14, and 109 proteins on a control, 4h LPS, and 24h LPS background, respectively. It is known that TMT-based proteomic studies may underestimate fold-change differences (166), and therefore these numbers may underestimate the impact of chronic EtOH exposure on the renal proteome. Specifically, a cluster of proteins that EtOH significantly decreased in abundance compared to control included Ehhadh, Acad11, Sqstm1, and Hnrnpc. Ehhadh, Acad11 and Sqstm1 are important peroxisomal proteins involved in oxidation of fatty acids and regulation of peroxisomal matrix composition. Many other proteins changed by EtOH are not known to play a role in EtOH-induced mechanisms in the kidney or other organs (Supplemental Data). However, EtOH also increased the abundance of a cluster of ribosomal proteins (Rpl6, Rpl8, Rpl13a, and Rps15) on a background of 24h LPS. Rpl13a (ribosomal protein L13a) has previously been described as a critical component of the interferon (IFN)-γ-activated inhibitor of translation or 'GAIT' system (166). The GAIT system is comprised of glutamyl-prolyl tRNA synthetase, NS1-associated protein 1, Rpl13a, and glyceraldehyde-3-phosphate

dehydrogenase. The increased abundance of a critical GAIT component in the EtOH + 24h LPS animals compared to the 24h LPS animals could contribute to an attenuated renal IFN-γ response in the two-hit model. Further investigation would be needed to confirm up-regulation of the GAIT system as a protective measure for experimental endotoxemia in Lieber-DeCarli EtOH-fed animals.

The transcriptomic study identified renal transcripts and pathways affected by EtOH and/or the early acute phase period following 4h LPS. Hierarchical clustering of transcriptomic data demonstrates 6-7 major dendrogram arms of robust LPS-dependent transcriptomic changes (Fig. 5.4C). For the renal transcriptome LPS had a 10-fold larger effect on regulated transcripts ($q<0.05$) and with larger fold-changes as compared to EtOH as the single hit (Table 1A). Quantitatively, chronic EtOH consumption consistently affected a sub-set of regulated transcripts (e.g. increased- KYNU, SLC7A12, decreased- CNTNAP5, CYP4A12A, GM6300, and KIF20B) even on a background of LPS exposure. The KYNU gene encodes the enzyme L-kynureninase that hydrolyzes kynurenine into anthranilate + L-alanine. Tryptophan metabolites such as kynurenine have been reported to inhibit aldehyde dehydrogenase (Aldh) activity (167), and increased KYNU expression suggests an EtOH-dependent compensatory mechanism to increase the kidneys capacity to metabolize acetaldehyde, a toxic intermediate in the oxidation of EtOH. SLC7A12 is an Asc-type cationic amino acid transporter (y+ system) and increased arginine uptake by endothelial Asc-type cationic amino acid transporters has been shown to blunt oxidative stress (168). GM6300 is a SLC7 pseudogene adjacent to SLC7A12 in

the murine genome. Transcriptomic studies of 15-week old OVE26 kidneys identified 638 genes regulated by the diabetic state. The single largest increased (SLC7A12) and decreased (GM6300) genes by informatics analyses were associated with endoplasmic reticulum (ER) stress (169). EtOH-independent/LPS-dependent mRNA expression (Table 5.1) changes modeled proteomic findings for acute phase stress response (Fga, Fgb, Fgg) or interferon-responsive gene products (Ifit1, Ifit2, Saa2, and Lcn2). Unlike previous studies in the liver and lung, LPS did not induce an EtOH-dependent synergistic increase the acute phase response gene products PAI-1 (1, 170). Our data for significant EtOH induction of renal CXCL1 (KC) (and CXCL10) transcript add to our prior report in plasma, liver and lung of the Lieber-DeCarli model requiring a two hit (EtOH + LPS) induction of KC (170). The comparison of GO terms impacted by transcript regulation by EtOH suggested coordinated effects on a few transcripts associated with interferon response, innate immunity response and skeletal muscle development. Consideration of GO features for transcripts regulated by EtOH pre-exposure on the LPS background clustered on terms for muscle cell proliferation and cell movement. LPS as a single hit or second hit induced large changes in transcript numbers, affecting expected GO terms: innate immune response, cytokine response and positive regulation of cytokine production. This more robust effect of 4h LPS on the transcriptome compared to EtOH is unsurprising, since LPS is well known to enhance and activate gene programs of transcription factors such as NF-κB (171, 172). Overall, the transcriptomic effect

of EtOH is muted as compared to the proteomic effect but in some regards parallels other murine disease models associated with ER stress.

The proteomic and transcriptomic effects of EtOH and/or LPS were integrated using pathways analysis. The integrated data revealed that EtOH, LPS, and EtOH + LPS have differential effects on unique protein canonical signaling pathways (Fig. 5.5A-B) related to transcription and translational signaling pathways, as well as stress response pathways, for example: inactivation of Nrf2 (EtOH) and activation of the acute phase response or LXR/RXR (LPS) pathways. Activation of hepatic LXRα is associated fatty liver pathogensis (172). Activation of renal LXR has been shown to decrease cystic fibrosis transmembrane conductance regulator (CFTR)-mediated chloride transport (173) and downregulate sodium-phosphate cotransporters (173). The expected finding that LPS activated the acute phase response pathway increased our confidence in the unpredicted and novel findings, such as the overall inactivation of the Nrf2-mediated oxidative stress response pathway (Fig. 5B).

EtOH-induced downregulation of select proteins in the Nrf2-mediated oxidative stress response pathway was an unexpected finding, as EtOH is known to induce Nrf2 through Cyp2E1 in the liver (174). Of the Nrf-2 targets, only Gclc was down-regulated by NextGen transcriptomic data (mRNA $\log_2$FC -1.38, q-value<0.007). In models of chronic kidney disease, Nrf2 pathway deactivation or knock-out is known to cause injury from increased oxidative stress and/or death (174-181). However, the EtOH-downregulation of proteins in the Nrf2 pathway was not accompanied by significant renal injury as indicated by histology and

magnitude of BUN increase. There are several possible explanations for this. First, EtOH activation of other transcription factors (e.g. Ahr, Sp1, or AP-1) successfully compensated for the downregulated components of the Nrf2 pathway and protected against injury (182-184). Second, the selective induction of Nqo1 or Sod2 may be based on the binding to the antioxidant response element (ARE) by unique Nrf2:cap n collar binding partner (e.g. Maf, MafF, MafB, MafG, or PMF-1) complexes with targeted transcriptional activity (185-187). Lastly, it is possible that neither the chronic, moderate EtOH consumption nor the acute endotoxemia in these mice caused sufficient oxidative stress for the decrease in select Nrf2 targets to be histologically deleterious.

EtOH-dependent reduction of Nrf2-related proteins may occur through one or more of several potential mechanisms. Nrf2 is regulated by several mechanisms, typically divided in to those dependent or independent of Kelch-like ECH-associated protein 1 (Keap1)(188). One mechanism involves Nrf2 activation through the Sqstm1/p62-mediated deactivation of Keap1 (189). In the present study, EtOH decreased Sqstm1/p62 abundance with or without LPS-exposure. EtOH exposure of neuronal cells in culture has been shown to lead to an activation of autophagic pathways that includes loss of Sqstm1/p62 (190). Therefore, EtOH may deactivate the Nrf2 stress response pathway by induction of autophagy, Sqstm1/p62 loss, and concomitant activation of Keap1. These and other potential mechanisms of EtOH-induced dysregulation of the Nrf2-mediated oxidative stress response pathway will be investigated in future studies.

Cat (a Nrf2 target) abundance in the Lieber-DeCarli model decreased by 40-50% while the CAT mRNA was stable ($Log_2FC$ -0.08, $q<0.999$). This suggests a post-translational mechanism for decreased Cat abundance in the chronic setting. We hypothesized this decrease would be more pronounced in a more severe, acute-on-chronic NIAAA model (98) that better mimics human drinking patterns. This would be an important finding as Cat plays a prominent role in hydrogen peroxide degradation and of the three known EtOH oxidizing enzymes (Ald, Cyp2E1, and Cat) is the most abundant in the renal cortex. Our data demonstrated that in the NIAAA model, the chronic (10-day), acute (9h gavage), and acute-on chronic EtOH consumption all decreased Cat abundance in the renal cortex. The direct effects of EtOH on Cat will be investigated in future studies.

# CHAPTER VI

# DISCUSSION AND CONCLUSIONS

## A. Restatement of goals and questions

The overall goal of the work described in this dissertation was to discover new potential mechanisms of alcohol-induced organ injury. The work summarized in Chapter III aimed to test a novel method of analyzing the hepatic matrisome and use that approach to determine the effects of chronic, moderate ethanol consumption and acute inflammation on the hepatic matrisome in mice. Chapter IV aimed to characterize the ECM degradome (peptidome) in AH patient plasma that will allow further investigation into the use of plasma ECM peptides as surrogate or mechanistic biomarkers. Finally, Chapter V of this dissertation used a discovery based 'omics approach to elucidate the effects of ethanol consumption on the kidneys. Taken together, these studies provide new understanding of the complex mechanisms of alcohol-induced organ injury.

## B. Major findings of this dissertation

### 1. The hepatic "matrisome" responds dynamically to stress

The important role of the hepatic ECM in ALD pathophysiology is well known. However, research on this topic has been largely 'collagenocentric' and 'fibrosocentric', that is, primarily focused on the role of the collagen matrix and the dramatic ECM changes in the fibrosis stage of disease. It is now understood that the ECM is not simply a collagen scaffold, but a complex microenvironment that may be comprised of as many as 100 or more proteins at a time (191). The group of proteins that makes up any specific ECM varies with organ and disease state, and is a dynamic subset of over 1000 known ECM-related proteins (92). It is therefore unsurprising that recent studies have shown that multiple ECM proteins contribute to fibrosis (111). However, it is also now known that the hepatic ECM is altered prior to fibrogenesis (89, 90). A limitation of previous studies focused on the role of the ECM in ALD is that they generally studied changes in one ECM protein at a time and did not consider structural changes that may accompany altered ECM protein turnover. Therefore the goal of Chapter III was to adapt a sequential protein extraction method originally developed for cardiac tissue (99, 114, 121) to allow proteomic analysis of global changes in the hepatic matrisome caused by chronic, moderate ethanol consumption and acute inflammation (LPS). Furthermore, the sequential protein extraction method reveals potential changes in ECM protein crosslinking, location, and other aspects. Overall, this approach provides new insight into novel matrisome protein changes caused by inflammatory stress.

This approach divided the hepatic ECM proteome into four distinct extracts: (1) loosely-associated ECM proteins (NaCl extract), (2) intracellular and

membrane-associated proteins (SDS extract), (3) tightly bound ECM proteins (GnHCl extract), and (4) highly insoluble ECM components (the remaining pellet). Qualitative analysis of the matrisome demonstrated that both ethanol and LPS caused dynamic changes, with each exposure producing unique protein abundance patterns across the four fractions. Indeed, ethanol and LPS each increased the number of matrisome proteins by ~25% compared to control. The combination of ethanol and LPS demonstrated patterns similar to each individual exposure but also exhibited unique patterns. The unique subsets of proteins qualitatively changed with ethanol and/or LPS may play critical roles in the hepatic response to stress. Ethanol and/or LPS also quantitatively changed abundance of many proteins that did not change qualitatively. These proteins are new potential key players in liver injury, whose roles can be determined in future studies. Furthermore, analysis of ethanol-specific matrisome changes may provide new insights into the mechanisms of ethanol-sensitized liver injury, which could reveal novel therapeutic targets. Most importantly, this work demonstrates the dynamic, global response of the hepatic matrisome to stress that opens a new, important area of future research. This work also lays the foundation for future studies, such as the investigation of the ECM degradome in the plasma of AH patients described in Chapter IV.

### 2. The plasma ECM degradome profile of alcoholic hepatitis patients changes between MELD groups

Chapter IV of this dissertation aimed to characterize the plasma peptidome in AH patients. This builds upon the work described in Chapter III of this dissertation, which demonstrated that the hepatic ECM undergoes significant remodeling during inflammatory liver injury in the absence of any apparent fibrosis (93). This remodeling involves protease cleavage of ECM proteins, which yields ECM peptide fragments (94). During remodeling, peptide fragments of the degraded ECM have been shown to increase in biologic fluids (e.g. plasma) (58, 59). Peptidomic analysis of the degraded ECM (i.e., 'degradome) has been identified as a useful diagnostic/prognostic tool in other diseases of ECM remodeling (such as metastatic cancers)(58, 59). Current methods of predicting AH outcome (i.e. clinical scores, e.g. MELD) are limited in their abilities to predict at-risk patients with moderate disease(84). We hypothesized that the severe inflammatory liver injury caused by AH would yield a unique degradome profile in patient plasma.

In the pilot study described herein, a workflow was developed for the peptidomic analysis of plasma from healthy participants or AH patients. AH severity was stratified by MELD score as mild (<12; n=45), moderate (12-19; n=23) or severe (>19; n=37). Hierarchical clustering of the peptidomic data identified three strong groupings of peptide abundance patterns that reflected combinations of (A) increased peptide levels in healthy controls, (B) increased peptide levels in Moderate + Severe and (C) increased peptide levels in Mild-A + Mild-B AH cohorts. Post-hoc filtering of the differentially abundant peptides identified strong relative abundance changes in ECM peptides with strong

differences noted in the collagen and fibrinogen peptides. The unique patterns of ECM and other plasma peptides 'features' across different severity groups of AH patients can be confirmed using large longitudinal studies and can be investigated further as potential mechanistic or surrogate biomarkers for patient outcome. The characterization of the AH plasma degradome also supports future mechanistic studies on the role of ECM remodeling in AH.

### 3. Alcohol consumption alters renal cortical oxidant response pathways

The studies in Chapter III and Chapter IV focus on the toxic effects of ethanol on its primary target organ, the liver. In contrast to the liver, the effects of ethanol consumption on the kidneys are poorly understood. Some human studies have reported benefits of chronic moderate EtOH consumption for preservation of renal function (85, 95). However, the small number of rodent studies on the effects of ethanol on the kidneys have reported that chronic ethanol consumption upregulates CYP2E1 (88), causes neutrophil infiltration (88), and increases acetylation of mitochondrial proteins (86) in the kidney. However, these previous studies have been limited by the hypothesis that ethanol affects the kidneys by mechanisms parallel to those in the liver. To bypass this limitation, the study in Chapter V used an unbiased proteomic and transcriptomic approach to discover novel players and pathways affected by ethanol and LPS in the renal cortex.

The proteomic analysis found that EtOH significantly changed 92, 14, and 109 proteins on a control, 4h LPS, and 24h LPS background, respectively.

Interestingly, ethanol significantly decreased the abundance of a cluster of peroxisomal proteins compared to control. Ethanol also increased the abundance of a cluster of ribosomal proteins on a background of 24-hour LPS. The effects of ethanol on the transcriptome were more muted than the effects on the proteome, suggesting that ethanol-induced protein may occur through degradation or other transcription-independent mechanisms. Pathways analysis of integrated proteomic and transcriptomic data revealed that ethanol caused overall inactivation of the Nrf2-mediated oxidative stress response pathway. This finding, which was confirmed with western blots, was surprising, as ethanol is known to induce Nrf2 in the liver (174). This demonstrates the benefit of an unbiased, discovery-based approach. Chronic ethanol consumption decreased Cat (a Nrf2 target) abundance by 40-50%. The EtOH-associated effects on Cat were confirmed using a separate chronic-plus-binge (NIAAA) model. This work uncovers novel potential mechanisms by which ethanol effects the kidneys that can be studied further in the future. Most importantly, these findings reveal that chronic, moderate ethanol consumption affects the renal cortex at the protein and transcript level in the absence of tissue-level changes.

### C. Significance of new findings

Chapter III describes a new method of analyzing the hepatic matrisome and revealed that the hepatic matrisome responds dynamically to stress. The significance of this new method is that it can be adapted for analysis of the matrisome in other liver pathologies (e.g., NAFLD) and in other organs (e.g., the

lung). The finding that the hepatic matrisome responds dynamically to inflammatory stress is significant in that it provides a mechanistic link between steatohepatitis and fibrogenesis. That 'link' is transitional ECM remodeling, which is thought to be a pivotal point between disease restitution and progression (1), and is therefore a promising target for new therapeutics. The work in Chapter III identified specific protein players involved in remodeling that can be investigated as drug targets in future studies. Furthermore, as ECM remodeling yields degradation products that can be secreted into bodily fluids, knowledge of remodeling also supports future investigations of the degradome (e.g. Chapter IV) and the eventual development of novel biomarkers.

Plasma peptidomics is a novel approach for prognosis stratification in AH. The work in Chapter IV found that peptides in the plasma of AH patients change across groups separated by MELD score. Interestingly, patients with lower MELD scores had dramatically higher abundances of plasma peptides than those with higher MELD scores. This suggests that the degradome may be a positive predictor of outcome in AH. Patient prognosis is a key factor in clinical risk-benefit decision making regarding the administration of anti-inflammatory pharmacotherapeutics. While this work could lead to novel surrogate biomarkers, understanding the peptidome can also provide insight into AH mechanisms. For example, the peptidome in Chapter IV can be used to predict the proteases that generated it. This protease activity can be validated and targeted in future studies, which could lead to new targeted therapies for AH. Furthermore, the plasma peptides resulting from the protease activity could serve

as mechanistic biomarkers for response to the targeted therapy. Even apart from these possibilities, the fact that this work demonstrated that acute hepatic inflammation yields widespread, measurable changes in the plasma peptidome is significant in itself.

The effects of ethanol consumption on the kidneys are poorly understood. The work in Chapter V demonstrated that although ethanol consumption does not cause histologically detectable changes in renal architecture, it does influence the renal cortex proteome and, to a lesser extent, transcriptome. For example, ethanol consumption caused overall inactivation of the Nrf2 pathway, decreased abundance of peroxisomal proteins, and attenuated induction of LPS-responsive genes. This suggests unique effects of ethanol on the kidney that do not parallel those in the liver. These data provide new hypotheses for future investigations on both the direct effects of ethanol on the kidneys and effects of ethanol on other renal pathologies. More broadly, insight into the effects of ethanol on the kidneys contributes to understanding of alcohol toxicity, which could lead to new hypotheses and therapeutic approaches in the study of ALD.

## D. Strengths and weaknesses of this dissertation

### 1. Strengths

There are several strengths of this dissertation. The first study provides insight into the role of transitional ECM changes in ethanol-sensitized hepatic inflammation (Chapter III) by characterizing the hepatic matrisome. This work used a well-established mouse model of chronic, moderate ethanol consumption

and subsequent LPS exposure. Ethanol-sensitized hepatic inflammation is a complex phenomenon that is not confined to a single organ or cell type and cannot be wholly recapitulated in a simpler model (e.g. cell culture). The use of an animal model as opposed to a human study allows many variables to be controlled, such as number of calories consumed, genetic variability, and environmental factors. This increases confidence that ethanol and/or LPS are the variables that caused the experiment results. Another strength is that a new method of protein extraction was validated for use with liver tissue, enabling the analysis of low-abundance and highly insoluble hepatic ECM proteins. This allowed for a discovery-based proteomic characterization of the matrisome that provides a foundation for new hypothesis-driven studies and the identification of new therapeutic targets. Importantly, this work also demonstrates that the hepatic matrisome responds dynamically to stress in the absence of fibrosis.

The second study in this dissertation examines the plasma peptidome from AH patients with disease severity stratified by MELD score. This investigation uses plasma from human patients, and so it does not rely on assumptions regarding the relevance of a model. Another strength is that several different methods for the purification of peptides were tested, and the method which yielded the most pure peptidome was chosen. Samples were handled randomly in flights that contained a number of samples from each group that was proportional to the total. This minimizes any bias caused by sample handling. Samples were also spiked with a peptide standard prior to LC-MS/MS analysis to control for time-dependent changes in the instrument. Additionally, the statistical

analysis of the peptidomic data accounted for several covariates, including participant age and sex. The analysis included in this dissertation is preliminary, and future analyses will ensure that all appropriate covariates are considered. Another strength of this study is that patient plasma, as opposed to liver tissue, was analyzed. This supports the future development of a minimally invasive diagnostic tool.

The third study in this dissertation examines the effects of ethanol consumption on the renal cortex proteome and transcriptome. This work employed the same mouse model of chronic, moderate ethanol consumption and a second 'hit' of LPS used in the first study in this dissertation. Therefore, the same strengths associated with this model apply. This model is well established and recapitulates the complexity of human alcohol consumption, while still controlling many variables. Another strength of this work is that the proteomic workflow included TMT labeling, which allows reliable relative quantification of proteins between experimental groups. This work also used a discovery-based 'omics approach, as opposed to a hypothesis driven approach. Hypotheses by nature rely on previous knowledge, but very little is currently known about the effects of ethanol on the kidneys. For this reason, a hypothesis-generating approach was chosen, which provides a foundation for future studies. Indeed, several effects of ethanol on the kidneys were identified which would not have previously been expected. It should also be noted that expected LPS-activation of the acute phase response pathway was observed, which can be viewed as a

“positive control” that increases confidence in the less expected results of this study.

### 2. Weaknesses

The experiments described in Chapter III identified changes in the hepatic matrisome after alcohol and LPS exposure. Although there are strengths associated with the use of a mouse model, there are also limitations that should be acknowledged. Although *in vivo* experiments may recapitulate human disease more completely compared to *in vitro* experiments, *in vivo* research introduces more complexity and less control of variables. Conversely, relevance to human disease may be questionable when mouse models are compared to human studies. It is therefore possible that the observed matrisome changes are mouse-specific and have little direct relevance to humans. While the inverse relationship between model relevance and ability to control variables can never be entirely avoided, it can be optimized for the question at hand and thoughtfully considered when interpreting results. Another limitation of this study is that the biological replicate samples from the same fraction and same experimental group were pooled prior to LC-MS/MS analysis due to cost and time constraints. This means that a sample from a single mouse could have driven the observed qualitative changes in protein abundance. For this reason, follow-up studies are needed to confirm specific matrisome protein changes caused by ethanol and/or LPS. Additionally, this study did not investigate the functional significance of specific protein changes, and so future studies should address this.

The work in Chapter IV identified plasma peptides that change with disease severity in AH patients. As with all human studies, there are many variables that cannot be controlled, and should therefore be included as covariates in statistical analyses. The analyses included herein consider age and sex as covariates, but do not include other covariates, such as body mass index or race. Plasma from different study groups was also collected at different sites, and so site-specific changes need to be statistically accounted for to the extent possible. Therefore, it is possible that variables other than AH severity may be involved in the observed changes in peptide abundances. As noted previously, the statistical analysis in this dissertation is a pilot study, and future analyses will more thoroughly address potential confounding variables. Another limitation of this study is that it is cross-sectional, and so large scale longitudinal follow-up studies are needed to confirm the use of select peptides for outcome prediction.

The work in Chapter V identifies proteins, transcripts and pathways affected by ethanol and/or LPS in the renal cortex. The same mouse model was used in Chapter III. Therefore, the same model-related limitations apply that were previously discussed. As with any animal model, the relevance of the experimental results to human disease is not guaranteed, and neither is the assumption that all potential confounding variables have been controlled. It should also be acknowledged that another study reported that a similar rat model of chronic ethanol consumption increased recruitment of MPO-positive cells into the kidney, whereas we did not observe this effect (87). Another limitation is that TMT labeling, which is used for relative quantification of protein abundance, is

known to cause signal suppression. Therefore, the observed protein-level changes caused by ethanol and/or LPS may actually be greater than what was observed. Additionally, it is standard practice to confirm phenomena of interest observed with an 'omics approach using an additional method (e.g. immunoblot to confirm proteomics). Some protein-level changes reported here were indeed confirmed with immunoblot, but other changes need to be confirmed in future studies.

## E. Future Directions

While the experiments described in this dissertation answered specific gaps in our knowledge of alcohol-induced organ injury, it has also created new questions that will need to be addressed in future studies. Three of these questions of these are discussed below.

### 1. Does targeting the regulated "matrisome" proteins identified in Chapter III prevent, halt, or reverse alcohol-induced organ injury?

The method described in Chapter III identified dynamic changes in the hepatic matrisome after ethanol and/or LPS exposure. However, whether any of these ECM proteins plays a critical role in alcohol-sensitized liver injury has yet to be determined. To carry out this investigation, a select matrisome protein that was strongly and uniquely affected by ethanol in Chapter III could be genetically or pharmacologically targeted in a mouse model. These mice could be administered the same model of chronic ethanol exposure followed by

inflammatory insult used in Chapter III. Hepatic inflammatory injury in these mice could be examined with histology or other methods. If targeting a protein mitigates damage, then that protein plays a critical role in damage. For example, previous studies from our group demonstrated that the integrin inhibitor CycloRGDfV protects against liver injury and inflammation caused by acute ethanol exposure and LPS (192). Such findings would support the targeting of the matrisome protein as a therapeutic strategy.

2. **Do the regulated peptides and features identified in Chapter IV predict alcoholic hepatitis patient outcome and/or response to treatment in longitudinal studies?**

The study in Chapter IV identifies plasma peptides of AH patients that change in abundance with disease severity. Earlier in the discussion, it was noted that a limitation of this study is that it is cross-sectional and therefore does not follow the same patients over time. Since this research asks the question whether peptide “features” can predict AH outcome, follow-up longitudinal outcome studies would help answer this question more definitively. Such studies could also investigate the ability of regulated peptide “features” to predict response to treatment

3. **What are the mechanisms by which alcohol consumption alters the oxidant response pathways identified in Chapter V in the renal cortex?**

The experiments described in Chapter V identified the effects of ethanol consumption on renal cortex proteins and pathways using a discovery-based ‘omics approach. The mechanisms by which ethanol elicits these effects are unknown. The transcriptomic analysis in Chapter V revealed that the effects of ethanol on the transcriptome were more muted than the effects on the proteome, suggesting that ethanol-induced protein changes may occur through altered protein degradation or other transcription-independent mechanisms. Targeting one of these mechanisms in the same model of ethanol consumption used in Chapter V would help determine the contribution of that mechanism to the observed ethanol-induced effects. Since the ethanol-induced effects have already been identified, they can now be detected with a more targeted method (e.g. immunoblot or PCR) instead of an ‘omics approach. Additionally, molecular signaling programs (e.g. phosphorylation cascades) likely play a role in regulating the observed changes in protein abundance, and could be investigated with a proteomic approach (e.g. phosphoproteomics), or other methods. It should be noted that others have used acetylomics to determine that chronic, moderate ethanol consumption causes mitochondrial hyperacetylation in rodent kidneys (86). Links between this acetylomic data and the results in Chapter V could be investigated in future studies.

## F. Summary and Conclusions

The overall goal of the work described in this dissertation was to elucidate mechanisms of alcohol-induced organ injury. Chapter III introduced a new

proteomic approach for characterizing the hepatic matrisome. That approach was used to characterize the dynamic response of the matrisome to the stress of chronic, moderate ethanol consumption and acute inflammation in mice. This provides a foundation for future experiments to identify new players in transitional ECM remodeling. Chapter IV demonstrated that AH causes detectable changes in the plasma ECM degradome/peptidome of patients. These findings will allow future investigations into the use of plasma peptide 'features' as biomarkers for AH outcome. Finally, Chapter V revealed the effects of chronic ethanol consumption and acute inflammation on the renal cortex proteome and transcriptome. This work provides new hypotheses for future studies examining the effects of ethanol on the kidneys. Taken together, this work reveals new insight into mechanisms by which ethanol affects the liver and kidneys.

# REFERENCES


1. Poole LG, Arteel GE. Transitional Remodeling of the Hepatic Extracellular Matrix in Alcohol-Induced Liver Injury. Biomed Res Int. 2016;2016:3162670. Epub 2016/11/16. doi: 10.1155/2016/3162670. PubMed PMID: 27843941; PMCID: PMC5098054.
2. 2015 National Survey on Drug Use and Health: Summary of the Effects of the 2015 NSDUH Questionnaire Redesign: Implications for Data Users. Rockville (MD)2016.
3. Peacock A, Leung J, Larney S, Colledge S, Hickman M, Rehm J, Giovino GA, West R, Hall W, Griffiths P, Ali R, Gowing L, Marsden J, Ferrari AJ, Grebely J, Farrell M, Degenhardt L. Global statistics on alcohol, tobacco and illicit drug use: 2017 status report. Addiction. 2018;113(10):1905-26. Epub 2018/05/12. doi: 10.1111/add.14234. PubMed PMID: 29749059.
4. Crews FT, Nixon K. Mechanisms of neurodegeneration and regeneration in alcoholism. Alcohol Alcohol. 2009;44(2):115-27. Epub 2008/10/23. doi: 10.1093/alcalc/agn079. PubMed PMID: 18940959; PMCID: PMC2948812.
5. Beier JI, Arteel GE, McClain CJ. Advances in alcoholic liver disease. Curr Gastroenterol Rep. 2011;13(1):56-64. Epub 2010/11/23. doi: 10.1007/s11894-010-0157-5. PubMed PMID: 21088999; PMCID: PMC3772541.
6. Guidot DM, Roman J. Chronic ethanol ingestion increases susceptibility to acute lung injury: role of oxidative stress and tissue remodeling. Chest. 2002;122(6 Suppl):309S-14S. Epub 2002/12/12. PubMed PMID: 12475807.
7. Adachi J, Asano M, Ueno Y, Niemela O, Ohlendieck K, Peters TJ, Preedy VR. Alcoholic muscle disease and biomembrane perturbations (review). J Nutr Biochem. 2003;14(11):616-25. Epub 2003/11/25. PubMed PMID: 14629892.
8. Pandol SJ, Raraty M. Pathobiology of alcoholic pancreatitis. Pancreatology. 2007;7(2-3):105-14. Epub 2007/06/27. doi: 10.1159/000104235. PubMed PMID: 17592222.
9. Global status report on alcohol and health 2018. Geneva: World Health Organization, 2018 Contract No.: Licence: CC BY-NC-SA 3.0 IGO.
10. Tuithof M, ten Have M, van den Brink W, Vollebergh W, de Graaf R. Alcohol consumption and symptoms as predictors for relapse of DSM-5 alcohol use disorder. Drug Alcohol Depend. 2014;140:85-91. Epub 2014/05/06. doi: 10.1016/j.drugalcdep.2014.03.035. PubMed PMID: 24793368.
11. Frantz C, Stewart KM, Weaver VM. The extracellular matrix at a glance. J Cell Sci. 2010;123(Pt 24):4195-200. Epub 2010/12/03. doi: 10.1242/jcs.023820. PubMed PMID: 21123617; PMCID: PMC2995612.
12. Sewry CA, Muntoni F. Inherited disorders of the extracellular matrix. Curr Opin Neurol. 1999;12(5):519-26. Epub 1999/12/11. PubMed PMID: 10590888.

13. Mao JR, Bristow J. The Ehlers-Danlos syndrome: on beyond collagens. J Clin Invest. 2001;107(9):1063-9. Epub 2001/05/09. doi: 10.1172/JCI12881. PubMed PMID: 11342567; PMCID: PMC209288.
14. Coulombe PA, Kerns ML, Fuchs E. Epidermolysis bullosa simplex: a paradigm for disorders of tissue fragility. J Clin Invest. 2009;119(7):1784-93. Epub 2009/07/10. doi: 10.1172/JCI38177. PubMed PMID: 19587453; PMCID: PMC2701872.
15. Guo XD, Johnson JJ, Kramer JM. Embryonic lethality caused by mutations in basement membrane collagen of C. elegans. Nature. 1991;349(6311):707-9. Epub 1991/02/21. doi: 10.1038/349707a0. PubMed PMID: 1996137.
16. Bonnans C, Chou J, Werb Z. Remodelling the extracellular matrix in development and disease. Nat Rev Mol Cell Biol. 2014;15(12):786-801. Epub 2014/11/22. doi: 10.1038/nrm3904. PubMed PMID: 25415508; PMCID: PMC4316204.
17. Bosman FT, Stamenkovic I. Functional structure and composition of the extracellular matrix. J Pathol. 2003;200(4):423-8. Epub 2003/07/08. doi: 10.1002/path.1437. PubMed PMID: 12845610.
18. Hynes RO. The extracellular matrix: not just pretty fibrils. Science. 2009;326(5957):1216-9. Epub 2009/12/08. doi: 10.1126/science.1176009. PubMed PMID: 19965464; PMCID: PMC3536535.
19. Rozario T, DeSimone DW. The extracellular matrix in development and morphogenesis: a dynamic view. Dev Biol. 2010;341(1):126-40. Epub 2009/10/27. doi: 10.1016/j.ydbio.2009.10.026. PubMed PMID: 19854168; PMCID: PMC2854274.
20. Mott JD, Werb Z. Regulation of matrix biology by matrix metalloproteinases. Curr Opin Cell Biol. 2004;16(5):558-64. Epub 2004/09/15. doi: 10.1016/j.ceb.2004.07.010. PubMed PMID: 15363807; PMCID: PMC2775446.
21. Lu P, Takai K, Weaver VM, Werb Z. Extracellular matrix degradation and remodeling in development and disease. Cold Spring Harb Perspect Biol. 2011;3(12). Epub 2011/09/16. doi: 10.1101/cshperspect.a005058. PubMed PMID: 21917992; PMCID: PMC3225943.
22. Page-McCaw A, Ewald AJ, Werb Z. Matrix metalloproteinases and the regulation of tissue remodelling. Nat Rev Mol Cell Biol. 2007;8(3):221-33. Epub 2007/02/24. doi: 10.1038/nrm2125. PubMed PMID: 17318226; PMCID: PMC2760082.
23. Streuli C. Extracellular matrix remodelling and cellular differentiation. Curr Opin Cell Biol. 1999;11(5):634-40. Epub 1999/10/06. PubMed PMID: 10508658.
24. Cawston TE, Young DA. Proteinases involved in matrix turnover during cartilage and bone breakdown. Cell Tissue Res. 2010;339(1):221-35. Epub 2009/11/17. doi: 10.1007/s00441-009-0887-6. PubMed PMID: 19915869.
25. Gaffney J, Solomonov I, Zehorai E, Sagi I. Multilevel regulation of matrix metalloproteinases in tissue homeostasis indicates their molecular specificity in vivo. Matrix Biol. 2015;44-46:191-9. Epub 2015/01/28. doi: 10.1016/j.matbio.2015.01.012. PubMed PMID: 25622911.

26. Gao B, Ahmad MF, Nagy LE, Tsukamoto H. Inflammatory pathways in alcoholic steatohepatitis. J Hepatol. 2019;70(2):249-59. Epub 2019/01/20. doi: 10.1016/j.jhep.2018.10.023. PubMed PMID: 30658726; PMCID: PMC6361545.
27. Poole LG, Dolin CE, Arteel GE. Organ-Organ Crosstalk and Alcoholic Liver Disease. Biomolecules. 2017;7(3). Epub 2017/08/17. doi: 10.3390/biom7030062. PubMed PMID: 28812994; PMCID: PMC5618243.
28. Federman S, Miller LM, Sagi I. Following matrix metalloproteinases activity near the cell boundary by infrared micro-spectroscopy. Matrix Biol. 2002;21(7):567-77. Epub 2002/12/12. PubMed PMID: 12475641.
29. Klaas M, Kangur T, Viil J, Maemets-Allas K, Minajeva A, Vadi K, Antsov M, Lapidus N, Jarvekulg M, Jaks V. The alterations in the extracellular matrix composition guide the repair of damaged liver tissue. Sci Rep. 2016;6:27398. Epub 2016/06/07. doi: 10.1038/srep27398. PubMed PMID: 27264108; PMCID: PMC4893701.
30. Cahalon L, Hershkoviz R, Gilat D, Miller A, Akiyama SK, Yamada KM, Lider O. Functional interactions of fibronectin and TNF alpha: a paradigm of physiological linkage between cytokines and extracellular matrix moieties. Cell Adhes Commun. 1994;2(3):269-73. Epub 1994/07/01. PubMed PMID: 7827964.
31. Gailit J, Clark RA. Wound repair in the context of extracellular matrix. Curr Opin Cell Biol. 1994;6(5):717-25. Epub 1994/10/01. PubMed PMID: 7530463.
32. Gilat D, Hershkoviz R, Mekori YA, Vlodavsky I, Lider O. Regulation of adhesion of CD4+ T lymphocytes to intact or heparinase-treated subendothelial extracellular matrix by diffusible or anchored RANTES and MIP-1 beta. J Immunol. 1994;153(11):4899-906. Epub 1994/12/01. PubMed PMID: 7525718.
33. Ley K, Laudanna C, Cybulsky MI, Nourshargh S. Getting to the site of inflammation: the leukocyte adhesion cascade updated. Nat Rev Immunol. 2007;7(9):678-89. Epub 2007/08/25. doi: 10.1038/nri2156. PubMed PMID: 17717539.
34. Wang S, Voisin MB, Larbi KY, Dangerfield J, Scheiermann C, Tran M, Maxwell PH, Sorokin L, Nourshargh S. Venular basement membranes contain specific matrix protein low expression regions that act as exit points for emigrating neutrophils. J Exp Med. 2006;203(6):1519-32. Epub 2006/06/07. doi: 10.1084/jem.20051210. PubMed PMID: 16754715; PMCID: PMC2118318.
35. Woodfin A, Voisin MB, Nourshargh S. Recent developments and complexities in neutrophil transmigration. Curr Opin Hematol. 2010;17(1):9-17. Epub 2009/10/30. doi: 10.1097/MOH.0b013e3283333930. PubMed PMID: 19864945; PMCID: PMC2882030.
36. Bataller R, Brenner DA. Liver fibrosis. J Clin Invest. 2005;115(2):209-18. Epub 2005/02/04. doi: 10.1172/JCI24282. PubMed PMID: 15690074; PMCID: PMC546435.
37. Schuppan D, Ruehl M, Somasundaram R, Hahn EG. Matrix as a modulator of hepatic fibrogenesis. Semin Liver Dis. 2001;21(3):351-72. Epub 2001/10/05. doi: 10.1055/s-2001-17556. PubMed PMID: 11586465.
38. Ebihara T, Venkatesan N, Tanaka R, Ludwig MS. Changes in extracellular matrix and tissue viscoelasticity in bleomycin-induced lung fibrosis. Temporal

aspects. Am J Respir Crit Care Med. 2000;162(4 Pt 1):1569-76. Epub 2000/10/13. doi: 10.1164/ajrccm.162.4.9912011. PubMed PMID: 11029378.
39. Meltzer EB, Noble PW. Idiopathic pulmonary fibrosis. Orphanet J Rare Dis. 2008;3:8. Epub 2008/03/28. doi: 10.1186/1750-1172-3-8. PubMed PMID: 18366757; PMCID: PMC2330030.
40. Rocco PR, Negri EM, Kurtz PM, Vasconcellos FP, Silva GH, Capelozzi VL, Romero PV, Zin WA. Lung tissue mechanics and extracellular matrix remodeling in acute lung injury. Am J Respir Crit Care Med. 2001;164(6):1067-71. Epub 2001/10/06. doi: 10.1164/ajrccm.164.6.2007062. PubMed PMID: 11587998.
41. Henriksen PA, Sallenave JM. Human neutrophil elastase: mediator and therapeutic target in atherosclerosis. Int J Biochem Cell Biol. 2008;40(6-7):1095-100. Epub 2008/02/22. doi: 10.1016/j.biocel.2008.01.004. PubMed PMID: 18289916.
42. Kougias P, Chai H, Lin PH, Yao Q, Lumsden AB, Chen C. Defensins and cathelicidins: neutrophil peptides with roles in inflammation, hyperlipidemia and atherosclerosis. J Cell Mol Med. 2005;9(1):3-10. Epub 2005/03/24. PubMed PMID: 15784160.
43. Levental KR, Yu H, Kass L, Lakins JN, Egeblad M, Erler JT, Fong SF, Csiszar K, Giaccia A, Weninger W, Yamauchi M, Gasser DL, Weaver VM. Matrix crosslinking forces tumor progression by enhancing integrin signaling. Cell. 2009;139(5):891-906. Epub 2009/11/26. doi: 10.1016/j.cell.2009.10.027. PubMed PMID: 19931152; PMCID: PMC2788004.
44. Provenzano PP, Inman DR, Eliceiri KW, Knittel JG, Yan L, Rueden CT, White JG, Keely PJ. Collagen density promotes mammary tumor initiation and progression. BMC Med. 2008;6:11. Epub 2008/04/30. doi: 10.1186/1741-7015-6-11. PubMed PMID: 18442412; PMCID: PMC2386807.
45. Friedman SL, Roll FJ, Boyles J, Bissell DM. Hepatic lipocytes: the principal collagen-producing cells of normal rat liver. Proc Natl Acad Sci U S A. 1985;82(24):8681-5. Epub 1985/12/01. PubMed PMID: 3909149; PMCID: PMC391500.
46. Arthur MJ, Iredale JP, Mann DA. Tissue inhibitors of metalloproteinases: role in liver fibrosis and alcoholic liver disease. Alcohol Clin Exp Res. 1999;23(5):940-3. Epub 1999/06/17. PubMed PMID: 10371419.
47. Berk BC, Fujiwara K, Lehoux S. ECM remodeling in hypertensive heart disease. J Clin Invest. 2007;117(3):568-75. Epub 2007/03/03. doi: 10.1172/JCI31044. PubMed PMID: 17332884; PMCID: PMC1804378.
48. Liu F, Mih JD, Shea BS, Kho AT, Sharif AS, Tager AM, Tschumperlin DJ. Feedback amplification of fibrosis through matrix stiffening and COX-2 suppression. J Cell Biol. 2010;190(4):693-706. Epub 2010/08/25. doi: 10.1083/jcb.201004082. PubMed PMID: 20733059; PMCID: PMC2928007.
49. Egeblad M, Rasch MG, Weaver VM. Dynamic interplay between the collagen scaffold and tumor evolution. Curr Opin Cell Biol. 2010;22(5):697-706. Epub 2010/09/09. doi: 10.1016/j.ceb.2010.08.015. PubMed PMID: 20822891; PMCID: PMC2948601.

50. Sorokin L. The impact of the extracellular matrix on inflammation. Nat Rev Immunol. 2010;10(10):712-23. Epub 2010/09/25. doi: 10.1038/nri2852. PubMed PMID: 20865019.
51. Benyon RC, Arthur MJ. Extracellular matrix degradation and the role of hepatic stellate cells. Semin Liver Dis. 2001;21(3):373-84. Epub 2001/10/05. doi: 10.1055/s-2001-17552. PubMed PMID: 11586466.
52. Calabro SR, Maczurek AE, Morgan AJ, Tu T, Wen VW, Yee C, Mridha A, Lee M, d'Avigdor W, Locarnini SA, McCaughan GW, Warner FJ, McLennan SV, Shackel NA. Hepatocyte produced matrix metalloproteinases are regulated by CD147 in liver fibrogenesis. PLoS One. 2014;9(7):e90571. Epub 2014/07/31. doi: 10.1371/journal.pone.0090571. PubMed PMID: 25076423; PMCID: PMC4116334.
53. Zang S, Wang L, Ma X, Zhu G, Zhuang Z, Xun Y, Zhao F, Yang W, Liu J, Luo Y, Liu Y, Ye D, Shi J. Neutrophils Play a Crucial Role in the Early Stage of Nonalcoholic Steatohepatitis via Neutrophil Elastase in Mice. Cell Biochem Biophys. 2015;73(2):479-87. Epub 2016/06/29. doi: 10.1007/s12013-015-0682-9. PubMed PMID: 27352342.
54. Ramachandran P, Pellicoro A, Vernon MA, Boulter L, Aucott RL, Ali A, Hartland SN, Snowdon VK, Cappon A, Gordon-Walker TT, Williams MJ, Dunbar DR, Manning JR, van Rooijen N, Fallowfield JA, Forbes SJ, Iredale JP. Differential Ly-6C expression identifies the recruited macrophage phenotype, which orchestrates the regression of murine liver fibrosis. Proc Natl Acad Sci U S A. 2012;109(46):E3186-95. Epub 2012/10/27. doi: 10.1073/pnas.1119964109. PubMed PMID: 23100531; PMCID: PMC3503234.
55. Duarte S, Baber J, Fujii T, Coito AJ. Matrix metalloproteinases in liver injury, repair and fibrosis. Matrix Biol. 2015;44-46:147-56. Epub 2015/01/21. doi: 10.1016/j.matbio.2015.01.004. PubMed PMID: 25599939; PMCID: PMC4495728.
56. Nargis NN, Aldredge RC, Guy RD. The influence of soluble fragments of extracellular matrix (ECM) on tumor growth and morphology. Math Biosci. 2018;296:1-16. Epub 2017/12/07. doi: 10.1016/j.mbs.2017.11.014. PubMed PMID: 29208360.
57. Randles M, Lennon R. Applying Proteomics to Investigate Extracellular Matrix in Health and Disease. Curr Top Membr. 2015;76:171-96. Epub 2015/11/28. doi: 10.1016/bs.ctm.2015.06.001. PubMed PMID: 26610914.
58. Sand JM, Leeming DJ, Byrjalsen I, Bihlet AR, Lange P, Tal-Singer R, Miller BE, Karsdal MA, Vestbo J. High levels of biomarkers of collagen remodeling are associated with increased mortality in COPD - results from the ECLIPSE study. Respir Res. 2016;17(1):125. Epub 2016/10/08. doi: 10.1186/s12931-016-0440-6. PubMed PMID: 27716343; PMCID: PMC5050854.
59. Lipton A, Leitzel K, Ali SM, Polimera HV, Nagabhairu V, Marks E, Richardson AE, Krecko L, Ali A, Koestler W, Esteva FJ, Leeming DJ, Karsdal MA, Willumsen N. High turnover of extracellular matrix reflected by specific protein fragments measured in serum is associated with poor outcomes in two metastatic breast cancer cohorts. Int J Cancer. 2018;143(11):3027-34. Epub 2018/06/21. doi: 10.1002/ijc.31627. PubMed PMID: 29923614.

60. Altamirano J, Bataller R. Alcoholic liver disease: pathogenesis and new targets for therapy. Nat Rev Gastroenterol Hepatol. 2011;8(9):491-501. Epub 2011/08/10. doi: 10.1038/nrgastro.2011.134. PubMed PMID: 21826088.
61. Schwartz JM, Reinus JF. Prevalence and natural history of alcoholic liver disease. Clin Liver Dis. 2012;16(4):659-66. Epub 2012/10/30. doi: 10.1016/j.cld.2012.08.001. PubMed PMID: 23101975.
62. Seth D, Haber PS, Syn WK, Diehl AM, Day CP. Pathogenesis of alcohol-induced liver disease: classical concepts and recent advances. J Gastroenterol Hepatol. 2011;26(7):1089-105. Epub 2011/05/07. doi: 10.1111/j.1440-1746.2011.06756.x. PubMed PMID: 21545524.
63. Levitt MD, Levitt DG, Furne J, DeMaster EG. Can the liver account for first-pass metabolism of ethanol in the rat? Am J Physiol. 1994;267(3 Pt 1):G452-7. Epub 1994/09/01. doi: 10.1152/ajpgi.1994.267.3.G452. PubMed PMID: 7943243.
64. Day CP, James OF. Steatohepatitis: a tale of two "hits"? Gastroenterology. 1998;114(4):842-5. Epub 1998/04/18. PubMed PMID: 9547102.
65. Yang SQ, Lin HZ, Lane MD, Clemens M, Diehl AM. Obesity increases sensitivity to endotoxin liver injury: implications for the pathogenesis of steatohepatitis. Proc Natl Acad Sci U S A. 1997;94(6):2557-62. Epub 1997/03/18. PubMed PMID: 9122234; PMCID: PMC20127.
66. Tilg H, Diehl AM. Cytokines in alcoholic and nonalcoholic steatohepatitis. N Engl J Med. 2000;343(20):1467-76. Epub 2000/11/18. doi: 10.1056/NEJM200011163432007. PubMed PMID: 11078773.
67. Nelson S, Kolls JK. Alcohol, host defence and society. Nat Rev Immunol. 2002;2(3):205-9. Epub 2002/03/27. doi: 10.1038/nri744. PubMed PMID: 11913071.
68. Diehl AM. Liver disease in alcohol abusers: clinical perspective. Alcohol. 2002;27(1):7-11. Epub 2002/06/14. PubMed PMID: 12062630.
69. Powell WJ, Jr., Klatskin G. Duration of survival in patients with Laennec's cirrhosis. Influence of alcohol withdrawal, and possible effects of recent changes in general management of the disease. Am J Med. 1968;44(3):406-20. Epub 1968/03/01. PubMed PMID: 5641303.
70. La Vecchia C, Negri E, D'Avanzo B, Boyle P, Franceschi S. Medical history and primary liver cancer. Cancer Res. 1990;50(19):6274-7. Epub 1990/10/01. PubMed PMID: 2400990.
71. Gogel BM, Goldstein RM, Kuhn JA, McCarty TM, Donahoe A, Glastad K. Diagnostic evaluation of hepatocellular carcinoma in a cirrhotic liver. Oncology (Williston Park). 2000;14(6 Suppl 3):15-20. Epub 2000/07/11. PubMed PMID: 10887647.
72. Lucey MR, Mathurin P, Morgan TR. Alcoholic hepatitis. N Engl J Med. 2009;360(26):2758-69. Epub 2009/06/26. doi: 10.1056/NEJMra0805786. PubMed PMID: 19553649.
73. Torok NJ. Update on Alcoholic Hepatitis. Biomolecules. 2015;5(4):2978-86. Epub 2015/11/06. doi: 10.3390/biom5042978. PubMed PMID: 26540078; PMCID: PMC4693265.

74. Moreau R, Jalan R, Gines P, Pavesi M, Angeli P, Cordoba J, Durand F, Gustot T, Saliba F, Domenicali M, Gerbes A, Wendon J, Alessandria C, Laleman W, Zeuzem S, Trebicka J, Bernardi M, Arroyo V, Consortium CSIotE-C. Acute-on-chronic liver failure is a distinct syndrome that develops in patients with acute decompensation of cirrhosis. Gastroenterology. 2013;144(7):1426-37, 37 e1-9. Epub 2013/03/12. doi: 10.1053/j.gastro.2013.02.042. PubMed PMID: 23474284.
75. Michelena J, Altamirano J, Abraldes JG, Affo S, Morales-Ibanez O, Sancho-Bru P, Dominguez M, Garcia-Pagan JC, Fernandez J, Arroyo V, Gines P, Louvet A, Mathurin P, Mehal WZ, Caballeria J, Bataller R. Systemic inflammatory response and serum lipopolysaccharide levels predict multiple organ failure and death in alcoholic hepatitis. Hepatology. 2015;62(3):762-72. Epub 2015/03/13. doi: 10.1002/hep.27779. PubMed PMID: 25761863; PMCID: PMC4549175.
76. Chayanupatkul M, Liangpunsakul S. Alcoholic hepatitis: a comprehensive review of pathogenesis and treatment. World J Gastroenterol. 2014;20(20):6279-86. Epub 2014/05/31. doi: 10.3748/wjg.v20.i20.6279. PubMed PMID: 24876748; PMCID: PMC4033465.
77. Cohen JA, Kaplan MM. The SGOT/SGPT ratio--an indicator of alcoholic liver disease. Dig Dis Sci. 1979;24(11):835-8. Epub 1979/11/01. PubMed PMID: 520102.
78. Yeluru A, Cuthbert JA, Casey L, Mitchell MC. Alcoholic Hepatitis: Risk Factors, Pathogenesis, and Approach to Treatment. Alcohol Clin Exp Res. 2016;40(2):246-55. Epub 2016/02/05. doi: 10.1111/acer.12956. PubMed PMID: 26842243.
79. Maddrey WC, Boitnott JK, Bedine MS, Weber FL, Jr., Mezey E, White RI, Jr. Corticosteroid therapy of alcoholic hepatitis. Gastroenterology. 1978;75(2):193-9. Epub 1978/08/01. PubMed PMID: 352788.
80. Srikureja W, Kyulo NL, Runyon BA, Hu KQ. MELD score is a better prognostic model than Child-Turcotte-Pugh score or Discriminant Function score in patients with alcoholic hepatitis. J Hepatol. 2005;42(5):700-6. Epub 2005/04/14. doi: 10.1016/j.jhep.2004.12.022. PubMed PMID: 15826720.
81. Cuthbert JA, Arslanlar S, Yepuri J, Montrose M, Ahn CW, Shah JP. Predicting short-term mortality and long-term survival for hospitalized US patients with alcoholic hepatitis. Dig Dis Sci. 2014;59(7):1594-602. Epub 2014/01/22. doi: 10.1007/s10620-013-3020-3. PubMed PMID: 24445730; PMCID: PMC4071136.
82. Dominguez M, Rincon D, Abraldes JG, Miquel R, Colmenero J, Bellot P, Garcia-Pagan JC, Fernandez R, Moreno M, Banares R, Arroyo V, Caballeria J, Gines P, Bataller R. A new scoring system for prognostic stratification of patients with alcoholic hepatitis. Am J Gastroenterol. 2008;103(11):2747-56. Epub 2008/08/30. doi: 10.1111/j.1572-0241.2008.02104.x. PubMed PMID: 18721242.
83. Forrest EH, Evans CD, Stewart S, Phillips M, Oo YH, McAvoy NC, Fisher NC, Singhal S, Brind A, Haydon G, O'Grady J, Day CP, Hayes PC, Murray LS, Morris AJ. Analysis of factors predictive of mortality in alcoholic hepatitis and derivation and validation of the Glasgow alcoholic hepatitis score. Gut. 2005;54(8):1174-9. Epub 2005/07/13. doi: 10.1136/gut.2004.050781. PubMed PMID: 16009691; PMCID: PMC1774903.

84. Dunn W, Jamil LH, Brown LS, Wiesner RH, Kim WR, Menon KV, Malinchoc M, Kamath PS, Shah V. MELD accurately predicts mortality in patients with alcoholic hepatitis. Hepatology. 2005;41(2):353-8. Epub 2005/01/22. doi: 10.1002/hep.20503. PubMed PMID: 15660383.
85. Koning SH, Gansevoort RT, Mukamal KJ, Rimm EB, Bakker SJ, Joosten MM, Group PS. Alcohol consumption is inversely associated with the risk of developing chronic kidney disease. Kidney Int. 2015;87(5):1009-16. Epub 2015/01/15. doi: 10.1038/ki.2014.414. PubMed PMID: 25587707.
86. Harris PS, Roy SR, Coughlan C, Orlicky DJ, Liang Y, Shearn CT, Roede JR, Fritz KS. Chronic ethanol consumption induces mitochondrial protein acetylation and oxidative stress in the kidney. Redox Biol. 2015;6:33-40. Epub 2015/07/16. doi: 10.1016/j.redox.2015.06.021. PubMed PMID: 26177469; PMCID: PMC4511634.
87. Latchoumycandane C, Nagy LE, McIntyre TM. Chronic ethanol ingestion induces oxidative kidney injury through taurine-inhibitable inflammation. Free Radic Biol Med. 2014;69:403-16. Epub 2014/01/15. doi: 10.1016/j.freeradbiomed.2014.01.001. PubMed PMID: 24412858; PMCID: PMC3960325.
88. Latchoumycandane C, Nagy LE, McIntyre TM. Myeloperoxidase formation of PAF receptor ligands induces PAF receptor-dependent kidney injury during ethanol consumption. Free Radic Biol Med. 2015;86:179-90. Epub 2015/05/25. doi: 10.1016/j.freeradbiomed.2015.05.020. PubMed PMID: 26003521; PMCID: PMC4554800.
89. Beier JI, Luyendyk JP, Guo L, von Montfort C, Staunton DE, Arteel GE. Fibrin accumulation plays a critical role in the sensitization to lipopolysaccharide-induced liver injury caused by ethanol in mice. Hepatology. 2009;49(5):1545-53. Epub 2009/03/18. doi: 10.1002/hep.22847. PubMed PMID: 19291788; PMCID: PMC2852109.
90. Gillis SE, Nagy LE. Deposition of cellular fibronectin increases before stellate cell activation in rat liver during ethanol feeding. Alcohol Clin Exp Res. 1997;21(5):857-61. Epub 1997/08/01. PubMed PMID: 9267535.
91. Thiele GM, Duryee MJ, Freeman TL, Sorrell MF, Willis MS, Tuma DJ, Klassen LW. Rat sinusoidal liver endothelial cells (SECs) produce pro-fibrotic factors in response to adducts formed from the metabolites of ethanol. Biochem Pharmacol. 2005;70(11):1593-600. Epub 2005/10/06. doi: 10.1016/j.bcp.2005.08.014. PubMed PMID: 16202982.
92. Naba A, Clauser KR, Ding H, Whittaker CA, Carr SA, Hynes RO. The extracellular matrix: Tools and insights for the "omics" era. Matrix Biol. 2016;49:10-24. Epub 2015/07/15. doi: 10.1016/j.matbio.2015.06.003. PubMed PMID: 26163349; PMCID: PMC5013529.
93. Massey VL, Dolin CE, Poole LG, Hudson SV, Siow DL, Brock GN, Merchant ML, Wilkey DW, Arteel GE. The hepatic "matrisome" responds dynamically to injury: Characterization of transitional changes to the extracellular matrix in mice. Hepatology. 2017;65(3):969-82. Epub 2016/12/31. doi: 10.1002/hep.28918. PubMed PMID: 28035785; PMCID: PMC5319876.

94. Daley WP, Peters SB, Larsen M. Extracellular matrix dynamics in development and regenerative medicine. J Cell Sci. 2008;121(Pt 3):255-64. Epub 2008/01/25. doi: 10.1242/jcs.006064. PubMed PMID: 18216330.
95. White SL, Polkinghorne KR, Cass A, Shaw JE, Atkins RC, Chadban SJ. Alcohol consumption and 5-year onset of chronic kidney disease: the AusDiab study. Nephrol Dial Transplant. 2009;24(8):2464-72. Epub 2009/03/25. doi: 10.1093/ndt/gfp114. PubMed PMID: 19307230.
96. von Montfort C, Beier JI, Kaiser JP, Guo L, Joshi-Barve S, Pritchard MT, States JC, Arteel GE. PAI-1 plays a protective role in CCl4-induced hepatic fibrosis in mice: role of hepatocyte division. Am J Physiol Gastrointest Liver Physiol. 2010;298(5):G657-66. Epub 2010/03/06. doi: 10.1152/ajpgi.00107.2009. PubMed PMID: 20203062; PMCID: PMC2867423.
97. Massey VL, Poole LG, Siow DL, Torres E, Warner NL, Schmidt RH, Ritzenthaler JD, Roman J, Arteel GE. Chronic Alcohol Exposure Enhances Lipopolysaccharide-Induced Lung Injury in Mice: Potential Role of Systemic Tumor Necrosis Factor-Alpha. Alcohol Clin Exp Res. 2015;39(10):1978-88. Epub 2015/09/19. doi: 10.1111/acer.12855. PubMed PMID: 26380957; PMCID: PMC4804458.
98. Bertola A, Mathews S, Ki SH, Wang H, Gao B. Mouse model of chronic and binge ethanol feeding (the NIAAA model). Nat Protoc. 2013;8(3):627-37. Epub 2013/03/02. doi: 10.1038/nprot.2013.032. PubMed PMID: 23449255; PMCID: PMC3788579.
99. de Castro Bras LE, Ramirez TA, DeLeon-Pennell KY, Chiao YA, Ma Y, Dai Q, Halade GV, Hakala K, Weintraub ST, Lindsey ML. Texas 3-step decellularization protocol: looking at the cardiac extracellular matrix. J Proteomics. 2013;86:43-52. Epub 2013/05/18. doi: 10.1016/j.jprot.2013.05.004. PubMed PMID: 23681174; PMCID: PMC3879953.
100. Wisniewski JR, Zougman A, Mann M. Combination of FASP and StageTip-based fractionation allows in-depth analysis of the hippocampal membrane proteome. J Proteome Res. 2009;8(12):5674-8. Epub 2009/10/24. doi: 10.1021/pr900748n. PubMed PMID: 19848406.
101. Rood IM, Merchant ML, Wilkey DW, Zhang T, Zabrouskov V, van der Vlag J, Dijkman HB, Willemsen BK, Wetzels JF, Klein JB, Deegens JK. Increased expression of lysosome membrane protein 2 in glomeruli of patients with idiopathic membranous nephropathy. Proteomics. 2015;15(21):3722-30. Epub 2015/08/26. doi: 10.1002/pmic.201500127. PubMed PMID: 26304790.
102. Keshishian H, Burgess MW, Gillette MA, Mertins P, Clauser KR, Mani DR, Kuhn EW, Farrell LA, Gerszten RE, Carr SA. Multiplexed, Quantitative Workflow for Sensitive Biomarker Discovery in Plasma Yields Novel Candidates for Early Myocardial Injury. Mol Cell Proteomics. 2015;14(9):2375-93. Epub 2015/03/01. doi: 10.1074/mcp.M114.046813. PubMed PMID: 25724909; PMCID: PMC4563722.
103. Barati MT, Powell DW, Kechavarzi BD, Isaacs SM, Zheng S, Epstein PN, Cai L, Coventry S, Rane MJ, Klein JB. Differential expression of endoplasmic reticulum stress-response proteins in different renal tubule subtypes of OVE26 diabetic mice. Cell Stress Chaperones. 2016;21(1):155-66. Epub 2015/10/21.

doi: 10.1007/s12192-015-0648-2. PubMed PMID: 26483256; PMCID: PMC4679738.
104. Crabb DW, Bataller R, Chalasani NP, Kamath PS, Lucey M, Mathurin P, McClain C, McCullough A, Mitchell MC, Morgan TR, Nagy L, Radaeva S, Sanyal A, Shah V, Szabo G, Consortia NAH. Standard Definitions and Common Data Elements for Clinical Trials in Patients With Alcoholic Hepatitis: Recommendation From the NIAAA Alcoholic Hepatitis Consortia. Gastroenterology. 2016;150(4):785-90. Epub 2016/02/28. doi: 10.1053/j.gastro.2016.02.042. PubMed PMID: 26921783; PMCID: PMC5287362.
105. Saunders JB, Aasland OG, Babor TF, de la Fuente JR, Grant M. Development of the Alcohol Use Disorders Identification Test (AUDIT): WHO Collaborative Project on Early Detection of Persons with Harmful Alcohol Consumption--II. Addiction. 1993;88(6):791-804. Epub 1993/06/01. PubMed PMID: 8329970.
106. Skinner HA, Sheu WJ. Reliability of alcohol use indices. The Lifetime Drinking History and the MAST. J Stud Alcohol. 1982;43(11):1157-70. Epub 1982/11/01. PubMed PMID: 7182675.
107. Parker BL, Burchfield JG, Clayton D, Geddes TA, Payne RJ, Kiens B, Wojtaszewski JFP, Richter EA, James DE. Multiplexed Temporal Quantification of the Exercise-regulated Plasma Peptidome. Mol Cell Proteomics. 2017;16(12):2055-68. Epub 2017/10/07. doi: 10.1074/mcp.RA117.000020. PubMed PMID: 28982716; PMCID: PMC5724171.
108. Bolstad BM, Irizarry RA, Astrand M, Speed TP. A comparison of normalization methods for high density oligonucleotide array data based on variance and bias. Bioinformatics. 2003;19(2):185-93. Epub 2003/01/23. PubMed PMID: 12538238.
109. Stacklies W, Redestig H, Scholz M, Walther D, Selbig J. pcaMethods--a bioconductor package providing PCA methods for incomplete data. Bioinformatics. 2007;23(9):1164-7. Epub 2007/03/09. doi: 10.1093/bioinformatics/btm069. PubMed PMID: 17344241.
110. Key M. A tutorial in displaying mass spectrometry-based proteomic data using heat maps. BMC Bioinformatics. 2012;13 Suppl 16:S10. Epub 2012/11/28. doi: 10.1186/1471-2105-13-S16-S10. PubMed PMID: 23176119; PMCID: PMC3489527.
111. Gressner OA, Weiskirchen R, Gressner AM. Evolving concepts of liver fibrogenesis provide new diagnostic and therapeutic options. Comp Hepatol. 2007;6:7. Epub 2007/08/01. doi: 10.1186/1476-5926-6-7. PubMed PMID: 17663771; PMCID: PMC1994681.
112. Bergheim I, Guo L, Davis MA, Lambert JC, Beier JI, Duveau I, Luyendyk JP, Roth RA, Arteel GE. Metformin prevents alcohol-induced liver injury in the mouse: Critical role of plasminogen activator inhibitor-1. Gastroenterology. 2006;130(7):2099-112. Epub 2006/06/10. doi: 10.1053/j.gastro.2006.03.020. PubMed PMID: 16762632; PMCID: PMC2648856.
113. Naba A, Clauser KR, Hynes RO. Enrichment of Extracellular Matrix Proteins from Tissues and Digestion into Peptides for Mass Spectrometry

Analysis. J Vis Exp. 2015(101):e53057. Epub 2015/08/15. doi: 10.3791/53057. PubMed PMID: 26273955; PMCID: PMC4545199.
114. Didangelos A, Yin X, Mandal K, Baumert M, Jahangiri M, Mayr M. Proteomics characterization of extracellular space components in the human aorta. Mol Cell Proteomics. 2010;9(9):2048-62. Epub 2010/06/17. doi: 10.1074/mcp.M110.001693. PubMed PMID: 20551380; PMCID: PMC2938114.
115. Mason RM, Mayes RW. Extraction of cartilage protein-polysaccharides with inorganic salt solutions. Biochem J. 1973;131(3):535-40. Epub 1973/03/01. PubMed PMID: 4269048; PMCID: PMC1177500.
116. Sajdera SW, Hascall VC. Proteinpolysaccharide complex from bovine nasal cartilage. A comparison of low and high shear extraction procedures. J Biol Chem. 1969;244(1):77-87. Epub 1969/01/10. PubMed PMID: 4237578.
117. Enomoto N, Ikejima K, Bradford B, Rivera C, Kono H, Brenner DA, Thurman RG. Alcohol causes both tolerance and sensitization of rat Kupffer cells via mechanisms dependent on endotoxin. Gastroenterology. 1998;115(2):443-51. Epub 1998/07/25. PubMed PMID: 9679050.
118. Eyre DR, Paz MA, Gallop PM. Cross-linking in collagen and elastin. Annu Rev Biochem. 1984;53:717-48. Epub 1984/01/01. doi: 10.1146/annurev.bi.53.070184.003441. PubMed PMID: 6148038.
119. Kobayashi J, Yamada S, Kawasaki H. Distribution of vitronectin in plasma and liver tissue: relationship to chronic liver disease. Hepatology. 1994;20(6):1412-7. Epub 1994/12/01. PubMed PMID: 7527001.
120. Koukoulis GK, Shen J, Virtanen I, Gould VE. Vitronectin in the cirrhotic liver: an immunomarker of mature fibrosis. Hum Pathol. 2001;32(12):1356-62. Epub 2002/01/05. doi: 10.1053/hupa.2001.29675. PubMed PMID: 11774169.
121. Didangelos A, Yin X, Mandal K, Saje A, Smith A, Xu Q, Jahangiri M, Mayr M. Extracellular matrix composition and remodeling in human abdominal aortic aneurysms: a proteomics approach. Mol Cell Proteomics. 2011;10(8):M111 008128. Epub 2011/05/20. doi: 10.1074/mcp.M111.008128. PubMed PMID: 21593211; PMCID: PMC3149094.
122. Holdsworth SR, Thomson NM, Glasgow EF, Atkins RC. The effect of defibrination on macrophage participation in rabbit nephrotoxic nephritis: studies using glomerular culture and electronmicroscopy. Clin Exp Immunol. 1979;37(1):38-43. Epub 1979/07/01. PubMed PMID: 487657; PMCID: PMC1537661.
123. Loike JD, el Khoury J, Cao L, Richards CP, Rascoff H, Mandeville JT, Maxfield FR, Silverstein SC. Fibrin regulates neutrophil migration in response to interleukin 8, leukotriene B4, tumor necrosis factor, and formyl-methionyl-leucyl-phenylalanine. J Exp Med. 1995;181(5):1763-72. Epub 1995/05/01. PubMed PMID: 7722453; PMCID: PMC2191980.
124. Lonai P. Epithelial mesenchymal interactions, the ECM and limb development. J Anat. 2003;202(1):43-50. Epub 2003/02/18. PubMed PMID: 12587919; PMCID: PMC1571048.
125. Hynes RO. Integrins: versatility, modulation, and signaling in cell adhesion. Cell. 1992;69(1):11-25. Epub 1992/04/03. PubMed PMID: 1555235.

126. Nastase MV, Young MF, Schaefer L. Biglycan: a multivalent proteoglycan providing structure and signals. J Histochem Cytochem. 2012;60(12):963-75. Epub 2012/07/24. doi: 10.1369/0022155412456380. PubMed PMID: 22821552; PMCID: PMC3527886.
127. Bode C, Kugler V, Bode JC. Endotoxemia in patients with alcoholic and non-alcoholic cirrhosis and in subjects with no evidence of chronic liver disease following acute alcohol excess. J Hepatol. 1987;4(1):8-14. Epub 1987/02/01. PubMed PMID: 3571935.
128. Mosesson MW. Fibrinogen gamma chain functions. J Thromb Haemost. 2003;1(2):231-8. Epub 2003/07/23. PubMed PMID: 12871494.
129. Migita K, Abiru S, Nakamura M, Komori A, Yoshida Y, Yokoyama T, Daikoku M, Ueki T, Takii Y, Yano K, Yastuhashi H, Eguchi K, Ishibashi H. Lipopolysaccharide signaling induces serum amyloid A (SAA) synthesis in human hepatocytes in vitro. FEBS Lett. 2004;569(1-3):235-9. Epub 2004/07/01. doi: 10.1016/j.febslet.2004.05.072. PubMed PMID: 15225640.
130. Pruett BS, Pruett SB. An explanation for the paradoxical induction and suppression of an acute phase response by ethanol. Alcohol. 2006;39(2):105-10. Epub 2006/12/01. doi: 10.1016/j.alcohol.2006.08.003. PubMed PMID: 17134663; PMCID: PMC1764540.
131. Bopst M, Haas C, Car B, Eugster HP. The combined inactivation of tumor necrosis factor and interleukin-6 prevents induction of the major acute phase proteins by endotoxin. Eur J Immunol. 1998;28(12):4130-7. Epub 1998/12/23. doi: 10.1002/(SICI)1521-4141(199812)28:12<4130::AID-IMMU4130>3.0.CO;2-W. PubMed PMID: 9862349.
132. Haziot A, Lin XY, Zhang F, Goyert SM. The induction of acute phase proteins by lipopolysaccharide uses a novel pathway that is CD14-independent. J Immunol. 1998;160(6):2570-2. Epub 1998/03/24. PubMed PMID: 9510153.
133. Sun S, Guo Y, Zhao G, Zhou X, Li J, Hu J, Yu H, Chen Y, Song H, Qiao F, Xu G, Yang F, Wu Y, Tomlinson S, Duan Z, Zhou Y. Complement and the alternative pathway play an important role in LPS/D-GalN-induced fulminant hepatic failure. PLoS One. 2011;6(11):e26838. Epub 2011/11/10. doi: 10.1371/journal.pone.0026838. PubMed PMID: 22069473; PMCID: PMC3206060.
134. Bacigalupo ML, Manzi M, Rabinovich GA, Troncoso MF. Hierarchical and selective roles of galectins in hepatocarcinogenesis, liver fibrosis and inflammation of hepatocellular carcinoma. World J Gastroenterol. 2013;19(47):8831-49. Epub 2014/01/01. doi: 10.3748/wjg.v19.i47.8831. PubMed PMID: 24379606; PMCID: PMC3870534.
135. Aziz-Seible RS, Lee SM, Kharbanda KK, McVicker BL, Casey CA. Ethanol feeding potentiates the pro-inflammatory response of Kupffer cells to cellular fibronectin. Alcohol Clin Exp Res. 2011;35(4):717-25. Epub 2011/01/13. doi: 10.1111/j.1530-0277.2010.01389.x. PubMed PMID: 21223308.
136. Schonherr E, Witsch-Prehm P, Harrach B, Robenek H, Rauterberg J, Kresse H. Interaction of biglycan with type I collagen. J Biol Chem. 1995;270(6):2776-83. Epub 1995/02/10. PubMed PMID: 7852349.

137. Mohan H, Krumbholz M, Sharma R, Eisele S, Junker A, Sixt M, Newcombe J, Wekerle H, Hohlfeld R, Lassmann H, Meinl E. Extracellular matrix in multiple sclerosis lesions: Fibrillar collagens, biglycan and decorin are upregulated and associated with infiltrating immune cells. Brain Pathol. 2010;20(5):966-75. Epub 2010/05/12. doi: 10.1111/j.1750-3639.2010.00399.x. PubMed PMID: 20456365.
138. Tufvesson E, Westergren-Thorsson G. Tumour necrosis factor-alpha interacts with biglycan and decorin. FEBS Lett. 2002;530(1-3):124-8. Epub 2002/10/22. PubMed PMID: 12387878.
139. Hengst U, Albrecht H, Hess D, Monard D. The phosphatidylethanolamine-binding protein is the prototype of a novel family of serine protease inhibitors. J Biol Chem. 2001;276(1):535-40. Epub 2000/10/18. doi: 10.1074/jbc.M002524200. PubMed PMID: 11034991.
140. Xu YF, Yi Y, Qiu SJ, Gao Q, Li YW, Dai CX, Cai MY, Ju MJ, Zhou J, Zhang BH, Fan J. PEBP1 downregulation is associated to poor prognosis in HCC related to hepatitis B infection. J Hepatol. 2010;53(5):872-9. Epub 2010/08/27. doi: 10.1016/j.jhep.2010.05.019. PubMed PMID: 20739083.
141. Keller ET, Fu Z, Brennan M. The biology of a prostate cancer metastasis suppressor protein: Raf kinase inhibitor protein. J Cell Biochem. 2005;94(2):273-8. Epub 2004/11/27. doi: 10.1002/jcb.20169. PubMed PMID: 15565643.
142. Wells RG. The role of matrix stiffness in regulating cell behavior. Hepatology. 2008;47(4):1394-400. Epub 2008/03/01. doi: 10.1002/hep.22193. PubMed PMID: 18307210.
143. Ford AJ, Jain G, Rajagopalan P. Designing a fibrotic microenvironment to investigate changes in human liver sinusoidal endothelial cell function. Acta Biomater. 2015;24:220-7. Epub 2015/06/29. doi: 10.1016/j.actbio.2015.06.028. PubMed PMID: 26117313.
144. Yang C, Zeisberg M, Lively JC, Nyberg P, Afdhal N, Kalluri R. Integrin alpha1beta1 and alpha2beta1 are the key regulators of hepatocarcinoma cell invasion across the fibrotic matrix microenvironment. Cancer Res. 2003;63(23):8312-7. Epub 2003/12/18. PubMed PMID: 14678990.
145. Seitz HK, Bataller R, Cortez-Pinto H, Gao B, Gual A, Lackner C, Mathurin P, Mueller S, Szabo G, Tsukamoto H. Alcoholic liver disease. Nat Rev Dis Primers. 2018;4(1):16. doi: 10.1038/s41572-018-0014-7. PubMed PMID: 30115921.
146. Savolainen VT, Liesto K, Mannikko A, Penttila A, Karhunen PJ. Alcohol consumption and alcoholic liver disease: evidence of a threshold level of effects of ethanol. Alcohol Clin Exp Res. 1993;17(5):1112-7. PubMed PMID: 8279675.
147. Louvet A, Labreuche J, Artru F, Boursier J, Kim DJ, O'Grady J, Trepo E, Nahon P, Ganne-Carrie N, Naveau S, Diaz E, Gustot T, Lassailly G, Cannesson-Leroy A, Canva-Delcambre V, Dharancy S, Park SH, Moreno C, Morgan TR, Duhamel A, Mathurin P. Combining Data From Liver Disease Scoring Systems Better Predicts Outcomes of Patients With Alcoholic Hepatitis. Gastroenterology. 2015;149(2):398-406 e8; quiz e16-7. doi: 10.1053/j.gastro.2015.04.044. PubMed PMID: 25935634.

148. Moss M, Burnham EL. Chronic alcohol abuse, acute respiratory distress syndrome, and multiple organ dysfunction. Crit Care Med. 2003;31(4 Suppl):S207-12. Epub 2003/04/12. doi: 10.1097/01.CCM.0000057845.77458.25. PubMed PMID: 12682442.
149. de Jong WJ, Cleveringa AM, Greijdanus B, Meyer P, Heineman E, Hulscher JB. The effect of acute alcohol intoxication on gut wall integrity in healthy male volunteers; a randomized controlled trial. Alcohol. 2015;49(1):65-70. Epub 2015/01/07. doi: 10.1016/j.alcohol.2014.09.033. PubMed PMID: 25559494.
150. Mueller S, Seitz HK, Rausch V. Non-invasive diagnosis of alcoholic liver disease. World J Gastroenterol. 2014;20(40):14626-41. Epub 2014/10/31. doi: 10.3748/wjg.v20.i40.14626. PubMed PMID: 25356026; PMCID: PMC4209529.
151. Lebedev SP. [Morphology and pathogenesis of visceral manifestations of chronic alcoholism]. Arkh Patol. 1982;44(5):80-6. Epub 1982/01/01. PubMed PMID: 7115139.
152. Nguyen TA, DeShazo JP, Thacker LR, Puri P, Sanyal AJ. The Worsening Profile of Alcoholic Hepatitis in the United States. Alcohol Clin Exp Res. 2016;40(6):1295-303. Epub 2016/05/06. doi: 10.1111/acer.13069. PubMed PMID: 27147285; PMCID: PMC4918810.
153. McKim SE, Uesugi T, Raleigh JA, McClain CJ, Arteel GE. Chronic intragastric alcohol exposure causes hypoxia and oxidative stress in the rat pancreas. Arch Biochem Biophys. 2003;417(1):34-43. Epub 2003/08/19. PubMed PMID: 12921777.
154. Kronenberg F. Emerging risk factors and markers of chronic kidney disease progression. Nat Rev Nephrol. 2009;5(12):677-89. Epub 2009/11/26. doi: 10.1038/nrneph.2009.173. PubMed PMID: 19935815.
155. Varga ZV, Matyas C, Paloczi J, Pacher P. Alcohol Misuse and Kidney Injury: Epidemiological Evidence and Potential Mechanisms. Alcohol Res. 2017;38(2):283-8. Epub 2017/10/11. PubMed PMID: 28988579; PMCID: PMC5513691.
156. Menon V, Katz R, Mukamal K, Kestenbaum B, de Boer IH, Siscovick DS, Sarnak MJ, Shlipak MG. Alcohol consumption and kidney function decline in the elderly: alcohol and kidney disease. Nephrol Dial Transplant. 2010;25(10):3301-7. Epub 2010/04/20. doi: 10.1093/ndt/gfq188. PubMed PMID: 20400446; PMCID: PMC2948837.
157. Knight EL, Stampfer MJ, Rimm EB, Hankinson SE, Curhan GC. Moderate alcohol intake and renal function decline in women: a prospective study. Nephrol Dial Transplant. 2003;18(8):1549-54. Epub 2003/08/05. PubMed PMID: 12897093.
158. Bundy JD, Bazzano LA, Xie D, Cohan J, Dolata J, Fink JC, Hsu CY, Jamerson K, Lash J, Makos G, Steigerwalt S, Wang X, Mills KT, Chen J, He J, Investigators CS. Self-Reported Tobacco, Alcohol, and Illicit Drug Use and Progression of Chronic Kidney Disease. Clin J Am Soc Nephrol. 2018;13(7):993-1001. Epub 2018/06/09. doi: 10.2215/CJN.11121017. PubMed PMID: 29880471; PMCID: PMC6032576.

159. Zelle DM, Agarwal PK, Ramirez JL, van der Heide JJ, Corpeleijn E, Gans RO, Navis G, Bakker SJ. Alcohol consumption, new onset of diabetes after transplantation, and all-cause mortality in renal transplant recipients. Transplantation. 2011;92(2):203-9. Epub 2011/06/21. doi: 10.1097/TP.0b013e318222ca10. PubMed PMID: 21685828.
160. Villafuerte BC, Barati MT, Rane MJ, Isaacs S, Li M, Wilkey DW, Merchant ML. Over-expression of insulin-response element binding protein-1 (IRE-BP1) in mouse pancreatic islets increases expression of RACK1 and TCTP: Beta cell markers of high glucose sensitivity. Biochim Biophys Acta Proteins Proteom. 2017;1865(2):186-94. Epub 2016/11/07. doi: 10.1016/j.bbapap.2016.10.015. PubMed PMID: 27816562; PMCID: PMC5233416.
161. Barati MT, Gould JC, Salyer SA, Isaacs S, Wilkey DW, Merchant ML. Influence of Acute High Glucose on Protein Abundance Changes in Murine Glomerular Mesangial Cells. J Diabetes Res. 2016;2016:3537863. Epub 2016/02/04. doi: 10.1155/2016/3537863. PubMed PMID: 26839892; PMCID: PMC4709621.
162. Barrett T, Wilhite SE, Ledoux P, Evangelista C, Kim IF, Tomashevsky M, Marshall KA, Phillippy KH, Sherman PM, Holko M, Yefanov A, Lee H, Zhang N, Robertson CL, Serova N, Davis S, Soboleva A. NCBI GEO: archive for functional genomics data sets--update. Nucleic Acids Res. 2013;41(Database issue):D991-5. Epub 2012/11/30. doi: 10.1093/nar/gks1193. PubMed PMID: 23193258; PMCID: PMC3531084.
163. Mundel P, Reiser J. Proteinuria: an enzymatic disease of the podocyte? Kidney Int. 2010;77(7):571-80. Epub 2009/11/20. doi: 10.1038/ki.2009.424. PubMed PMID: 19924101; PMCID: PMC4109304.
164. Reiser J, von Gersdorff G, Loos M, Oh J, Asanuma K, Giardino L, Rastaldi MP, Calvaresi N, Watanabe H, Schwarz K, Faul C, Kretzler M, Davidson A, Sugimoto H, Kalluri R, Sharpe AH, Kreidberg JA, Mundel P. Induction of B7-1 in podocytes is associated with nephrotic syndrome. J Clin Invest. 2004;113(10):1390-7. Epub 2004/05/18. doi: 10.1172/JCI20402. PubMed PMID: 15146236; PMCID: PMC406528.
165. Lu XM, Ma L, Jin YN, Yu YQ. Lumican overexpression exacerbates lipopolysaccharide-induced renal injury in mice. Mol Med Rep. 2015;12(3):4089-94. Epub 2015/06/18. doi: 10.3892/mmr.2015.3940. PubMed PMID: 26081832; PMCID: PMC4526055.
166. Savitski MM, Mathieson T, Zinn N, Sweetman G, Doce C, Becher I, Pachl F, Kuster B, Bantscheff M. Measuring and managing ratio compression for accurate iTRAQ/TMT quantification. J Proteome Res. 2013;12(8):3586-98. Epub 2013/06/19. doi: 10.1021/pr400098r. PubMed PMID: 23768245.
167. Badawy AA, Bano S, Steptoe A. Tryptophan in alcoholism treatment I: kynurenine metabolites inhibit the rat liver mitochondrial low Km aldehyde dehydrogenase activity, elevate blood acetaldehyde concentration and induce aversion to alcohol. Alcohol Alcohol. 2011;46(6):651-60. Epub 2011/09/08. doi: 10.1093/alcalc/agr134. PubMed PMID: 21896552; PMCID: PMC3196366.
168. Rajapakse NW, Konstantinidis G, Evans RG, Nguyen-Huu TP, Kaye DM, Head GA. Endothelial cationic amino acid transporter-1 overexpression blunts

the effects of oxidative stress on pressor responses to behavioural stress in mice. Clin Exp Pharmacol Physiol. 2014;41(12):1031-7. Epub 2014/08/15. doi: 10.1111/1440-1681.12279. PubMed PMID: 25115333.
169. Komers R, Xu B, Fu Y, McClelland A, Kantharidis P, Mittal A, Cohen HT, Cohen DM. Transcriptome-based analysis of kidney gene expression changes associated with diabetes in OVE26 mice, in the presence and absence of losartan treatment. PLoS One. 2014;9(5):e96987. Epub 2014/05/16. doi: 10.1371/journal.pone.0096987. PubMed PMID: 24827579; PMCID: PMC4020814.
170. Poole LG, Massey VL, Siow DL, Torres-Gonzales E, Warner NL, Luyendyk JP, Ritzenthaler JD, Roman J, Arteel GE. Plasminogen Activator Inhibitor-1 Is Critical in Alcohol-Enhanced Acute Lung Injury in Mice. Am J Respir Cell Mol Biol. 2017;57(3):315-23. Epub 2017/04/27. doi: 10.1165/rcmb.2016-0184OC. PubMed PMID: 28445073; PMCID: PMC5625219.
171. O'Neill LA, Golenbock D, Bowie AG. The history of Toll-like receptors - redefining innate immunity. Nat Rev Immunol. 2013;13(6):453-60. Epub 2013/05/18. doi: 10.1038/nri3446. PubMed PMID: 23681101.
172. Gobejishvili L, Barve S, Joshi-Barve S, Uriarte S, Song Z, McClain C. Chronic ethanol-mediated decrease in cAMP primes macrophages to enhanced LPS-inducible NF-kappaB activity and TNF expression: relevance to alcoholic liver disease. Am J Physiol Gastrointest Liver Physiol. 2006;291(4):G681-8. Epub 2006/06/06. doi: 10.1152/ajpgi.00098.2006. PubMed PMID: 16751174.
173. Raksaseri P, Chatsudthipong V, Muanprasat C, Soodvilai S. Activation of liver X receptors reduces CFTR-mediated Cl(-) transport in kidney collecting duct cells. Am J Physiol Renal Physiol. 2013;305(4):F583-91. Epub 2013/05/31. doi: 10.1152/ajprenal.00579.2012. PubMed PMID: 23720350.
174. Gong P, Cederbaum AI. Nrf2 is increased by CYP2E1 in rodent liver and HepG2 cells and protects against oxidative stress caused by CYP2E1. Hepatology. 2006;43(1):144-53. Epub 2005/12/24. doi: 10.1002/hep.21004. PubMed PMID: 16374848.
175. Aminzadeh MA, Nicholas SB, Norris KC, Vaziri ND. Role of impaired Nrf2 activation in the pathogenesis of oxidative stress and inflammation in chronic tubulo-interstitial nephropathy. Nephrol Dial Transplant. 2013;28(8):2038-45. Epub 2013/03/21. doi: 10.1093/ndt/gft022. PubMed PMID: 23512109; PMCID: PMC3765021.
176. Jiang T, Tian F, Zheng H, Whitman SA, Lin Y, Zhang Z, Zhang N, Zhang DD. Nrf2 suppresses lupus nephritis through inhibition of oxidative injury and the NF-kappaB-mediated inflammatory response. Kidney Int. 2014;85(2):333-43. Epub 2013/09/13. doi: 10.1038/ki.2013.343. PubMed PMID: 24025640; PMCID: PMC3992978.
177. Liu M, Reddy NM, Higbee EM, Potteti HR, Noel S, Racusen L, Kensler TW, Sporn MB, Reddy SP, Rabb H. The Nrf2 triterpenoid activator, CDDO-imidazolide, protects kidneys from ischemia-reperfusion injury in mice. Kidney Int. 2014;85(1):134-41. Epub 2013/10/04. doi: 10.1038/ki.2013.357. PubMed PMID: 24088953; PMCID: PMC5282962.

178. Potteti HR, Tamatam CR, Marreddy R, Reddy NM, Noel S, Rabb H, Reddy SP. Nrf2-AKT interactions regulate heme oxygenase 1 expression in kidney epithelia during hypoxia and hypoxia-reoxygenation. Am J Physiol Renal Physiol. 2016;311(5):F1025-F34. Epub 2016/09/02. doi: 10.1152/ajprenal.00362.2016. PubMed PMID: 27582105; PMCID: PMC5130454.
179. Jimenez-Osorio AS, Garcia-Nino WR, Gonzalez-Reyes S, Alvarez-Mejia AE, Guerra-Leon S, Salazar-Segovia J, Falcon I, Montes de Oca-Solano H, Madero M, Pedraza-Chaverri J. The Effect of Dietary Supplementation With Curcumin on Redox Status and Nrf2 Activation in Patients With Nondiabetic or Diabetic Proteinuric Chronic Kidney Disease: A Pilot Study. J Ren Nutr. 2016;26(4):237-44. Epub 2016/02/27. doi: 10.1053/j.jrn.2016.01.013. PubMed PMID: 26915483.
180. Atilano-Roque A, Wen X, Aleksunes LM, Joy MS. Nrf2 activators as potential modulators of injury in human kidney cells. Toxicol Rep. 2016;3:153-9. Epub 2016/01/12. doi: 10.1016/j.toxrep.2016.01.006. PubMed PMID: 28959534; PMCID: PMC5615789.
181. Hall ET, Bhalla V. Is there a sweet spot for Nrf2 activation in the treatment of diabetic kidney disease? Diabetes. 2014;63(9):2904-5. Epub 2014/08/26. doi: 10.2337/db14-0829. PubMed PMID: 25146471; PMCID: PMC4141365.
182. Jaiswal AK. Regulation of genes encoding NAD(P)H:quinone oxidoreductases. Free Radic Biol Med. 2000;29(3-4):254-62. Epub 2000/10/18. PubMed PMID: 11035254.
183. Ross D, Siegel D. Functions of NQO1 in Cellular Protection and CoQ10 Metabolism and its Potential Role as a Redox Sensitive Molecular Switch. Front Physiol. 2017;8:595. Epub 2017/09/09. doi: 10.3389/fphys.2017.00595. PubMed PMID: 28883796; PMCID: PMC5573868.
184. Shin S, Wakabayashi N, Misra V, Biswal S, Lee GH, Agoston ES, Yamamoto M, Kensler TW. NRF2 modulates aryl hydrocarbon receptor signaling: influence on adipogenesis. Mol Cell Biol. 2007;27(20):7188-97. Epub 2007/08/22. doi: 10.1128/MCB.00915-07. PubMed PMID: 17709388; PMCID: PMC2168916.
185. Kataoka K, Igarashi K, Itoh K, Fujiwara KT, Noda M, Yamamoto M, Nishizawa M. Small Maf proteins heterodimerize with Fos and may act as competitive repressors of the NF-E2 transcription factor. Mol Cell Biol. 1995;15(4):2180-90. Epub 1995/04/01. PubMed PMID: 7891713; PMCID: PMC230446.
186. Kimura M, Yamamoto T, Zhang J, Itoh K, Kyo M, Kamiya T, Aburatani H, Katsuoka F, Kurokawa H, Tanaka T, Motohashi H, Yamamoto M. Molecular basis distinguishing the DNA binding profile of Nrf2-Maf heterodimer from that of Maf homodimer. J Biol Chem. 2007;282(46):33681-90. Epub 2007/09/19. doi: 10.1074/jbc.M706863200. PubMed PMID: 17875642.
187. Yamamoto T, Kyo M, Kamiya T, Tanaka T, Engel JD, Motohashi H, Yamamoto M. Predictive base substitution rules that determine the binding and transcriptional specificity of Maf recognition elements. Genes Cells. 2006;11(6):575-91. Epub 2006/05/24. doi: 10.1111/j.1365-2443.2006.00965.x. PubMed PMID: 16716189.

188. Bryan HK, Olayanju A, Goldring CE, Park BK. The Nrf2 cell defence pathway: Keap1-dependent and -independent mechanisms of regulation. Biochem Pharmacol. 2013;85(6):705-17. Epub 2012/12/12. doi: 10.1016/j.bcp.2012.11.016. PubMed PMID: 23219527.
189. Jain A, Lamark T, Sjottem E, Larsen KB, Awuh JA, Overvatn A, McMahon M, Hayes JD, Johansen T. p62/SQSTM1 is a target gene for transcription factor NRF2 and creates a positive feedback loop by inducing antioxidant response element-driven gene transcription. J Biol Chem. 2010;285(29):22576-91. Epub 2010/05/11. doi: 10.1074/jbc.M110.118976. PubMed PMID: 20452972; PMCID: PMC2903417.
190. Luo J. Autophagy and ethanol neurotoxicity. Autophagy. 2014;10(12):2099-108. Epub 2014/12/09. doi: 10.4161/15548627.2014.981916. PubMed PMID: 25484085; PMCID: PMC4502825.
191. Naba A, Clauser KR, Hoersch S, Liu H, Carr SA, Hynes RO. The matrisome: in silico definition and in vivo characterization by proteomics of normal and tumor extracellular matrices. Mol Cell Proteomics. 2012;11(4):M111 014647. Epub 2011/12/14. doi: 10.1074/mcp.M111.014647. PubMed PMID: 22159717; PMCID: PMC3322572.
192. Massey VL, Arteel GE. Acute alcohol-induced liver injury. Front Physiol. 2012;3:193. Epub 2012/06/16. doi: 10.3389/fphys.2012.00193. PubMed PMID: 22701432; PMCID: PMC3372892.

# ABBREVIATIONS

| | |
|---|---|
| Adh | Alcohol dehydrogenase |
| AH | Alcoholic hepatitis |
| Ahr | Aryl hydrocarbon receptor |
| ALD | Alcoholic liver disease |
| ANOVA | Analysis of variance |
| Aldh | Aldehyde dehydrogenase |
| ALT | Alanine aminotransferase |
| APP | Acute phase protein |
| ARE | Antioxidant response element |
| ASH | Alcoholic steatohepatitis |
| AST | Aspartate aminotransferase |
| AUC | Area under the curve |
| AUD | Alcohol use disorder |
| AUDIT | Alcohol use disorder identification test |
| BH | Benjamini-Hochberg |
| BSA | Bovine serum albumin |
| BUN | Blood urea nitrogen |
| Cat | Catalase |
| CCL2 | C-C Motif Chemokine Ligand 2 |
| CID | Collision induced dissociation |
| COL | Collagen |
| CRELD2 | Cysteine-rich with EGF-like domain protein 2 |
| CTP | Child-Turcotte-Pugh score |
| Cyp2e1 | Cytochrome P450 2E1 |
| DAMP | Damage-associated molecular pattern |

| | |
|---|---|
| DSM | Diagnostic and Statistical Manual of Mental Disorders |
| DTT | Dithiothreitol |
| ECM | Extracellular matrix |
| EDTA | Ethylenediaminetetraacetic acid |
| ER | Endoplasmic reticulum |
| ETD | Electron transfer dissociation |
| EtOH | Ethanol |
| FA | Formic acid |
| FASP | Filter-aided sample preparation |
| FC | Fold change |
| FDR | False discovery rate |
| FTMS | Fourier-transform mass spectrometry |
| GAPDH | Glyceraldehyde 3-phosphate dehydrogenase |
| Gclc | Glutamate-cysteine ligase catalytic subunit |
| GnHCl | Guanidine hydrochloride |
| GO | Gene ontology |
| H&E | Hematoxylin & eosin |
| HC | Healthy control |
| HCC | Hepatocellular carcinoma |
| HCD | Higher energy collision dissociation |
| HEPES | 4-(2-hydroxyethyl)-1-piperazineethanesulfonic acid |
| HF | Hepatic fibrosis |
| HLB | Hydrophilic-lipophilic balance |
| HMGB1 | High mobility group protein B1 |
| HRS | Hepatorenal syndrome |
| HSCs | Hepatic stellate cells |
| IFN-γ | Interferon gamma |
| IB | Immunoblot |
| i.p. | Intraperitoneal |

| | |
|---|---|
| IHC | Immunohistochemistry |
| INR | International normalized ratio |
| IPA | Ingenuity Pathways Analysis |
| ITMS | Ion trap mobility spectrometry |
| KCl | Potassium chloride |
| KCs | Kupffer cells |
| Keap1 | Kelch-like ECH-associated protein 1 |
| LC-MS/MS | Liquid chromatography and tandem mass spectrometry |
| LPS | Lipopolysaccharide |
| LTDH | Lifetime drinking history |
| LXR | Liver X receptor |
| M/z | Mass-to-charge ratio |
| MD | Maltose-dextrin |
| MDE | Matrix-degrading enzymes |
| MELD | Model for end-stage liver disease |
| MMPs | Matrix metalloproteinases |
| Mpo | Myeloperoxidase |
| mRNA | Messenger ribonucleic acid |
| MS | Mass spectrometry |
| NaCl | Sodium chloride |
| NaF | Sodium fluoride |
| NAFLD | Non-alcoholic fatty liver disease |
| NASH | Non-alcoholic steatohepatitis |
| $NaVO_3$ | Sodium metavanadate |
| NIAAA | National Institute on Alcohol Abuse and Alcoholism |
| NIH | National Institutes of Health |
| NP-40 | Nonidet p-40 |
| Nqo1 | NAD(P)H quinone dehydrogenase 1 |
| Nrf2 | Nuclear factor erythroid 2–related factor 2 |

| | |
|---|---|
| PAI-1 | Plasminogen activator inhibitor |
| PAMP | Pathogen-associated molecular pattern |
| PAS | Periodic acid-Schiff |
| PBDC | Proteomics Biomarkers Discovery Core |
| PCA | Principle component analysis |
| PEBP1 | Phosphatidylethanolamine-binding protein |
| PMN | Polymorphonuclear leukocyte |
| PRR | Pathogen recognition receptor |
| PT | Prothrombin time |
| RANTES | Regulated on activation, normal T cell expressed and secreted |
| RIN | RNA integrity number |
| RIPA | Radioimmunoprecipitation assay |
| RNA | Ribonucleic acid |
| RXR | Retinoid X receptor |
| SAA1 | Serum amyloid A1 |
| SAA2 | Serum amyloid A2 |
| SCX | Strong cation exchange |
| SDS | Sodium dodecyl sulfate |
| SGOT | Serum glutamic oxaloacetic transaminase |
| SGPT | Serum glutamic-pyruvic transaminase |
| SIRS | Systemic inflammatory response syndrome |
| Sod1 | Superoxide dismutase 1 |
| Sod2 | Superoxide dismutase 2 |
| Sqstm | Sequestrome-1 |
| Tbili | Total bilirubin |
| TBST | Tris-buffered saline and Tween |
| TCA | Trichloroacetic acid |
| TEABC | Triethylammonium bicarbonate |
| TGFβ | Transforming growth factor beta |

| | |
|---|---|
| TIC | Total ion current |
| TIMP | Tissue inhibitor of matrix metalloproteinases |
| TLR4 | Toll-like receptor 4 |
| TNFα | Tumor necrosis factor-alpha |
| TMT | Tandem mass tag |
| UHPLC | Ultra-high-performance liquid chromatography |

PUBLISHER'S NOTICE OF APPROVAL

Dear Dr. Mike Merchant,

**Hepatology**
**"The hepatic "matrisome" responds dynamically to injury: characterization of transitional changes to the extracellular matrix"**
**Article ID: HEP28918**

Thank you for your recent communication regarding the use of data and figures of the above-mentioned article.

We wish to advise that Christine Dolin can use the article for her dissertation as long as the material to be used is less than half of the article. For further clarifications, please contact our Permissions Team at Permissions@wiley.com. It should also be for non-commercial purpose or for financial consideration.

Full and accurate credit must be given to the Contribution. We hope this information helps.

Please do not hesitate to contact us if you require any further assistance.

Kind regards,

**Marie Bautista**
Wiley Author Support

WILEY

CURRICULUM VITAE

Christine E. Dolin
University of Louisville School of Medicine
Department of Pharmacology and Toxicology
Louisville, KY 40292

---

## 1. EDUCATION

| | |
|---|---|
| (2019) | Ph.D. in Pharmacology and Toxicology |
| | University of Louisville, Louisville, KY |
| 2017 | M.S. in Pharmacology and Toxicology |
| | University of Louisville, Louisville, KY |
| 2015 | B.S. in Chemistry, conc. Biochemistry, Minor in Biology |
| | University of Louisville, Louisville, KY |

## 2. PROFESSIONAL EXPERIENCE

| | |
|---|---|
| 08/2015 - present | Graduate Research Assistant (Advisor: Michael Merchant, Ph.D., formerly Gavin Arteel, Ph.D., until he moved in June 2018), Department of Pharmacology and Toxicology, University of Louisville |
| 08/2014 - 07/2015 | Undergraduate Research Assistant (Advisor: Gavin Arteel, Ph.D.), Department of Pharmacology and Toxicology, University of Louisville |
| 05/2014 - 07/2014 | National Cancer Institute R25 Cancer Education Program Trainee (Advisor: Gavin Arteel, Ph.D.), Department of Pharmacology and Toxicology, University of Louisville |
| 01/2013 - 08/2013 | Undergraduate Research Assistant (Advisor: Teresa Fan, Ph.D.), Department of Chemistry, University of Louisville |

## 3. PROFESSIONAL MEMBERSHIPS AND ACTIVITIES

| | |
|---|---|
| 2018-present | Kentucky Academy of Science (KAS) |
| 2016-2018 | Kentucky Biomedical Research Infrastructure and Network (KBRIN) Journal Club |
| 2016-2017 | American Society of Nephrology (ASN) |

| | |
|---|---|
| 2015-present | American Association for the Study of Liver Diseases (AASLD) |
| 2014-present | University of Louisville Alcohol Research Center (ULARC) |
| 2014-present | Society of Toxicology (SOT), Student Member |
| 2014-present | Ohio Valley Society of Toxicology (OVSOT) |

## 4. AWARDS AND HONORS

| | |
|---|---|
| 2018 | Abstract awarded “Best of the Liver Meeting”, AASLD’s Liver Meeting |
| 2018 | Invited to speak at Early Morning Workshop, AASLD’s Liver Meeting |
| 2018 | Abstract selected for oral presentation, AASLD’s Liver Meeting |
| 2017 | Abstract selected for oral presentation, OVSOT Fall Meeting |
| 2017 | Finalist in University of Louisville Three-Minute Thesis Competition |
| 2016 | Graduate Student Council Travel Award |
| 2016 | Abstract selected for oral presentation, OVSOT Summer Meeting |
| 2015 | Poster selected for third and final round of judging, Research!Louisville |
| 2015 | Abstract selected for oral presentation, OVSOT Summer Meeting |
| 2015 | One of seven University of Louisville undergraduate students selected to present research at the Atlantic Coast Conference Meeting of the Minds |
| 2010 | Valedictorian and *Summa cum Laude*, South Oldham High School |
| 2009 | Kentucky Governor’s Scholars Program, focus in Biological and Environmental Issues |

## 5. SERVICE AND LEADERSHIP ACTIVITIES

| | |
|---|---|
| 02/2019 | Organized and led presentation and activity for Westport Middle School Girls’ STEM Club, through the Kentucky Academy of Science |
| 08/2018 | Served on Q&A panel for new student welcome event, Department of Pharmacology and Toxicology, University of Louisville |
| 07/2018 | Collected clinical data for Superfund “Project Greenheart”, University of Louisville |
| 07/2018 | Led roundtable discussion for National Cancer Institute R25 Cancer Education Program students, University of Louisville |
| 07/2016 | Led roundtable discussion for National Cancer Institute R25 Cancer Education Program students, University of Louisville |
| 08/2012-05/2013 | Served on the University of Louisville Housing and Residence Life “Green Committee”, which promotes sustainability in residence halls |

## 6. FUNDING

| | |
|---|---|
| 2017-present | National Institute of Environmental Health Sciences NRSA Institutional Training Grant (T32) Predoctoral Fellowship, University of Louisville, Department of Pharmacology and Toxicology |
| 2015-2017 | Graduate Research Fellowship, Integrated Program in Biomedical Sciences, University of Louisville |

## 7. ABSTRACTS AND PRESENTATIONS

### A. Abstracts

#### *Local/Regional*

1. **Dolin CE**, Wilkey DW, Vatsalya V, McClain CJ, Merchant ML, Arteel GE. Poster, (2018) Peptidomic analysis of alcoholic hepatitis: a new prognostic tool? Research!Louisville, Louisville, KY.
2. **Dolin CE**, Poole LG, Wilkey DW, Arteel GE, Rouchka EC, Barati MT, Merchant ML. (2017) A novel effect of alcohol on the kidney: Chronic and acute alcohol exposure alter peroxisomal protein abundance in the renal cortex. Ohio Valley Society of Toxicology Annual Meeting, West Lafayette, IN.
3. Hudson SV, **Dolin CE,** Merchant ML, Arteel GE (2017) Arsenic Attenuates LPS-stimulated Polarization in Murine Bone Marrow Derived Macrophages: Potential Role of miR-301b. Research!Louisville, Louisville, KY.
4. **Dolin CE**, Poole LG, Wilkey DW, Arteel GE, Rouchka EC, Barati MT, Merchant ML. (2017) A novel effect of alcohol on the kidney: Chronic and acute alcohol exposure alter peroxisomal protein abundance in the renal cortex. Research!Louisville, Louisville, KY.
5. **Dolin CE**, Poole LG, Wilkey DW, Rouchka EC, Arteel GE, Barati MT, Michael L. Merchant. (2017) Effects of ethanol and lipopolysaccharide on the renal cortex proteome and transcriptome. UT-KBRIN Bioinformatics Summit, Burns, TN.
6. **Dolin CE**, Poole LG, Wilkey DW, Rouchka EC, Arteel GE, Barati MT, Michael L. Merchant. (2017) Effects of ethanol and lipopolysaccharide on the renal cortex proteome and transcriptome. Graduate Student Council Research Symposium, Louisville, KY.
7. **Dolin CE**, Poole LG, Wilkey DW, Arteel GE, Rouchka EC, Barati MT, Merchant ML. (2016) Effects of Ethanol and Lipopolysaccharide on the Renal Cortex Proteome and Transcriptome. Ohio Valley Society of Toxicology Annual Meeting, Indianapolis, IN.
8. Poole LG, Beier JI, Torres-Gonzalez E, Anwar-Mohamed A, Warner N, **Dolin CE**, Nguyen-Ho C, Hudson SV, Roman J, Arteel GE. (2016) Acute-on-chronic Alcohol Exposure Concomitantly Damages the Liver and Lung. Research!Louisville, Louisville, KY.
9. Hudson SV, **Dolin CE**, Poole LP, Massey VL, Wilkey DW, Merchant ML, Frieboes H, Arteel GE. (2016) Modeling Binding Kinetics of Integrin

Mediators of EtOH-enhanced LPS Liver Injury. Research!Louisville, Louisville, KY.

10. **Dolin CE**, Poole LG, Wilkey DW, Arteel GE, Rouchka EC, Barati MT, Merchant ML. (2016) Effects of Ethanol and Lipopolysaccharide on the Renal Cortex Proteome and Transcriptome. Research!Louisville, Louisville, KY.
11. **Dolin CE**, Poole LG, Wilkey DW, Barati MT, Arteel GE, Merchant ML. (2016) Characterization of the Impact of Ethanol and Lipopolysaccharide on the Renal Cortex Proteome. Ohio Valley Society of Toxicology Summer Meeting, Cincinnati, OH.
12. **Dolin CE**, Poole LG, Wilkey DW, Barati MT, Arteel GE, Merchant ML. (2016) Characterization of the Impact of Ethanol and Lipopolysaccharide on the Renal Cortex Proteome. University of Kentucky Postdoctoral Symposium, Lexington, KY.
13. **Dolin CE**, Massey VL, Poole LG, Siow DL, Merchant ML, Wilkey DW, Roman J, Arteel GE. (2016) The Hepatic and Pulmonary "Matrisomes" Respond Dynamically to Inflammatory Injury: Proteomic Characterization of Transitional ECM Changes in the Liver and Lung. Graduate Student Council Research Symposium, Louisville, KY.
14. Poole LG, Massey VL, Torres-Gonzalez E, Warner N, Siow D, **Dolin CE**, Lang AL, Hudson SV, Roman J, Arteel GE. (2015) Alcohol enhances endotoxemia-induced acute lung injury: role of plasminogen activator inhibitor-1. Research!Louisville, Louisville, KY.
15. Hudson SV, **Dolin CE**, Poole LP, Massey VL, Wilkey DW, Merchant ML, Frieboes H, Arteel GE. (2015) Modeling the Kinetics of Integrin Receptor Binding to Extracellular Matrix Proteins. Research!Louisville, Louisville, KY.
16. **Dolin CE**, Massey VL, Poole LG, Siow DL, Merchant ML, Wilkey DW, Roman J, Arteel GE. (2015) The Hepatic and Pulmonary "Matrisome" Responds Dynamically to Inflammatory Injury: Proteomic Characterization of the Transitional ECM Changes. Research!Louisville, Louisville, KY.
17. **Dolin CE,** Massey VL, Poole LG, Siow DL, Merchant ML, Wilkey DW, Arteel GE. (2015) The Hepatic "Matrisome" Responds Dynamically to Inflammatory Injury: Proteomic Characterization of the Transitional ECM Changes in the Liver. Ohio Valley Society of Toxicology Summer Meeting, Cincinnati, OH.
18. **Dolin CE**, Massey VL, Poole LG, Siow DL, Merchant ML, Wilkey DW, Arteel GE. (2015) The Hepatic "Matrisome" Responds Dynamically to Stress: Novel Characterization of the ECM Proteome. Atlantic Coast Conference Meeting of the Minds, Raleigh, NC.
19. **Dolin CE**, Massey VL, Poole LG, Siow DL, Merchant ML, Wilkey DW, Arteel GE. (2015) The Hepatic "Matrisome" Responds Dynamically to Stress: Novel Characterization of the ECM Proteome. Posters at the Capitol, Frankfort, KY.
20. Poole LG, Massey VL, **Dolin CE**, Siow DL, Merchant ML, Beier JI, Roman J, Arteel GE. (2014) Ethanol-induced changes in the hepatic ECM directly

enhance the pro-inflammatory response of macrophages. Ohio Valley Society of Toxicology Annual Meeting, Dayton, OH.

21. **Dolin CE**, Massey VL, Poole LG, Siow DL, Merchant ML, Wilkey DW, Arteel GE. (2014) The Hepatic "Matrisome" Responds Dynamically to Stress: Novel Characterization of the ECM Proteome. Ohio Valley Society of Toxicology Annual Meeting, Dayton, OH.
22. Massey VL, Poole LG, Torres E, **Dolin CE**, Merchant ML, Ritzenthaler J, Roman J, Arteel GE. (2014) Characterization of the liver:lung axis in alcohol-induced lung damage. Research!Louisville, Louisville, KY.
23. Poole LG, Massey VL, **Dolin CE**, Merchant ML, Beier JI, Roman J, Arteel GE. (2014) Ethanol-induced changes in the hepatic ECM directly enhance the pro-inflammatory response of macrophages. Research!Louisville, Louisville, KY.
24. **Dolin CE**, Massey VL, Poole LG, Siow DL, Merchant ML, Wilkey DW, Arteel GE (2014) The Hepatic "Matrisome" Responds Dynamically to Stress: Novel Characterization of the ECM Proteome. Research!Louisville, Louisville, KY.
25. **Dolin CE**, Massey VL, Poole LG, Siow DL, Merchant ML, Wilkey DW, Arteel GE (2014) The Hepatic "Matrisome" Responds Dynamically to Stress: Novel Characterization of the ECM Proteome. University of Louisville R25 Cancer Education Program, Louisville, KY.

***National***

1. **Dolin CE**, Wilkey DW, Vatsalya V, Srivastava S, McClain CJ, Rai SN, Merchant ML, Arteel GA (2018) Novel Biomarkers in Alcoholic Hepatitis: Analysis of the Plasma Peptidome/Degradome. *Hepatology* 68(6):1444A.
2. Hudson SV, Anwar-Mohamed A, **Dolin CE**, Merchant ML, Arteel GE (2017) Arsenic Attenuates Lipopolysaccharide-Stimulated Polarization in Murine Bone Marrow Derived Macrophages: Potential Role of miR-301b. *The Toxicologist Supplement* 2017:2992.
3. Hudson SV, **Dolin CE**, Merchant ML, Arteel GE (2017) Role of miR-301b in arsenic-altered macrophage polarization: potential insight into impact of arsenic exposure on innate immune response. *Hepatology* 66(S1):653.
4. Poole LG, Beier JI, Torres-Gonzalez E, Anwar-Mohamed A, Warner N, **Dolin CE**, Nguyen-Ho C, Ritzenthaler JD, Roman J, Arteel GE (2016) Acute-on-chronic alcohol exposure using the 'NIAAA model' concomitantly damages the liver and lung. *Hepatology* 64(S1):1221.
5. Hudson SV, **Dolin CE**, Poole LG, Massey VL, Wilkey DW, Brock GN, Merchant ML, Frieboes HB, Arteel GE (2016) Modeling Concurrent Binding of Mixed Integrin Species to Multiple ECM Ligands. *The Toxicologist Supplement* 2016:2211.
6. **Dolin CE,** Poole LG, Wilkey DW, Arteel GE, Rouchka EC, Barati MT, Merchant ML (2016) Omics Characterization of Ethanol and Lipopolysaccharide Impact on the Renal Cortex. *JASN Abstract Supplement* 2016 27:

7. **Dolin CE,** Massey VL, Poole LG, Siow DL, Merchant ML, Wilkey DW, Arteel GE. (2015) The Hepatic and Pulmonary "Matrisome" Responds Dynamically to Inflammatory Injury: Proteomic Characterization of the Transitional ECM Changes in the Liver. *Hepatology* 62(S1):587.
8. **Dolin CE,** Massey VL, Poole LG, Siow DL, Merchant ML, Wilkey DW, Arteel GE. (2015) The Hepatic "Matrisome" Responds Dynamically to Stress: Novel Characterization of the ECM Proteome. *The Toxicologist Supplement* 2015:693.

## B. Oral Presentations

### *Local/Regional*

1. 12/2018. Research Seminar. Using proteomics to discover new mechanisms and biomarkers in alcohol-induced organ injury. Department of Pathology and Laboratory Medicine, University of Kentucky, Lexington, KY.
2. 3/2018. Journal Club Presentation. Time and compartment resolved proteome profiling of the extracellular niche in lung injury and repair- Schiller *et al*. Kentucky Biomedical Research Infrastructure Network (KBRIN) Journal Club, Louisville, KY.
3. 12/2017. Platform Presentation, 12/2017, A novel effect of alcohol on the kidney: Chronic and acute alcohol exposure alter peroxisomal protein abundance in the renal cortex. Ohio Valley Society of Toxicology Annual Meeting, West Lafayette, IN.
4. 4/2017. Research Seminar. A systems-based approach to discover alcohol-induced mechanisms in the liver, lung, and kidney. Department of Pharmacology and Toxicology, University of Louisville, Louisville, KY.
5. 3/2017. Platform Presentation. Effects of ethanol and lipopolysaccharide on the renal cortex proteome and transcriptome. Graduate Student Council Research Symposium, Louisville, KY.
6. 3/2017. Research Seminar. A systems-based approach to discover alcohol-induced mechanisms in the liver, lung, and kidney. KBRIN Bioinformatics Group, University of Louisville, Louisville, KY.
7. 6/2016. Platform Presentation. Characterization of the Impact of Ethanol and Lipopolysaccharide on the Renal Cortex Proteome. Ohio Valley Society of Toxicology Summer Meeting, Cincinnati, OH.
8. 6/2016. Research Seminar. Proteomic Characterization of the Impact of Alcohol-Enhanced Inflammatory Injury on the Liver, Lung, and Kidney. Department of Pharmacology and Toxicology, University of Louisville, Louisville, KY.
9. 6/2015. Platform Presentation. The Hepatic "Matrisome" Responds Dynamically to Inflammatory Injury: Proteomic Characterization of the Transitional ECM Changes in the Liver. Ohio Valley Society of Toxicology Summer Meeting, Cincinnati, OH.

### *National*

1. 11/2018. Platform Presentation. Novel biomarkers in alcoholic hepatitis: analysis of the plasma peptidome/degradome. American Association for the Study of Liver Diseases' The Liver Meeting, San Francisco, CA.
2. 11/2018. Early Morning Workshop Presentation. The hepatic "matrisome" responds dynamically to injury: characterization of transitional changes to the extracellular matrix in mice. American Association for the Study of Liver Diseases' The Liver Meeting, San Francisco, CA.

## C. Posters

### *Local/Regional*

1. 10/2018. Peptidomic analysis of alcoholic hepatitis: a new prognostic tool? Research!Louisville, Louisville, KY.
2. 9/2017. A novel effect of alcohol on the kidney: Chronic and acute alcohol exposure alter peroxisomal protein abundance in the renal cortex, Research!Louisville, Louisville, KY.
3. 4/2017. Effects of ethanol and lipopolysaccharide on the renal cortex proteome and transcriptome, UT-KBRIN Bioinformatics Summit, Burns, TN.
4. 10/2016. Effects of Ethanol and Lipopolysaccharide on the Renal Cortex Proteome and Transcriptome. Ohio Valley Society of Toxicology Annual Meeting, Indianapolis, IN.
5. 10/2016. Effects of Ethanol and Lipopolysaccharide on the Renal Cortex Proteome and Transcriptome. Research!Louisville, Louisville, KY.
6. 6/2016. Characterization of the Impact of Ethanol and Lipopolysaccharide on the Renal Cortex Proteome. University of Kentucky Postdoctoral Symposium, Lexington, KY.
7. 4/2016. The Hepatic and Pulmonary "Matrisomes" Respond Dynamically to Inflammatory Injury: Proteomic Characterization of Transitional ECM Changes in the Liver and Lung. Graduate Student Council Research Symposium, Louisville, KY.
8. 10/2015. The Hepatic and Pulmonary "Matrisome" Responds Dynamically to Inflammatory Injury: Proteomic Characterization of the Transitional ECM Changes. Research!Louisville, Louisville, KY.
9. 2015. The Hepatic "Matrisome" Responds Dynamically to Stress: Novel Characterization of the ECM Proteome. Atlantic Coast Conference Meeting of the Minds, Raleigh, NC.
10. 2014. The Hepatic "Matrisome" Responds Dynamically to Stress: Novel Characterization of the ECM Proteome. Ohio Valley Society of Toxicology Annual Meeting, Dayton, OH.
11. 9/2014. The Hepatic "Matrisome" Responds Dynamically to Stress: Novel Characterization of the ECM Proteome. Research!Louisville, Louisville, KY.
12. 2014. The Hepatic "Matrisome" Responds Dynamically to Stress: Novel Characterization of the ECM Proteome. University of Louisville National Cancer Institute R25 Cancer Education Program, Louisville, KY.

***National***

1. 11/2016. Omics Characterization of Ethanol and Lipopolysaccharide Impact on the Renal Cortex. American Society of Nephrology Kidney Week, Chicago, IL.
2. 11/2015. The Hepatic and Pulmonary "Matrisome" Responds Dynamically to Inflammatory Injury: Proteomic Characterization of the Transitional ECM Changes in the Liver. American Association for the Study of Liver Diseases' The Liver Meeting, San Francisco, CA.
3. 3/2015. The Hepatic "Matrisome" Responds Dynamically to Stress: Novel Characterization of the ECM Proteome. Society of Toxicology Annual Meeting, San Diego, CA.

## 8. PUBLICATIONS

### A. Papers

***As coauthor***

1. Hudson SV, **Dolin CE**, Merchant ML, and Arteel GE. Arsenic attenuates lipopolysaccharide-stimulated polarization in murine bone marrow derived macrophages. (*Toxicol. Appl. Pharmacol.* 2018, submitted)
2. Poole LG, Beier JI, Torres-Gonzales E, Schlueter CF, Hudson SV, Artis A, Warner NL, Nguyen-Ho CT, **Dolin CE**, Ritzenthaler JD, Hoyle GW, Roman J, Arteel GE. Chronic + binge alcohol exposure promotes inflammation and alters airway mechanics in the lung. (*Alcohol*. 2018, in press)
3. Hudson SV, **Dolin CE**, Poole LG, Massey VL, Wilkey DW, Beier JI, Merchant ML, Frieboes HB, and Arteel GE. Modeling the Kinetics of Integrin Receptor Binding to Hepatic Extracellular Matrix Proteins. *Sci Rep.* 2017; 7(1): 12444. PMID: 28963535. PMCID: PMC5622105
4. Poole LG, **Dolin CE**, Arteel GE. Organ-Organ Crosstalk and Alcoholic Liver Disease. *Biomolecules*. 2017; 7(3): 62. PMID: 28812994. PMCID: PMC5618243

***As primary author***

5. **Dolin CE**, Poole LG, Wilkey DW, Isaacs SM, Arteel GE, Rouchka EC, Barati MT, Merchant ML. Proteotranscriptomics demonstrates chronic moderate alcohol consumption influences renal cortical oxidant response pathways. (2019, in preparation)
6. Massey VL*, **Dolin CE***, Poole LG, Hudson SV, Siow DL, Brock GN, Merchant ML, Wilkey DW, and Arteel GE. The hepatic "matrisome" responds dynamically to injury: characterization of transitional changes to the extracellular matrix in mice. *Hepatology*. 2017; 65(3): 969-982. PMID: 28035785. PMCID: PMC5319876. [*co-first authors listed by seniority]